AD_____

Award Number: W81XWH-11-1-0836

TITLE: Technologies for Hemostasis and Stabilization of the Acute Traumatic Wound

PRINCIPAL INVESTIGATOR: Carlson, Mark A.

CONTRACTING ORGANIZATION: University of Nebraska
Omaha, NE 68198-6810

REPORT DATE: October 2012

TYPE OF REPORT: Annual

PREPARED FOR: U.S. Army Medical Research and Materiel Command
Fort Detrick, Maryland 21702-5012

DISTRIBUTION STATEMENT: Approved for Public Release;
Distribution Unlimited

REPORT DOCUMENTATION PAGE

Form Approved
OMB No. 0704-0188

1. REPORT DATE	**2. REPORT TYPE**	**3. DATES COVERED**
25 October 2012	Annual	26 September 2011 – 25 September 2012

4. TITLE AND SUBTITLE
Technologies for Hemostasis and Stabilization of the Acute Traumatic Wound

5a. CONTRACT NUMBER

5b. GRANT NUMBER
W81XWH-11-1-0836

5c. PROGRAM ELEMENT NUMBER

6. AUTHOR(S)
Carlson, Mark A. Velander, William H. Larsen, Gustavo Nuñez, Luis
Burgess, Wilson H.

E-Mail: macarlso@unmc.edu

5d. PROJECT NUMBER

5e. TASK NUMBER

5f. WORK UNIT NUMBER

7. PERFORMING ORGANIZATION NAME(S) AND ADDRESS(ES)

University of Nebraska
Omaha, NE 68198-6810

8. PERFORMING ORGANIZATION REPORT NUMBER

9. SPONSORING / MONITORING AGENCY NAME(S) AND ADDRESS(ES)
U.S. Army Medical Research and Materiel Command
Fort Detrick, Maryland 21702-5012

10. SPONSOR/MONITOR'S ACRONYM(S)

11. SPONSOR/MONITOR'S REPORT NUMBER(S)

12. DISTRIBUTION / AVAILABILITY STATEMENT
Approved for Public Release; Distribution Unlimited

13. SUPPLEMENTARY NOTES

14. ABSTRACT

The purpose of this research is to advance hemostasis technology, and to develop effective hemostatic devices for two difficult types of hemorrhage: (1) traumatic noncompressible (also known as truncal) hemorrhage; and (2) traumatic hemorrhage in the cold coagulopathic subject. The scope of this research will include both military and civilian trauma victims, particularly those suffering from hemorrhagic truncal injury and/or coagulopathic hemorrhage, from both penetrating and blunt mechanism. During the first year of this project, we successfully generated stocks of two vitally important clotting factors (fibrinogen and Factor XIII), which we will need for the development and manufacture of our hemostatic devices. In addition, we developed prototypical methods to deliver foaming technology for the treatment of noncompressible hemorrhage, and created iterations of resorbable synthetic gauze for use as hemostatic bandages. We also generated preliminary preclinical data using both the noncompressible and the cold coagulopathic hemorrhage models (both in swine), and are positioned to perform extensive testing during the next year of the project.

15. SUBJECT TERMS
Trauma, hemorrhage, hemostasis, liver injury, biologics, clotting factors, biomaterial, bandage, wound

16. SECURITY CLASSIFICATION OF:			**17. LIMITATION OF ABSTRACT**	**18. NUMBER OF PAGES**	**19a. NAME OF RESPONSIBLE PERSON**
a. REPORT	**b. ABSTRACT**	**c. THIS PAGE**			USAMRMC
U	U	U	UU	126	**19b. TELEPHONE NUMBER** *(include area code)*

Table of Contents

	Pages
Introduction……..…..	**4**
Body……..	**5-15**
Key Research Accomplishments……..	**16**
Reportable Outcomes……	**17**
Conclusion……	**18**
References……	**19-20**
Figures……	**21-46**
Appendices……	**47-125**

INTRODUCTION

Project Title: Technologies for Hemostasis and Stabilization of the Acute Traumatic Wound

The subject of this research project is the treatment of hemorrhagic in two difficult clinical scenarios: (1) traumatic noncompressible (also known as truncal) hemorrhage; and (2) traumatic hemorrhage in the cold coagulopathic subject. The purpose of this research is to advance the technology of hemostasis, and to use preclinical large animal models to test hemostatic technologies on the two difficult types of hemorrhage named above. The scope of this research will include both military and civilian trauma victims, particularly those suffering from hemorrhagic truncal injury and/or coagulopathic hemorrhage, from both penetrating and blunt mechanism. In addition, the technologies under development in this research should be useful in nontrauma surgical procedures, both elective and emergency, in which solid organ, coagulopathic, and/or noncompressible hemorrhage might occur.

BODY

The description of the work performed during the past year will be organized according to the Tasks delineated in the project's Statement of work, which has been reproduced in the Appendix A1. For a timeline of Task execution, refer to the Gantt chart in Figure 1. For a list of acronyms used in this report, see Appendix A2.

Task 1. Purification/generation of pd-FI and rFXIIIA

Overview. Essential to the goals of the proposed research is the stable and economical supply of fibrinogen of equal or greater quality to commercially made fibrinogen. To meet that need, we have developed a scalable process which incorporates lipid coat virus inactivation using solvent detergent. This process produces a fibrinogen product at equivalent or greater yield, purity and activity (Table 1) to that of commercially-made fibrinogen (Figure 2) while having the important viral inactivation treatment advantage of being solvent-detergent treated. Commercially available fibrinogens made in the US market use heat pasteurization, and do not use solvent detergent inactivation (*1*). Solvent detergent is the most effective treatment for lipid coat virus inactivation, but frequently adversely affects fibrinogen activity. We have circumvented that disadvantage with our ethanol precipitation process, and by using activated recombinant FXIIIA (rFXIIIA2-a) in the formulation of our liquid fibrin sealant (LFS). When the FI produced by our ethanol fractionation process is used in our LFS formulation, it produces kinetically fast forming and strong fibrin clots (Figure 3).

Table 1. Typical yields for ethanol fractionation and ammonium sulfate processes.

	Ethanol Precipitation	Ammonium Sulfate Precipitation
Starting plasma volume (L)	13	13
Purity (%)	95	90
Yield (g)	17	16.7
Maximum clot strength (dyn/cm^2)	3278.9 ± 829.6	5811.7 ± 139.4
Fibronectin (%)	3.9	8.1
DEAE fractionation	N/A	8% yield; 1:1 FI/FN

DEAE = diethylaminoethanol

Fibrinogen:fibronectin complex. To meet the additional potential need of decreasing the fibrinogen used in liquid fibrin sealant devices (i.e., sprays, bandages and foams) while retaining components which improve healing characteristics, we have developed an alternative fibrinogen purification process which isolates a broadly temperature stabile, 1:1 stoichiometric, fibrinogen:fibronectin (FI:FN) complex. A similar species heretofore was reported to be isolated in abnormal plasmas but, to our knowledge, it has not been reported to have been isolated from normal human plasma pool (nhpp) (*2*). Fibronectin clearly is present in many commercially available LFS (*3*, *4*). The past reports that studied the interactions formed between FI and FN have not identified, however, a broadly temperature stable FI:FN complex (*5*). This is likely reflected by the variability in FI and FN content of commercial grade preparations of FI, which may disrupt the complex and which were used in the studies. Indeed, our process enables this complex to be preserved and isolated relative to most classical processes, which either disrupt the complex and/or do not directly isolate it from nhpp (Figure 4.). Using the more gentle conditions provided by ammonium sulfate fractionation to fully capture and preserve the complex as it exists in starting nhpp, we were able to isolate 8-10% of the total FI existing within nhpp as this complex with >98% purity. Importantly, this purified FI: FN complex produces a

more rapidly forming and stronger clot at the same total protein concentration than pure FI (Figure 3). This is the first report of the thromboelastographic properties of an FI:FN complex.

γ′/γ Subvariant. Surprisingly, we also observed that the complex appears to consist entirely of FI containing the naturally occurring γ′/γ subvariant. The yield is consistent with essentially all of the γ′/γ population of plasma FI being involved with FN complex formation. The γ′ chain of variant of FI has been shown to interact with Factor XIII (*6, 7*). It also has been correlated with protective effect in the risk of venous thrombosis and an increased risk of arterial thrombosis in the general patient population (*8*). It is well known that FN plays a central role in wound healing, as FN in the extracellular matrix is a strong chemotactic agent and supports cell proliferation (*9-11*). In addition to its healing benefits, the presence of FN can reduce the amount of FI needed to achieve an equivalent clot by >50% over that obtained with LFS containing pure FI.

Fibrinogen produced. We have produced 80 grams of pure FI using an ethanol fractionation process and >2 grams of FI:FN complex using an ammonium sulfate process (Table 2). This amount of FI is sufficient to supply LFS to the dual foam development for the next 6 months. The FI:FN produced thus far can enable probative experiments with LFS. We intend to use several applications utilizing the FI:FN complex on liver injury models.

Table 2. Proteins supplied to the project for the last year.

Protein	Material Supplied
Recombinant Factor XIIIa	1,000,000 U
Recombinant fibrinogen	2.5 g
Plasma-derived fibrinogen	80 g

Factor XIII generation. Liquid fibrin sealants are formed from the concerted action of thrombin (FIIa) and activation of tetrameric, zymogen factor XIII on fibrinogen which results in the formation of crosslinked fibrin polymer. We have developed a process for producing recombinant, activated factor XIIIA (rFXIIIA2-a) in *Pichia pastoris.* This contrasts the zymogen recombinant factor XIIIA catalytic unit (rFXIIIA2) made in *Saccharomyces cerevisiae* currently in commercial development by Novo Nordisk (*12*). Our recombinant rFXIIIA2-a specifically ameliorates both (i) the kinetic lag in crosslinking when activating tetrameric, zymogen factor XIII and (ii) the diffusional limitation of factor XIII activity, which arise from the rapid increase in viscosity that accompanies the acceleration of fibrin formation with high thrombin levels.

Factor XIII produced. The rFXIIIA2-a made using our process is highly pure (Figure 5). It also is highly stable at 4˚C for >2 years when using our liquid formulation. We have produced and supplied the project with 1M units of rFXIIIA2-a for use in LFS foam development and for current LFS bandage surgical efforts (Table 2). We also have begun incorporating a chromophore-based activity assay to complement our TEG base analysis of rFXIIIA2-a activity for purposes of quality control documentation. This assay was provided to us by Dr. Helen Philippou of Leeds University, UK.

Task 2. Generation of ultrafine particles for tamponade carrier foam

Preparation of polymer ultrafine particles for foam stabilization was performed. It was found that particle shape depends on the solvent used for EHD processing. Conditions were determined in order to fabricate elongated particles with aspect ratio greater than 1. The results of production of two particle types with different aspect ratios are shown in Figure 6. These materials are being produced in quantities suitable for testing the degree of stabilization of the foam formulations in Task 3.

Task 3. Testing of candidate tamponade carrier & FS foams

Preliminary foam studies. A series of surfactants, emulsifiers and thickening agents were studied to determine their optimal concentrations for foam stability. These components were: Tween® 20, Laureth-23, triethanolamine (TEA), sorbitol, hydroxypropylcellulose (HPC) and xanthan gum. Foaming tests were performed by discharging the liquid formulation as foam, using a foaming nozzle, and filling identical graduated beakers. The volume of foam and drained liquid were measured over time. Tests were performed in triplicate. The plot shown in Figure 7 shows the foam stability over time generated by a series of component combinations.

One formulation produced a foam that was stable (up to 87% of the initial volume) for ~60 minutes. The composition of this formulation was: Tween® 20 = 2%; Laureth-23 = 15%; TEA = 0.5%; HPC = 0.5%; Xanthan gum = 0.1%. Triplicate tests of this formulation were repeated in order to confirm the results. Further research will determine whether the addition of polymer particles can improve foam stability; in addition, foaming device/nozzle hardware will be developed.

Hydrophilicity of polymeric mesh and foam filler particles. One of the desired properties in a mesh to be used as a hemostatic bandage or in foam filler particles is rapid blood adsorption, a process which is governed by polymer surface hydrophilicity. Since our focus remains on FDA-approved implantable polymers and additives for our devices, all nano- and micro-structures have been constructed from polylactic acid (PLA). The same chemistry principles that impart hydrophilicity apply to both foam filler particles and bandage materials; we investigated hydrophilicity enhancement of the latter. Although our native ultrafine polymer mesh displayed zero hydrophilicity, we found that this can be improved by using very small amounts of FDA-friendly surfactants. Up until recently, we had been using aqueous polysorbate solutions at relatively high concentrations to deposit the surfactant (polysorbate) onto the surface of the mesh fibers. An improvement to this process that was developed this year was the replacement of the thick, dense polysorbate coating solutions with sodium cholate formulations, leading to the use of much lower surfactant concentration, and yielding faster liquid absorption. This change in surfactant utilization not only makes the process more economic, but also decreases the use of non-procoagulant additives.

Task 4. Testing of single foams in rabbits (tamponade carrier & FS foams separately)

This Task currently is delayed. During the first year the rabbit noncompressible hemorrhage model (*13*) was attempted in seven subjects. The investigators then had some correspondence with the Scientific Officers of this project in August of 2012 (see emails in Appendix A3), and it was decided to stop using the rabbit model and convert all the planned investigation that was to use rabbit subjects into investigation that would use swine subjects. The rationale for this change was that the swine were less expensive to use than rabbits, while arguably having more clinical relevance (secondary to its larger size). At this point in time, the necessary changes to the animal protocol are being reviewed by the Omaha VA IACUC. After the local IACUC has reviewed and approved the changes to the animal protocol, the protocol will be sent to ACURO for their review and approval. After the ACURO approval has been obtained, the investigation of Task 4 will resume. The results obtained with the seven rabbit subjects mentioned above were reported in previous Quarterly Reports and will not be reiterated here, because the rabbit data no longer are relevant to this project.

Task 5. Development & engineering of dual foam candidate devices

Our research and development effort for the last year on dual foam fibrin sealant (FS) hemostatic devices has focused upon the optimization of hydrodynamic effects upon LFS mixing and carrier foam coverage. These are two key variables in the design effort to minimize LFS usage. We have used a viscoelastic LFS mimetic fluid to study these effects, and will transition to LFS when these studies begin early in the next funding year. The mimetic LFS consists of two differently dyed (red and blue) input

steams containing a viscosity modifier (Figure 8). Mixing of the LFS component input streams first is tested with no carrier foam flow, since the two streams do not form a contact interface until near the exit of the applicator nozzle. When fully mixed, the FS mimetic appears as a purple foam upon exit from the nozzle (Figure 9). The blue and red streams (facsimiles for fibrinogen/rFXIIIA2-a and thrombin inputs) are injected by air pressure into a foaming frit mounted just prior to entrance of the outer annular space of the applicator nozzle. The nozzle has an outer annular diameter of 12.9 mm. The inner (carrier foam) annular space has a diameter of 7.5 mm, leaving an annular radial space of 1.75 mm. The foaming frit can be removed for hydrodynamic studies in which the LFS is not foamed. The results of engineering studies presented below are using the LFS mimetic in a foaming mode for the LFS fluid.

1. We elucidated a mixing regime to control and obtain complete mixing of thrombin with plasma-derived fibrinogen/recombinant factor XIII input streams prior to exiting the outer annular space of the foam generator nozzle. In all cases used here, the LFS mimetic is fully mixed by the frit as indicated by the uniform purple color of the outer FS mimetic layer (Figure 9). The next step is to evaluate coverage of the carrier foam by the fully mixed LFS mimetic.

2. We studied a flow regime which provides the carrier foam at a flow rate that is predicted to be sufficiently rapid for a delivery of 4 L of dual foam to a closed abdominal cavity wound in a range of 1.3-8 min. We estimate that an 80 kg body weight adult has up to 4 L of intraabdominal (intraperitoneal) void volume. This translates to carrier foam flow rates of 0.5 and 3 L/min. Ultimately, the outer LFS flow rate will not contribute significantly to the total dual foam flow rate. The role of the carrier foam is two-fold: the carrier foam delivery of the LFS to a maximal amount of intra-abdominal surface, while exerting a transient and mild pressure force (tamponade effect) to the surface. The pressure flow behavior of the viscoelastic FS foam mimetic is shown for a carrier foam flow rate of 3 L/min and also for a carrier foam flow rate of 0.5 L/min (Figure 10).

3. In order to minimize the amount of LFS needed to achieve a cost effective hemostatic device product, we directed our efforts at ascertaining the amount of FS foam necessary for complete carrier foam coverage at a given carrier foam flow rate (Figure 11). Therefore, the first goal of our engineering studies has been to control the coating of the carrier film by FS foam by understanding the hydrodynamic properties of pressure versus flow rate of the viscoelastic LFS mimetic liquid input stream. It is important to note that the early flow pattern of an actual FS foam at a lower extent of fibrinogen polymerization would be characterized as a non-Newtonian fluid within the applicator nozzle. As the FS foam polymerizes, the rising viscosity inhibits mixing of the LFS liquid that exists within the interfacial (bubble) structure, making it difficult to react further in an efficient manner. This rising viscosity also limits the efficient coating of the carrier foam as the FS and carrier foams meet and form an interface at the nozzle exit. Ideally, once the dual foam has exited the nozzle, the carrier foam should drag the FS foam along. While the extent of polymerization will be manipulated in future work with actual LFS inputs, the viscous nature of the FS foam will both facilitate its delivery by the carrier foam to abdominal surfaces without inefficient LFS pooling, and also prevent its separation from the carrier foam. Complete coverage of the carrier foam was thinnest (Figure 12) with the lowest carrier flow rate of 0.5 L/min, while at a 0.25-0.5 mL/min of LFS mimetic liquid input.

4. The amount of LFS will be minimized by understanding the changes in hemostatic behavior that are affected by using a low density (therefore lowest possible content LFS), outer foam FS foam layer, in comparison to a non-foamed LFS that forms an extremely thin, polymerized film. Our previous studies demonstrated that a hemostatic layer using our nonfoamed, optimized LFS can be as little as 100 μm thick (see submitted manuscript to *Biomacromolecules* in Appendix A4). Thus, our prototype dual foam generator has been designed to be able to make an outer foam

layer or to easily adjust to injecting rapidly polymerizing LFS without foaming. During the next year, we will use pd-FI in our optimized LFS as a foamed and nonfoamed outer layer.

Task 6. Testing of dual foam in rabbits

This Task currently is delayed. All investigation involving rabbit subjects will be converted into investigation utilizing swine subjects; see explanation under Task 4.

Task 7. Engineering scale-up of optimized candidate particles

This task has yet to start.

Task 8. Testing of dual foam in swine noncompressible model (laparotomy with 2˚ closure)

This task has yet to start. Although the dual foam device for this Task is not yet available for use, we undertook some preliminary investigation with the swine noncompressible hemorrhage model. Currently there is no published version of such a model which uses a laparotomy followed by temporary closure after the injury. Dr. Bochicchio, a Co-Investigator on this project, does have preliminary data on a closed noncompressible hemorrhage model that employs laparoscopy, which will be utilized in Task 10. Since a description of an open model of noncompressible hemorrhage in swine was not available, we proceeded to develop such a model.

The initial strategy in the development of this open noncompressible hemorrhage model was to use the central liver injury model in a swine subject without hemodilution or hypothermia. The rational for this approach was that in the field, a warfighter who had suffered penetrating truncal trauma would not have pre-existing hypothermia and hypofibrinogenemia. A hypothetical treatment for life-threatening noncompressible hemorrhage would be best administered in the field, prior to establishment of hypothermia and/or hypofibrinogenemia. So we reasoned it would be best to develop this model in normothermic, normovolemic subjects.

Per the approved protocol, a central liver injury (*14*) was performed in five normothermic, normovolemic, splenectomized swine through a midline incision; no treatment was administered, other than clipping the midline incision shut and giving warm LR resuscitation (limited to 100 mL/kg). A 60 min observation period was chosen, because the outcome of interest was death from acute exsanguination, not death from prolonged shock. The outcome data is summarized in Table 3. Interestingly, all five swine survived the 60 min observation period with relative ease; three of them lost less than 1 L of blood. The final MAP fell to ~60 mm Hg, and the final Hb averaged ~8 g/dL. There was no discernable effect on the protime, but the mean fibrinogen level decreased to ~50% of the starting value. The median number of large hepatic veins transected in these five subjects was three. Photographs from one of these subjects are shown in Figures 13-19.

The severity of the central liver can be appreciated in Figure 18. Multiple large hepatic veins typically are shredded (Figure 16) by the liver injury clamp, which has tines in an X-configuration (Figure 20). Neither the portal vein (Figure 17) nor the vena cava (Figure 19) is injured when the tines are positioned superiorly over the dome of the liver, anterior to the IVC. Given the severity of this injury, it was somewhat surprising that all five animals survived the 60 min observation period, some with only minor physiologic disturbance. Close inspection of the subjects revealed the probable mechanism for this survival: an injury in this location (i.e., the liver dome) in swine becomes sealed against the diaphragm, which effectively tamponades the bleeding (as long as the subject has a reasonably intact clotting system). Specifically, all subjects had a tenacious clot which had sealed the dome of the liver to the diaphragm (Figures 14-15), which was appreciated upon re-opening the abdomen after the 60 min observation period. In light of this anatomical arrangement and the swine's relative hypercoagulable state (discussed under Task 14), the survival results may seem a little less surprising.

Table 3. Outcome data on five normothermic normovolemic swine subjects with untreated central liver injury.

No.	Pre-injury MAP (mm Hg)	15 min MAP (mm Hg)	60 min MAP (mm Hg)	Blood loss (mL)	Survival	Pre-injury Hb (g/dL)	15 min Hb (g/dL)	60 min Hb (g/dL)	Pre-injury PT (s)	15 min PT (s)	60 min PT (s)	Pre-injury FI (mg/dL)	15 min FI (mg/dL)	60 min FI (mg/dL)	#HV cut	#strikes
92	120	61	101	604	Y	12.0	9.7	10.4	12.2	11.6	12.1	104	63	60	1	2
93	95	78	63	688	Y	12.0	9.8	9.9	11.5	11.0	11.5	113	70	63	3	2
94	113	42	31	2362	Y	13.2	6.1	4.3	11.7	na	15.1	117	na	37	3	3
95	119	30	51	1537	Y	12.4	5.7	5.7	11.4	13.3	12.3	138	51	59	3	3
96	115	97	78	802	Y	13.0	9.7	10.7	12.7	12.2	11.8	74	45	47	4	3
mean	112.4	61.6	64.8	1198.6		12.5	8.2	8.2	11.9	12.0	12.6	109	57	53	2.8	2.6
sd	10.1	26.9	26.6	748.3		0.6	2.1	3.0	0.5	1.0	1.5	23	11	11	1.1	0.5
median	115	61	63	802		12.4	9.7	9.9	11.7	11.9	12.1	113	57	59	3	3

Swine subjects were 3 months old, male, weighing 33.9 ± 2.5 kg (range 30.6-37.4 kg). Immediately after central liver injury, the midline incision was closed with towel clips. Each subject was resuscitated with IV Lactated Ringers solution (37˚C) at 150 mL/min, with a resuscitation target = 90% of pre-injury MAP, and with the maximum resuscitation volume set at 100 mL/kg.

FI = quantitative fibrinogen assay (after von Clauss); PT = protime; #HV cut = number of hepatic veins lacerated by the injury; #strikes = number of strikes (i.e., hits, applications) of liver injury clamp to the region of the liver directly anterior to the inferior vena cava. Times given are post-injury.

Since the injury described above appears to be self-sealing against the diaphragm, this injury cannot really be used for a "noncompressible" hemorrhage model. A different injury mechanism is needed, in which tamponade of the bleeding against an adjacent structure (like the diaphragm) is less likely, particularly when the subject's endogenous clotting potential is strong. Alternative injury mechanisms may involve a similar injury in the background of hypothermia and hemodilution (though this would go against the warfighter rationale discussed above), or placement of the injury in a different location where tamponade would be more difficult. An example of the latter might be a portal vein injury in the infrahepatic space. A reasonable goal for such a model would be a no-treatment control group which has a greater than 50% mortality after 60 min, a terminal or near-terminal drop in MAP in all subjects, and an average blood loss of 2-3 L. Development of this porcine noncompressible hemorrhage model in anticipation of the foam testing for Tasks 4, 6, and 8 will continue.

Task 9. Delivery of candidate field-ready dual foam device

This task has yet to start.

Task 10. Testing of dual foam in swine noncompressible model (closed penetrating wound)

This task has yet to start.

Task 11. Delivery of report on final recommended product description for dual foam device for treatment of noncompressible hemorrhage

This task has yet to start.

Task 12. Delivery of resorbable bandage for final preclinical study in hypothermic coagulopathic model

Overview. During an April 2012 meeting that the investigators of this project had with the project's Scientific Officers at the ISR in San Antonio, recommendations were made by ISR's Dr. Bijan Kheirabadi to the LNK representative in attendance (Dr. Gustavo Larsen) to specifically gear resorbable gauze designs toward production of materials that biodegrade at intermediate rates. For wound stabilization, the existing resorbable gauzes either degrade too fast (within hours, when the blood clot still needs mechanical stability), to many days or weeks (when interference with the natural would healing process becomes important). Research thus aimed at formulating a resorbable mesh that degrades in a 1-2 day timeframe was initiated. Since both fiber diameter and polymer type are key parameters determining mesh degradation rate, both are being considered. As arguably one of the slowest FDA-approved implantable polymer is polycaprolactone (PCL), it was initially hypothesized that by blending it with PLA, an optimum between polymer composition and fiber strand diameter could be found to provide excellent short-term mechanical stability and degradation in a few short days. Results are summarized below.

Production of microfibrous, macroporous mesh. The team has determined that for large, open and irregular wounds structures, any non-foam approach will require more open and "fluffier" structures (akin to cotton gauze) than our original nanomesh used to model elective surgery situations. Concentrated solutions of PLA and PCL in a wide range of molecular weights, concentrations and solvents have been and continue to be studied for the production of thicker fibers (microfibers) by electrohydrodynamic (EHD) processing techniques that require higher flow rates and lower voltages than what is used for production of nanomesh samples. The method actually is a hybrid between EHD and dry fiber spinning. We also will target resorbable polymer formulations that are expected to degrade between 1 and 2 days, which is faster than polyglactin 910 mesh (Vicryl®; Ethicon®), and but slower than oxidized cellulose

(Surgicel®; Ethicon®). The goal with this mesh production is to provide adequate mechanical stabilization of the wound, while minimizing influence on the healing process.

PLA and PCL meshes with "tunable" openings are being produced by the above hybrid method which combines dry fiber spinning with EHD technology. The macropores of the microfibrous mesh can be controlled during processing. Figure 21 shows macroscopic views of these mesh products. PCL mesh with optimal mechanical strength was produced by processing PCL (45 kDa) in dichloromethane (SEM shown in Figure 22). The average fiber diameter was ~25 μm (Figure 23).

We also determined that a mixture of a high molecular weight PLA (240 kDa) and a low molecular weight PLA (70 kDa) was needed to obtain material with adequate mechanical properties. Humidity also was a factor in the collection of fibers with the new method; a fluffier material was collected at higher humidity, regardless of the polymer type being processed. These structures, which were naturally hydrophobic, could be sprayed with dilute surfactant when hydrophilicity was required.

As a test of hydrophilicity, mesh samples were tested for blood absorption. The PCL mesh had a more rigid structure (though still pliable) than the PLA mesh, which resulted in less mesh shrinkage when saturated with blood. In an attempt to combine the rigidity of PCL with the faster biodegradability of PLA, a PCL/PLA composite mesh also was investigated. Two 5 x 5 cm portions of hydrophobic and hydrophilic meshes were placed simultaneously in with fresh untreated swine blood. Blood absorption into the hydrophilic PLA and PCL mesh occurred in 21 and 5 sec, respectively; the hydrophobic mesh samples did not absorb any blood after 5 min (Figure 24). The hydrophilic meshes (200 mg of PLA and 900 mg of PCL, both 20 x10 cm) also were inspected after a 1 h *in vivo* incubation (i.e., treatment of a swine hepatic injury; see Task 14). After this 1 h period, the PCL mesh still retained its initial structure, while PLA did not (Figure 25).

Ongoing work is being focused on generating a resorbable mesh that degrades in 1-2 days. Both fiber diameter and polymer type are being considered, since both are key parameters determining mesh degradation rate. Since one of the slowest FDA-approved implantable polymers is PCL, it initially was hypothesized that a blend of PCL and PLA with an optimal fiber strand diameter could provide excellent short-term mechanical stability, with degradation in several days. *In vitro* tests were performed on three different mesh materials, in duplicates. The composition of each mesh is shown in Table 4. Samples were cut into rectangular shapes (2 x 3 cm), placed on tissue culture plates and immersed in simulated body fluid (SBF) (*15*). Samples were kept in an incubator at 37˚C, with 5% CO_2. The SBF was exchanged every 7 days. Samples were then removed after 2, 3, 7, 14 and 21 days, rinsed three times with deionized water, and dried under vacuum overnight. Each sample was weighted and compared with its initial weight. Degradation results are shown in Figure 26.

Table 4. Composition of resorbable synthetic bandages.

Bandage type	Component	% by weight
1. Pure PLA	PLA 70 kDa	90.13
	PLA 250 kDa	9.87
2. Pure PCL	PCL 45 kDa	100.00
3. PCL/PLA blend	PCL 45 kDa	33.33
	PLA 70 kDa	60.00
	PLA 250 kDa	6.67

From the results shown in Figures 25-26, it is apparent that both texture and polymer(monomer) release from the synthetic mesh can be controlled. The target will remain retention of the mechanical quality of the bandage for ~1 day, but with degradation after several days. The LNK team expects to narrow down the selection of polymer type and fiber diameter further during the next quarter in order to achieve the degradation target without sacrificing initial mechanical sturdiness.

Task 13. Delivery of fibrin sealant for final preclinical study in hypothermic coagulopathic model

We have assessed the quality of our plasma derived FI products using thromboelastography (Figure 3). This is the primary tool used to assure that all LFS formulations meet specifications for a fast acting LFS that forms an acceptably strong fibrin polymer upon application by spray to bandages, directly onto wounded tissue or for use in the development of the project's dual foam LFS technology. We expect that we will be able to generate LFS for the remainder of the project on the scale described in Table 2.

Task 14. Final preclinical study of resorbable bandage in for hypothermic coagulopathic model (swine)

The swine model used for Task 14 has been well-described by other investigators (*14, 16-18*), and we have successfully reiterated this model in our laboratory. The injury is similar to the one described above in Task 8, in which a central liver injury (Figure 18) is created with an injury clamp (Figure tf28) in a splenectomized subject, except that the subject undergoes hemodilution (60% blood volume exchange with hetastarch) and is made hypothermic (down to ~32˚C) prior to injury. The standard experimental set-up includes a carotid arterial line (for blood pressure monitoring and laboratory tests), a jugular venous line (for rapid IV fluid administration via a roller pump), a femoral arterial line (for large-volume phlebotomy during the hemodilution procedure), a transabdominal cystotomy, EKG leads, and an ETCO2 monitor. Vital signs are continuously monitored with a Bionet BM5 monitor (see Appendix A5); a sample of laboratory values which are obtained on each subject are shown in Appendix A6. TEG also is performed at the time points shown in Appendix A6 (see below discussion). A detailed data sheet is maintained for each subject (sample shown in Appendix A7). In addition, each procedure is recorded on digital video using a camera that is suspended from the operating room light directly over the incision. All of the above information was collected on every swine in this project to date (i.e., from Tasks 8 and 14).

Some of the responsibilities of the UNL team has been to assess the time course of coagulation for the swine subjects used in swine hemorrhage models. By doing so, the hemostatic response to an LFS bandage or dual foam application can be put into perspective, which aids the iterative development of these devices. In general, the swine subjects (N = 68; some of the data collected prior to initiation of the present award) possessed an initial coagulation profile typical of a hypercoagulable state relative to humans (Figure 27). During progression to exsanguination or in the hypothermic/hemodiluted state, all subjects exhibited a decrease in coagulation potential (Figure 28). The baseline relative hypercoagulable state in swine might explain in part their ability to survive the injuries described under Task 8.

In our initial attempts with the hypothermic hemodilutional liver injury model, we noted that the negative control swine subjects (injured but treated with cotton gauze only) were not dying, and were not experiencing the degree of blood loss seen by other investigators experienced with this model (the results of these initial swine subjects were described in earlier Quarterly Reports, and will not be reiterated here). In order to address this discrepancy, we met with the project's Scientific Officers at the ISR (San Antonio) in April, 2012. The outcome of these discussions was that (1) a post-injury 30 sec free-bleeding period would be instituted prior to the application of any treatment, (2) the post-injury observation time would be increased to 120 min, and (3) warm Hextend™ (6% hetastarch in LR) would be used for resuscitation in the post-injury phase. These changes to the animal protocol were approved by the local animal committee and then by ACURO. After the changes were approved, five swine underwent the hypothermic coagulopathic central liver injury using the above changes, with a control treatment of cotton gauze only. The mortality was 100% (none survived longer than 30 min after injury), with a mean blood loss >4 L; see data summarized in Table 5. None of the subjects reached their target MAP, and all received the maximum allowed Hextend™ resuscitation (3 L). This was the expected outcome for the negative control (cotton gauze treatment only) in this model.

With the negative control results conforming to previously-published standards, we began the testing of our resorbable synthetic bandage with and without LFS supplementation. In brief, the initial bandage iterations we tried were not hemostatic in this model. Preliminary data that we obtained in

investigations prior to this award demonstrated that the bandages were hemostatic for major hepatic injury in normothermic, normovolemic swine, but this result did not translate to the hypothermic, hemodiluted subject. The primary problem with the latter subjects is that the synthetic bandage did not adhere to the wound surface, even when pre-wetted with LFS (up to 100 mg total FI).

Table 5. Vital sign, laboratory, and other data from swine (N =5) undergoing central liver injury with the hypothermic/hemodilutional protocol.

Timed data

	Time point			
Value	Initial	Pre-injury	15 min post-injury	At death
MAP (mm Hg)	107 ± 9	67 ± 9	46 ± 9	—
Temp (˚C)	38.5 ± 1.0	32.5 ± 0.5	32.3 ± 0.4	—
Hb (g/dL)	10.7 ± 0.5	4.0 ± 0.6	1.5 ± 0.8	0.4 ± 0.2
PT (s)	11.4 ± 0.5	16.9 ± 1.7	fail*	fail
Fibrinogen (mg/dL)	120 ± 22	37 ± 5	fail	fail

Other data

Pre-procedure weight (kg)	34.8 ± 4.5 (29.6 – 40.8)
#Hepatic veins cut (median)	2
Duration of survival post-injury (min)	33 ± 12 (25 – 53)
Blood loss, free-bleed period (mL)	354 ± 69 (292 – 451)
Blood loss, post-treatment phase (mL)	4364 ± 469 (3858 – 4994)

*fail = assay failed because of severe clotting disturbance. Values are given as mean ± sd, unless indicated. Ranges are given in parentheses.

A typical result which demonstrates the failure of the initial bandage configurations is shown in Figure 29. After the injury is created, a 30 second free-bleeding period ensues, in which the subject loses 300-400 mL of blood (Table 5). After the free-bleed period, the synthetic bandage material (wetted with LFS immediately prior to application) is inserted into the cavitary liver wound, followed by three cotton laparotomy pads placed over the top of the synthetic bandage. The abdomen is closed rapidly with towel clips, and resuscitation with 37˚C Hextend™ is begun, with a target resuscitation MAP equal to 90% of the pre-injury MAP, and with a maximum resuscitation volume of 3 L of Hextend™ (i.e., the same protocol used with the cotton gauze negative controls). All subjects (N = 4) treated with various iterations of the synthetic gauze + LFS died from exsanguination in <1 h. None of the bandages adhered to the liver injury site. The bandage material typically formed a cast of the cavity wound (Figure 29), but the bandage mass slipped out of the wound immediately at the postmortem examination, with no evidence of clotting or adhesion to the liver parenchyma.

The suboptimal performance of the synthetic gauze + LFS in treating central liver injury in the cold coagulopathic subject was somewhat surprising, as this same treatment combination was highly effective in treating severe hepatic injuries in swine with normal coagulation (demonstrated in studies done prior to the present award; refer to Appendix A11). In the subjects with normal clotting, the synthetic bandage adhered tenaciously to the wounded liver parenchyma, consistently stopping both venous and arterial hemorrhage. The decrease in hemostatic performance of the LFS-supplemented gauze in the cold coagulopathic subject is another demonstration of how difficult it is to achieve hemostasis in this model. On the other hand, this same difficulty should make any positive result with this model quite powerful.

The plan at this point for Task 14 is to improve the adhesion of the synthetic bandage to the injured liver surface in a cold coagulopathic subject. In order to do this, we will submit a proposal to the project's Scientific Officers to perform some additional swine experiments that will focus on the adhesion

phenomenon between the bandage and the wound surface in the cold coagulopathic background. We will propose to do these additional experiments as a no-cost addition to the project. If this no-cost addition is approved, then we will submit the necessary protocol changes to the animal committees.

Possible alternative to address the inadequate bandage adhesion in Task 14 might include the following: (1) changing the macro-, micro- and/or nanostructure of the synthetic mesh; (2) increasing or optimizing the amount of fibrinogen and/or other clotting factors in the bandage; (3) using a foaming agent to increase the tamponade effect of the synthetic material.

Task 15. Delivery of report on final recommended product description for resorbable fibrin sealant bandage for treatment of compressible coagulopathic hemorrhage

This task has yet to start.

KEY RESEARCH ACCOMPLISHMENTS

Below is a list of key research accomplishments from this past year's work:

1. A scalable purification process using ethanol fractionation to produce FI that uniquely includes solvent detergent viral inactivation. This contrasts viral inactivation by heat pasteurization that is used by current US manufacturers. The quality and yield of FI is equivalent to current industrial processes.

2. The discovery of a unique 1:1 stoichiometric FI:FN complex in nhpp consisting exclusively of the FI subvariant population containing the γ′/γ heterodimeric chains. This species possesses more rapid clotting kinetics and greater clot strength then our pure FI in our optimized LFS. The complex binds up to 10% of the FI in nhpp.

3. A scalable process using ammonium sulfate precipitation that quantitatively captures and preserves the FI:FN complex from nhpp.

4. A prototypical dual foam generator-applicator device was made and tested. This device facilitates both the control of the outer FS film thickness and carrier foam coverage. These studies will enable us to ascertain the minimal amount of FS foam needed to achieve hemostasis when those studies begin in swine surgical models in the second year of funding.

5. Generation of purified fibrinogen from USARMY donated plasma.

6. Generation of purified recombinant activated Factor XIII (*rFXIIIA2-a*) made from yeast fermentation using *Pichia pastoris.*

7. Generation of optimized, formulated, quality-controlled fibrin sealant for use in swine models of traumatic hemorrhage.

8. Replication and validation of the porcine cold coagulopathic central liver injury model, with initial testing of bandage/LFS devices therein.

9. Thromboelastographic analysis of the coagulation time course for the swine models of traumatic hemorrhage.

10. Initial studies on an open (laparotomy) model of noncompressible hemorrhage in swine.

11. Drs. Carlson (UNMC) and Nuñez (LNK) have been provided a letter of program approval (see Appendix A8) by the State of Nebraska for a separate but related project entitled "Hemostatic Patch," which will study elective surgical applications for the synthetic resorbable mesh + LFS devices. This program will fund work at $100,000 for the first year, starting in late 2012, and has a "phase II" option of $400,000 at the end of the initial period.

REPORTABLE OUTCOMES

[From the template: "Provide a list of reportable outcomes that have resulted from this research to include: manuscripts, abstracts, presentations; patents and licenses applied for and/or issued; degrees obtained that are supported by this award; development of cell lines, tissue or serum repositories; informatics such as databases and animal models, etc.; funding applied for based on work supported by this award; employment or research opportunities applied for and/or received based on experience/training supported by this award."]

List of reportable outcomes:

1. Manuscript submitted/under review at *Biomacromolecules* (title: "A recombinant human fibrinogen that produces thick fibrin fibers with increased wound adhesion and clot density"); see Appendix A4. This represents work done prior to this award.

2. Meeting abstract on recombinant LFS *vs.* Tisseel™ (J Surg Res 2011;165:317); see Appendix A9. This represents work done prior to this award.

3. Portions of the investigators' work were reported at an invited talk to the Instituto Vital Brazil, Rio de Janiero, Brazil, January 9th, 2012 in a talk on "Transgenic Production of Blood Proteins for Treating Hemorrhage", and also the 21st International Congress on Fibrinolysis and Proteolysis in Brighton England on July 1-5 2012 in a talk on "Hemostasis, Adhesion and Clot Stability characteristics of Human Fibrinogen Produced in the Milk of Transgenic Cows" (see abstract in Appendix A10).

4. A poster presentation "Development of Novel Hemostatic Devices in Swine Hemorrhage Models" was given at the 2011 Clinical Congress of the American College of Surgeons; see Appendix A11. This represents work done prior to this award.

5. A manuscript entitled "A totally recombinant human fibrin sealant containing fibrinogen, thrombin, and Factor XIII" is in preparation; a preliminary draft is attached in Appendix A12. This represents work done prior to this award.

6. A manuscript entitled "A room and low temperature stable fibrinogen heterodimeric γ′/γ:fibronectin complex with improved clot formation" is in preparation, and will tentatively to be submitted to *Vox Sang*.

CONCLUSIONS

This overall goal of this project is to develop hemostatic technology for two severe clinical scenarios: (1) noncompressible (truncal) hemorrhage, which is the topic of Aim 1 of the original proposal; and (2) solid organ hemorrhage in a cold coagulopathic subject, which is the topic of Aim 2. Conclusions drawn from the work during the first year of this project are as follows:

1. Our hydrodynamic studies of dual foam technology show that a device with tunable FS coverage and film thickness can be melded to a carrier foam flow rate that is commensurate with the predicted needs of an economical hemostatic device for treatment of closed cavity abdominal wounds. Our discovery and isolation of a unique FI:FN complex using a scalable purification process that has improved *in vitro* clotting kinetics and clot strength over that of LFS formulations using FI alone, merits future *in vivo* study.

2. The hypothermic hemodilutional model with central liver injury has been successfully reproduced in our animal laboratory. As expected, the control group treated with cotton gauze only suffered 100% mortality in less than one hour after injury.

3. Initial iterations of the resorbable synthetic bandage wet with LFS (up to 100 mg total fibrinogen) were not hemostatic in treating the central injury in the cold coagulopathic background. Previous work in our laboratory had shown that this type of bandage was highly effective in treating severe hepatic injuries in swine with normal coagulation. Work during the next year will focus on engineering the bandage to improve its wound adhesion properties. In addition, we will propose additional (no-cost) studies that will examine the bandage-wound interface in the cold coagulopathic subject.

4. Initial attempts using the approved version of the open noncompressible hemorrhage model were not able to demonstrate an adequate amount of blood loss or lethality. This result suggests that the model as is (central liver injury in a swine subject with normal clotting) may not be “severe” enough to study noncompressible truncal hemorrhage. A reasonable negative (no treatment) control with this model would produce death from exsanguination within 30-60 min of injury, including 2-3 L of blood loss. More rapid exsanguination/earlier death probably would make it too difficult to see treatment effect (i.e., increase the false negative rate); on the other hand, a slower rate of blood loss (as we had with our initial efforts) would likely exaggerate treatment effect (i.e., increase the false positive rate). Variations of the open noncompressible hemorrhage model will be considered in anticipation of needing it for the studies of Task 8, which should get underway during year 2 of this project.

The relevance of studying hemostatic devices in the treatment of hemorrhage in the two scenarios described above is in this project is that both noncompressible and coagulopathic hemorrhage remain difficult clinical problems. Noncompressible truncal hemorrhage in particular is emerging as the leading cause of preventable hemorrhagic death in the injured warfighter (*19*), and coagulopathic hemorrhage remains a perennial problem (*20*) with imperfect solutions that is faced by surgeons during emergency and elective procedures, in both military and civilian environments.

REFERENCES

1. M. R. Jackson, Fibrin sealants in surgical practice: an overview. *The American journal of surgery* **182**, S1 (2001).

2. K. Nagamatsu, M. Komori, S. Kuroda, K. Tanaka, Dynamic light scattering studies on hydrodynamic properties of fibrinogen-fibronectin complex. *J Biomolec Struct Dynam* **9**, 807 (1992).

3. J. Chabbat, M. Tellier, P. Porte, M. Steinbuch, Properties of a new fibrin glue stable in liquid state. *Thromb Res* **76**, 525 (1994).

4. K. I. Schexneider, Fibrin sealants in surgical or traumatic hemorrhage. *Current opinion in hematology* **11**, 323 (Sep, 2004).

5. E. Makogonenko, G. Tsurupa, K. Ingham, L. Medved, Interaction of Fibrin(ogen) with Fibronectin: Further Characterization and Localization of the Fibronectin-Binding Site. *Biochemistry* **41**, 7907 (2002).

6. R. A. Ariens, T. S. Lai, J. W. Weisel, C. S. Greenberg, P. J. Grant, Role of factor XIII in fibrin clot formation and effects of genetic polymorphisms. *Blood* **100**, 743 (Aug 1, 2002).

7. M. W. Mosesson, Fibrinogen and fibrin structure and functions. *J Thromb Haemost* **3**, 1894 (2005).

8. S. Uitte de Willige, K. F. Standeven, H. Philippou, R. A. S. Ariens, The pleiotropic role of the fibrinogen gamma' chain in hemostasis. *Blood* **114**, 3994 (2009).

9. R. A. F. Clark, Fibrin glue for wound repair: facts and fancy. *Thromb Haemost* **90**, 1003 (2003).

10. D. L. Amrani, J. P. Diorio, Y. Delmotte, Wound healing: Role of commercial fibrin sealants. *Annals of the New York Academy of Sciences* **936**, 566 (2001).

11. M.-G. M. Lee, D. Jones, Applications of fibrin sealant in surgery. *Surg Innov* **12**, 203 (2005).

12. P. D. Bishop *et al.*, Expression, purification, and characterization of human factor XIII in Saccharomyces cerevisiae. *Biochemistry* **29**, 1861 (1990).

13. B. S. Kheirabadi *et al.*, High-pressure fibrin sealant foam: an effective hemostatic agent for treating severe parenchymal hemorrhage. *J Surg Res* **144**, 145 (Jan, 2008).

14. A. V. Delgado *et al.*, A novel biologic hemostatic dressing (fibrin patch) reduces blood loss and resuscitation volume and improves survival in hypothermic, coagulopathic Swine with grade V liver injury. *J Trauma* **64**, 75 (Jan, 2008).

15. M. R. C. Marques, R. Loebenberg, M. Almukainzi, Simulated biological fluids with possible application in dissolution testing. *Dissolution Technol* **18**, 15 (2011).

16. G. Bochicchio *et al.*, Use of a modified chitosan dressing in a hypothermic coagulopathic grade V liver injury model. *Am J Surg* **198**, 617 (Nov, 2009).

17. J. B. Holcomb *et al.*, Dry fibrin sealant dressings reduce blood loss, resuscitation volume, and improve survival in hypothermic coagulopathic swine with grade V liver injuries. *J Trauma* **47**, 233 (Aug, 1999).

18. U. Martinowitz *et al.*, Intravenous rFVIIa administered for hemorrhage control in hypothermic coagulopathic swine with grade V liver injuries. *J Trauma* **50**, 721 (Apr, 2001).

19. J. F. Kelly *et al.*, Injury severity and causes of death from Operation Iraqi Freedom and Operation Enduring Freedom: 2003-2004 versus 2006. *J Trauma* **64**, S21 (Feb, 2008).

20. J. B. Holcomb *et al.*, Damage control resuscitation: directly addressing the early coagulopathy of trauma. *J Trauma* **62**, 307 (Feb, 2007).

Figure 1

Project Title: “Technologies for Hemostasis and Stabilization of the Acute Traumatic Wound”
Award Number: W81XWH-11-1-0836
PI: Carlson, Mark A.
Annual Report (Y1, Q1-Q4)
Reporting period: 10-01-2011 to 09-30-2012

Figure 1. Gantt Chart (current year in boldface). See Appendix A1 for definitions of Tasks.

Task	**Y1Q1**	**Y1Q2**	**Y1Q3**	**Y1Q4**	Y2Q1	Y2Q2	Y2Q3	Y2Q4	Y3Q1	Y3Q2	Y3Q3	Y3Q4	Y4Q1	Y4Q2	Y4Q3	Y4Q4	Status
1																	On schedule
2																	On schedule
3																	On schedule
4																	Delayed
5																	Delayed
6																	Delayed
7																	Yet to start
8																	Yet to start
9																	Yet to start
10																	Yet to start
11																	Yet to start
12																	On schedule
13																	On schedule
14																	On schedule
15																	Yet to start

Key

- Task completed
- Task on schedule & active
- Task delayed
- Anticipated span of delayed task
- Task yet to start

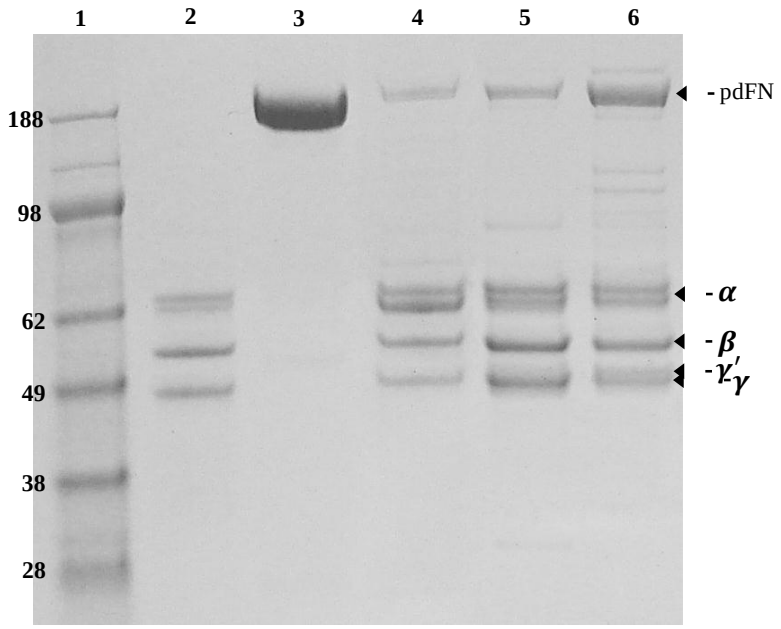

Figure 2. SDS PAGE of pdFI purified by ethanol or ammonium sulfate fractionation. Lane 1: molecular weight marker. Lane 2: Enzyme Research fibrinogen. Lane 3: fibronectin (pdFN). Lane 4: pdFI, purified by classical cryoprecipitation. Lane 5: pdFI, purified by ethanol fractionation. Lane 6: pdFI, purified by ammonium sulfate fractionation.

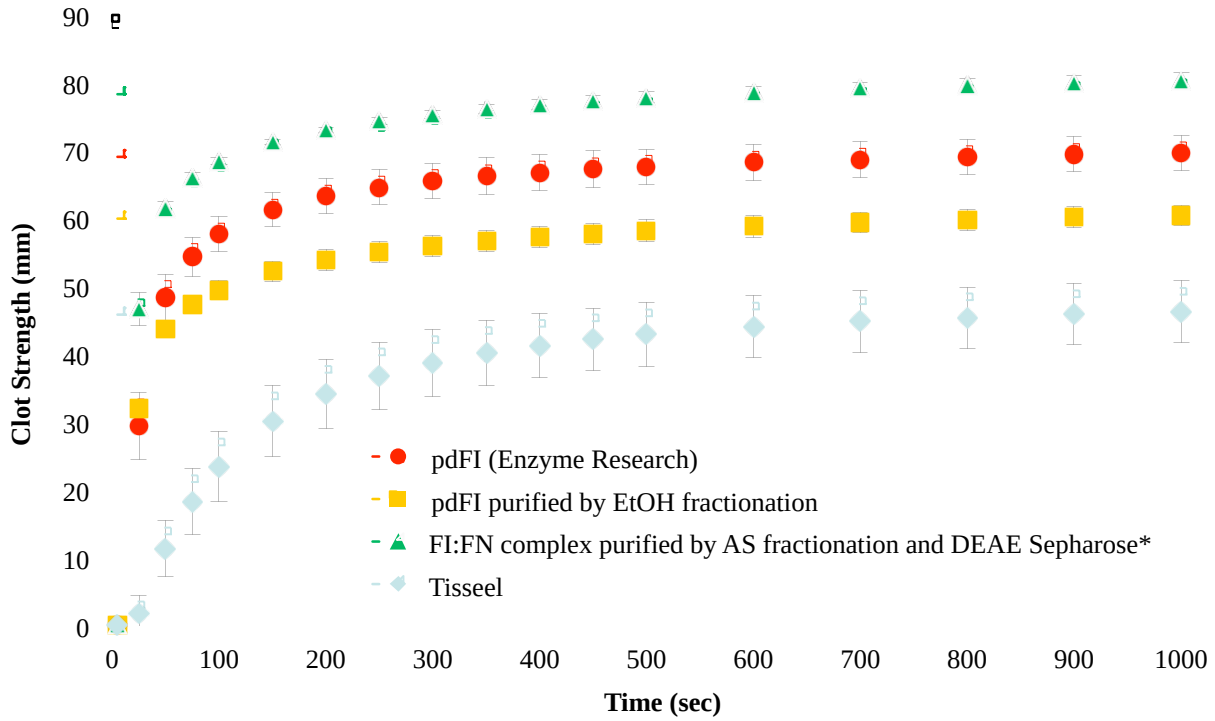

Figure 3. Thromboelastographic analysis of fibrinogen made by ethanol (EtOH) or ammonium sulfate (AS) fractionation, when formulated at 9 mg/mL FI, 2500 U/mL rFXIIIA2-a, and 106 U/mL rFIIa. *Note: FI:FN complex contained 9 mg/mL total protein (3.69 mg/mL FI), 2500 U/mL rFXIIIA2-a, and 106 U/mL rFIIa.

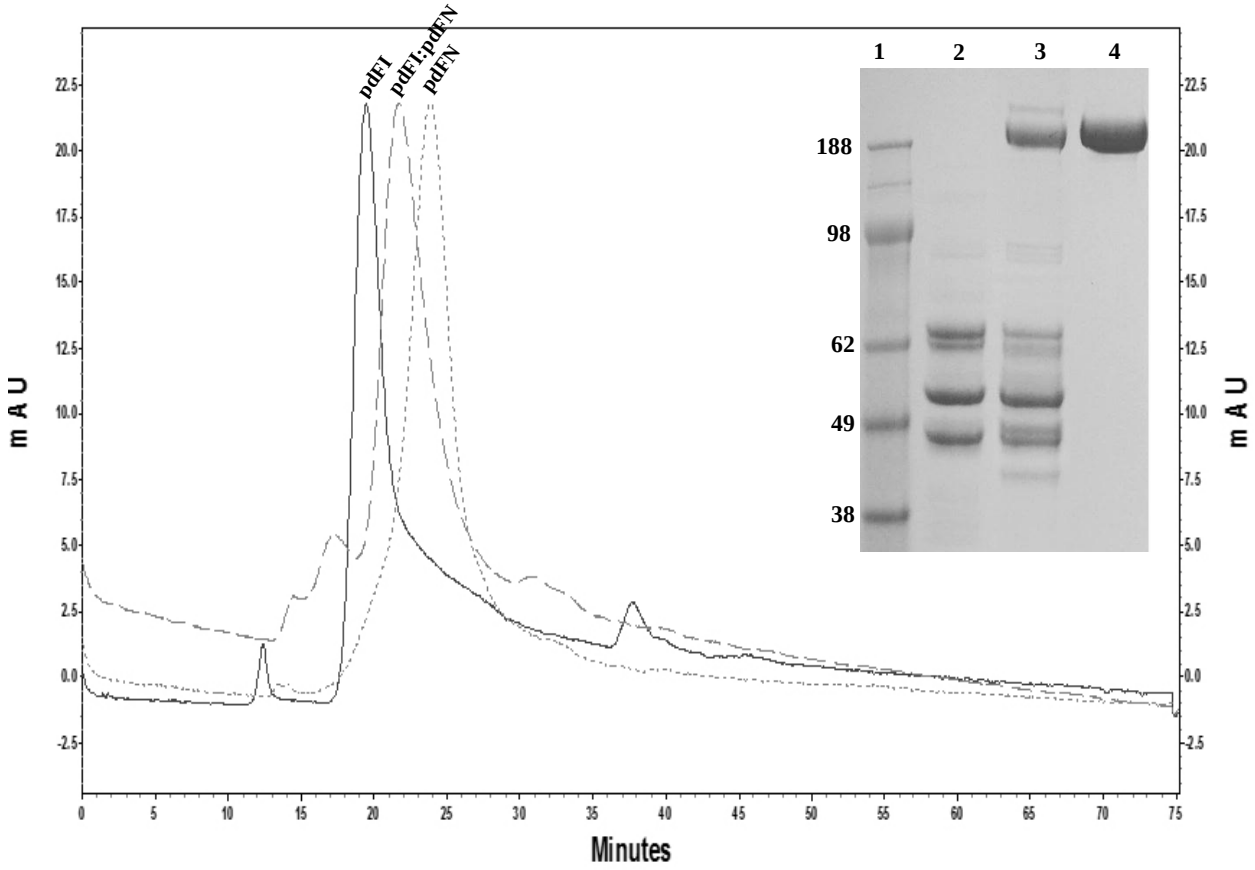

Figure 4. HPSEC analysis of a novel fibrinogen:fibronectin complex made by ammonium sulfate fractionation, with corresponding SDS-PAGE insert (Lane 1: molecular weight marker; lane 2: Enzyme Research fibrinogen (pdFI); lane 3: DEAE complex (pdFI:pdFN); lane 4: fibronectin (pdFN).

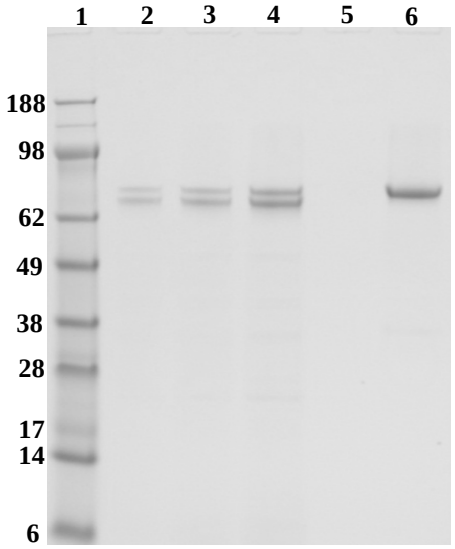

Figure 5. SDS-PAGE of purified recombinant activated Factor XIII, from fermentation of *Pichia pastoris.* Lane 1: molecular weight marker. Lanes 2-4: rFXIIIa reference (0.5, 1.0 and 2.0 µg). Lane 5: blank. Lane 6: purified rFXIIIa.

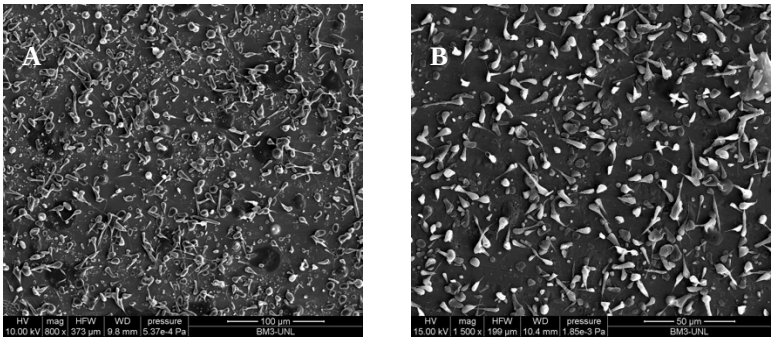

Figure 6. Examples of oblong particles produced by EHD with aspect ratio 4 (A) and 2.5 (B). Measure bars in lower right of each panel are 100 µm (A) and 50 µm (B).

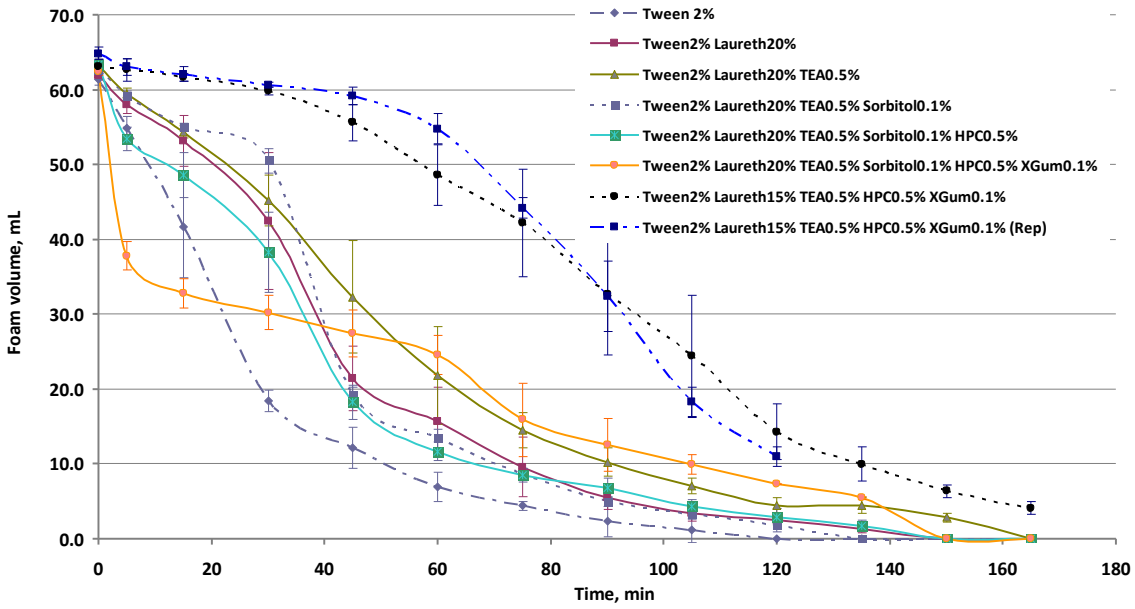

Figure 7. Foam formulation studies. Laureth = Laureth 23; TEA = triethanolamine; HPC = hydroxypropylcellulose; Xgum = xanthan gum; Rep = repeat.

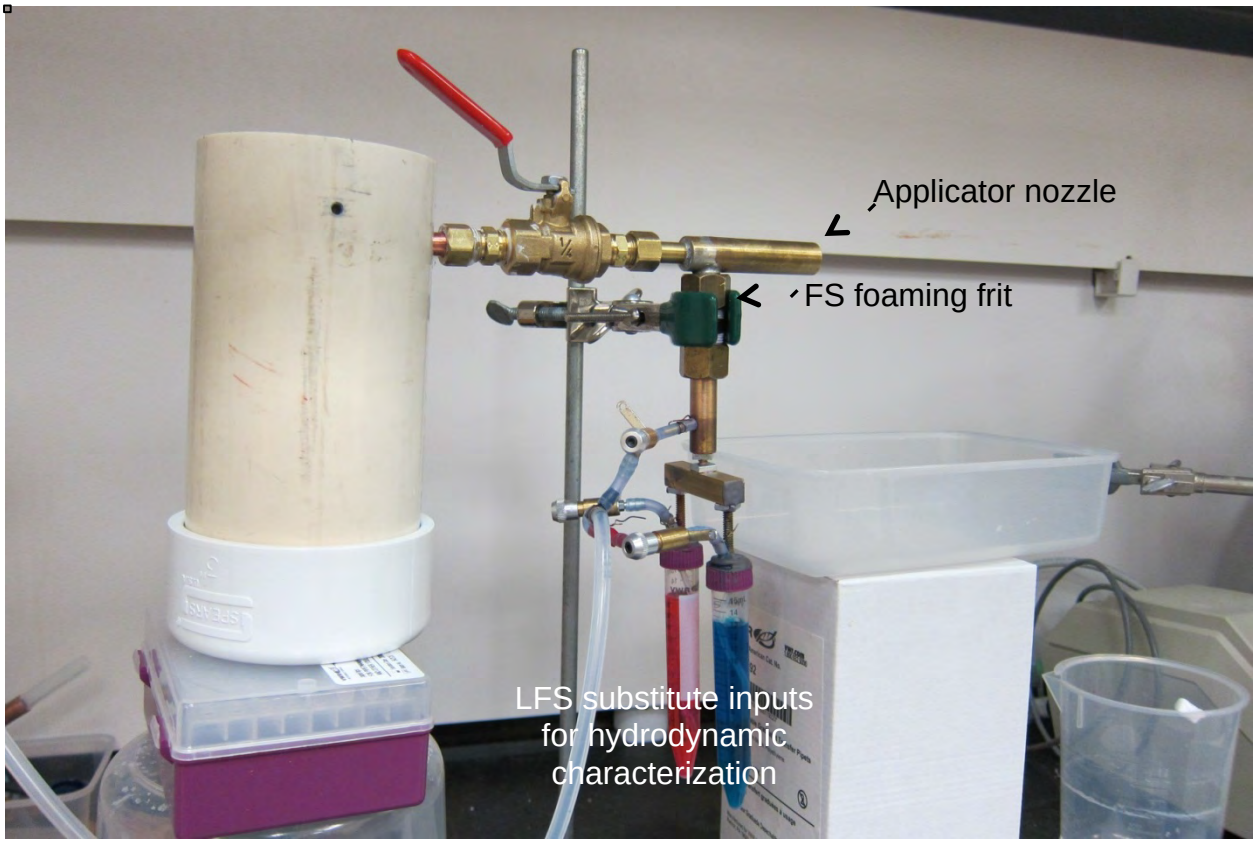

Figure 8. Protypical dual foam generator for hydrodynamic performace optimization using liquid fibrin sealant (LFS) viscoelastic fluid mimetic.

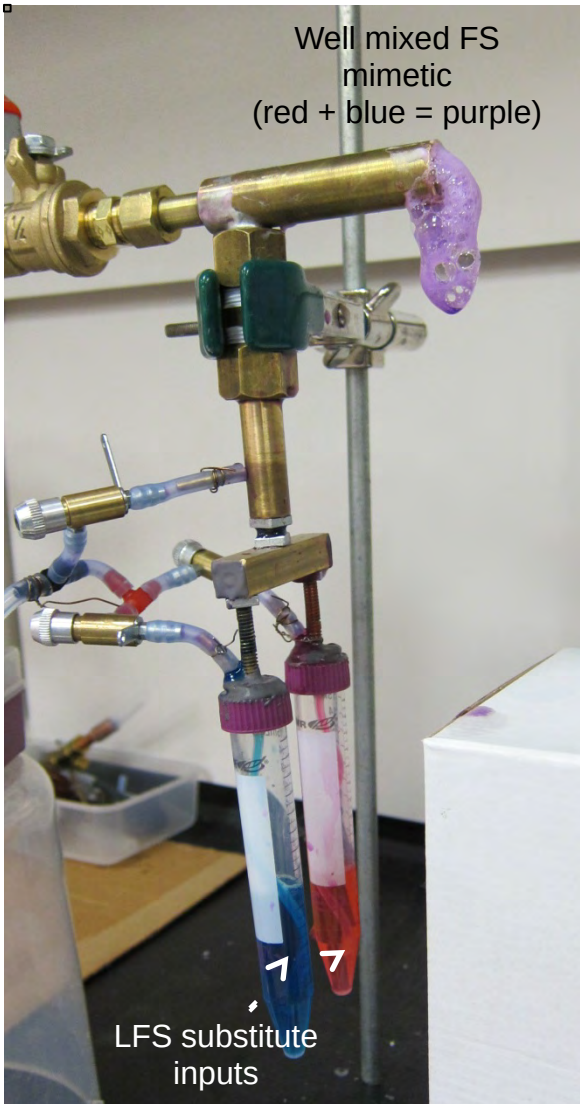

Figure 9. Mixing of fibrin sealant viscoelastic mimetic liquid inputs (fluid to foam).

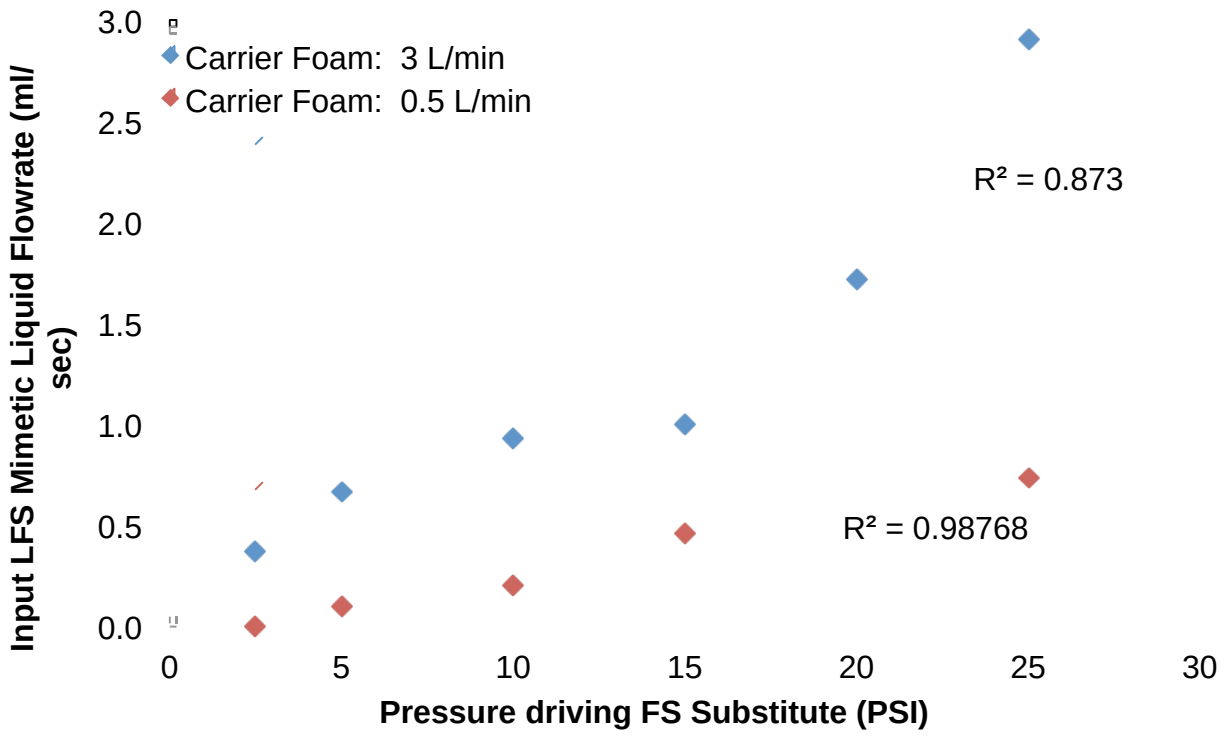

Figure 10. LFS mimetic input flow rates as a function of nozzle feed air pressure at fixed carrier foam flow rate.

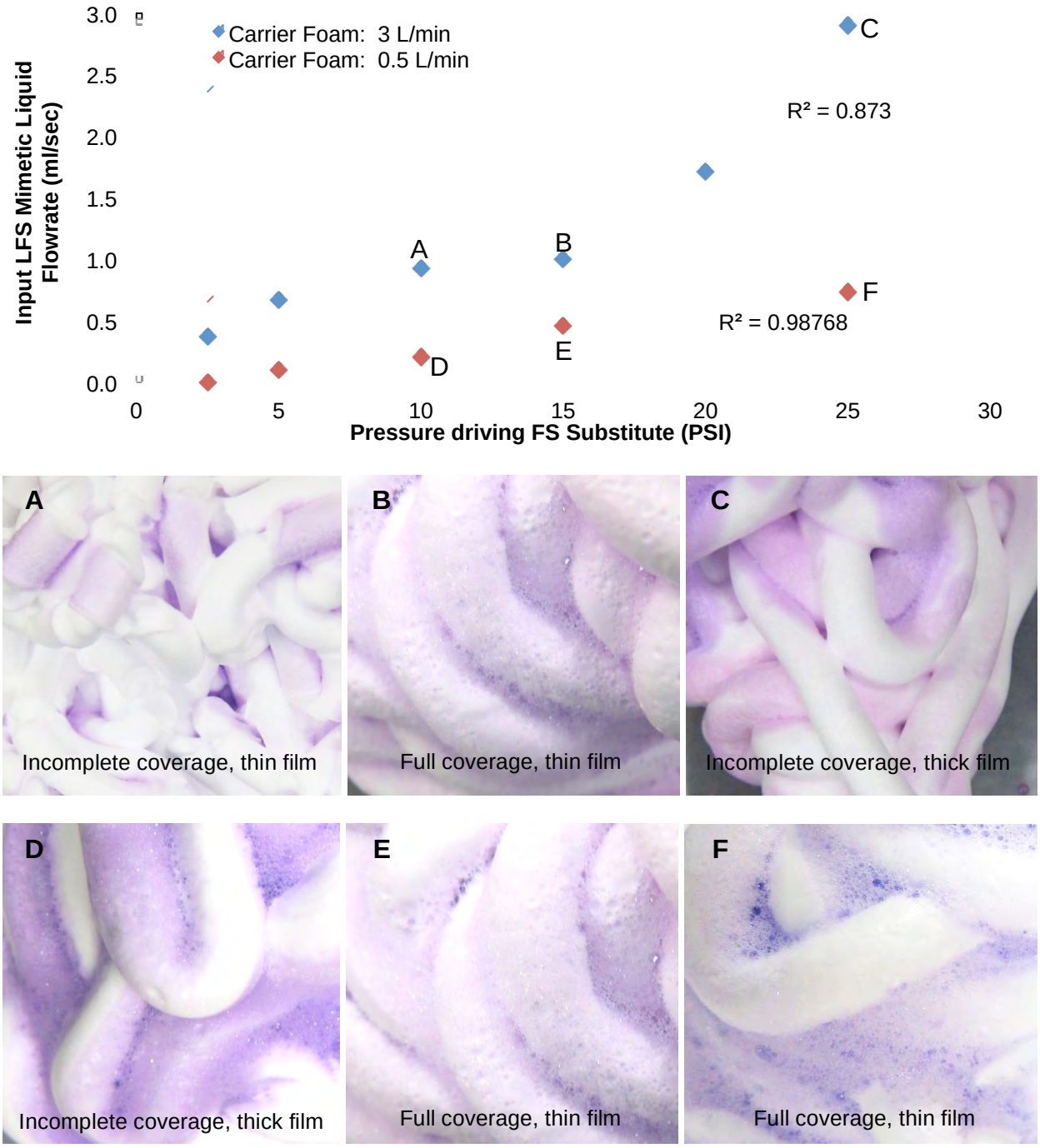

Figure 11. Dual foam mode outer coating efficiency as a function of fibrin sealant viscoelastic foam flow rates.

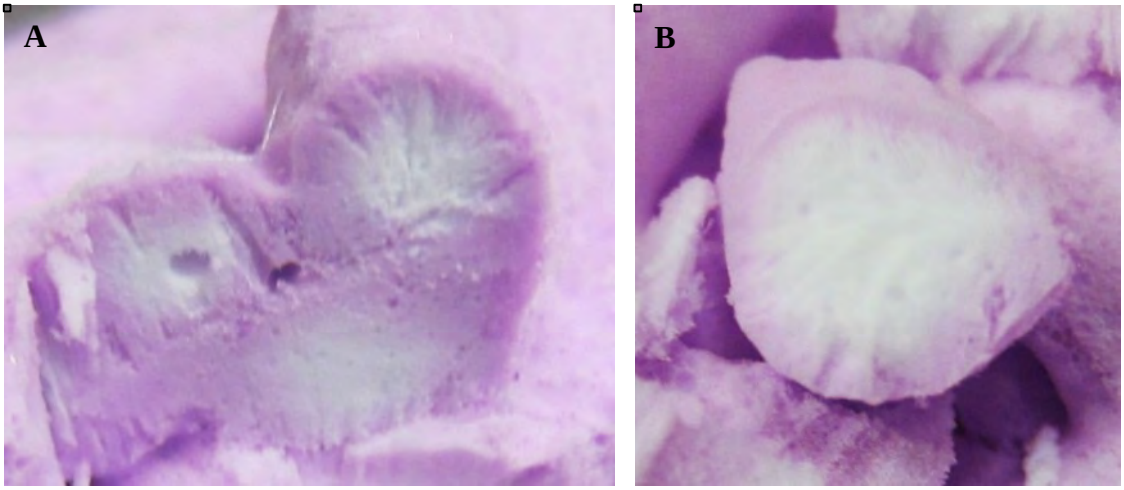

Figure 12. Fibrin sealant viscoelastic foam coating thickness in dual foam cross-section. (A) Thick film cross-section. (B) Thin film cross-section.

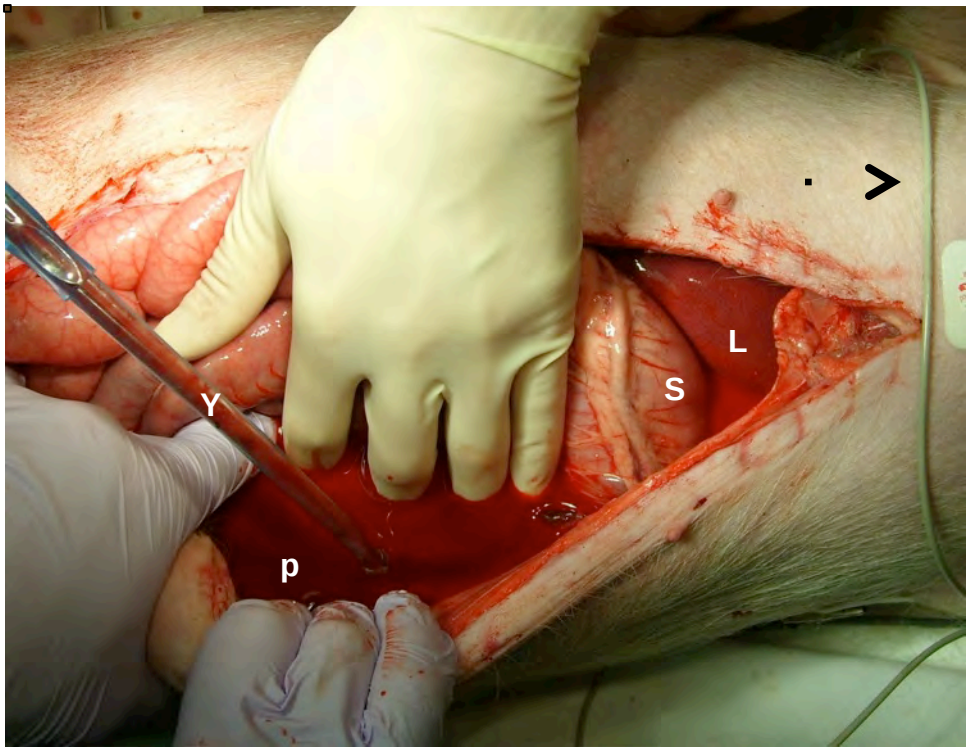

Figure 13: overhead view of swine subject 96, immediately after the 60 min observation period. Subject is supine, with ventral midline incision. Large black arrow = cephalad; p = pool of blood in left paracolic gutter; Y = Yankauer sucker; S = stomach; L = liver.

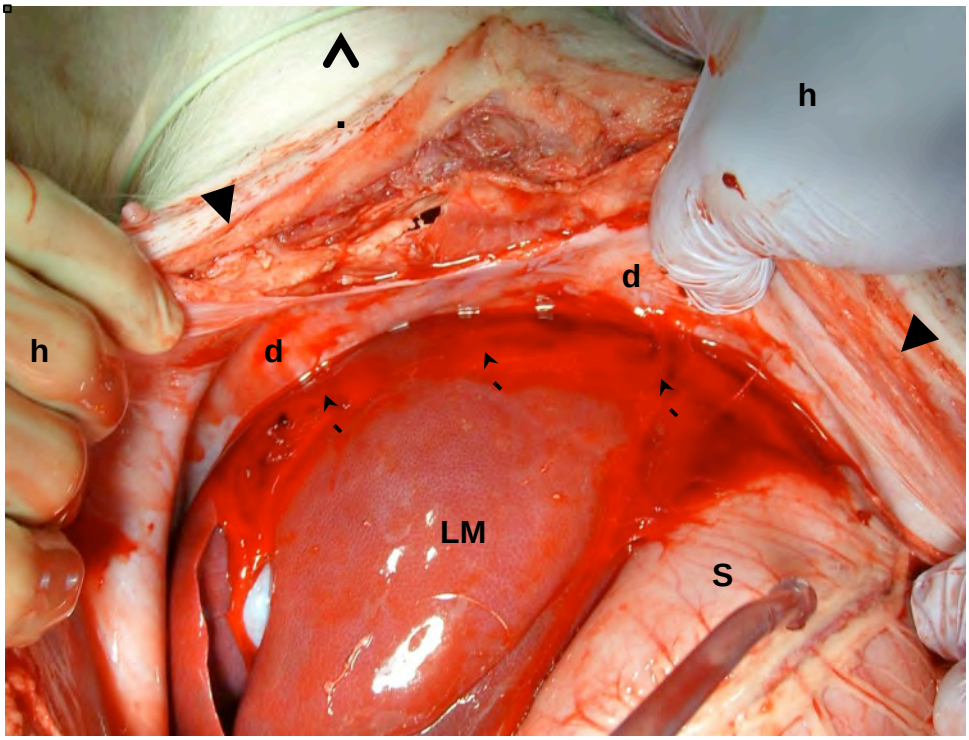

Figure 14: overhead view of liver *in vivo* from swine 96, immediately after the 60 min observation period. Subject is supine, with ventral midline incision. Large black arrow = cephalad; small black arrows = clot sealing liver against the diaphragm; arrowheads = edge of incision; d = diaphragm; LM = left medial lobe; S = stomach; h = surgeon hand.

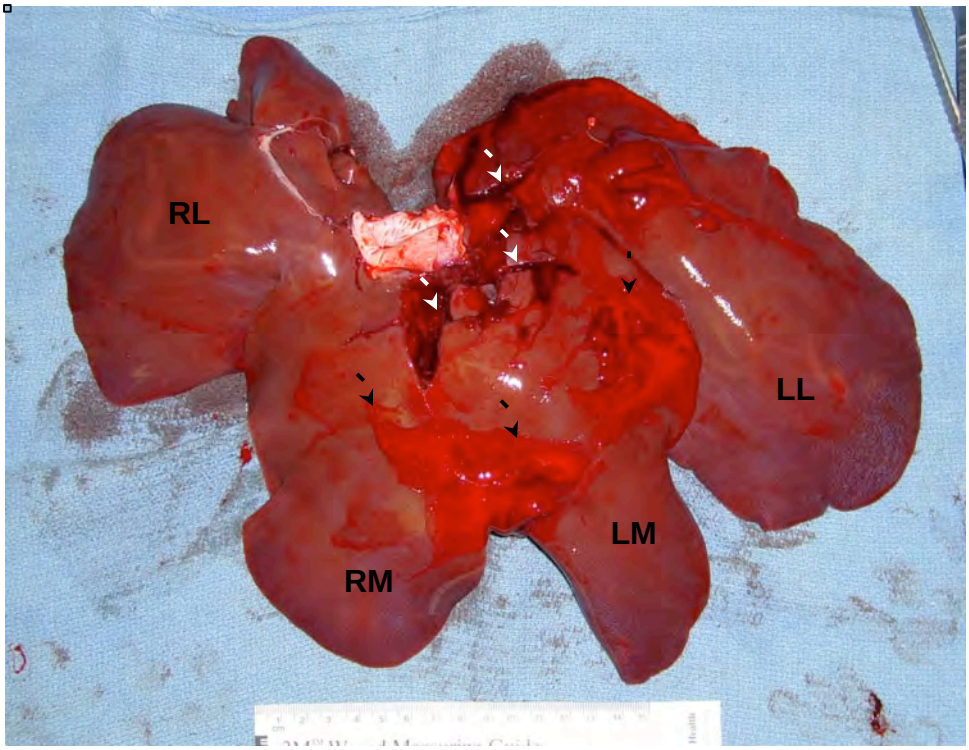

Figure 15: liver *ex vivo* from swine 96, superior aspect. RL = right lateral lobe; RM = right medial lobe; LM = left medial lobe; LL = left medial lobe. Three black arrows indicate clot that sealed off the injury. Three white arrows indicate the injury itself.

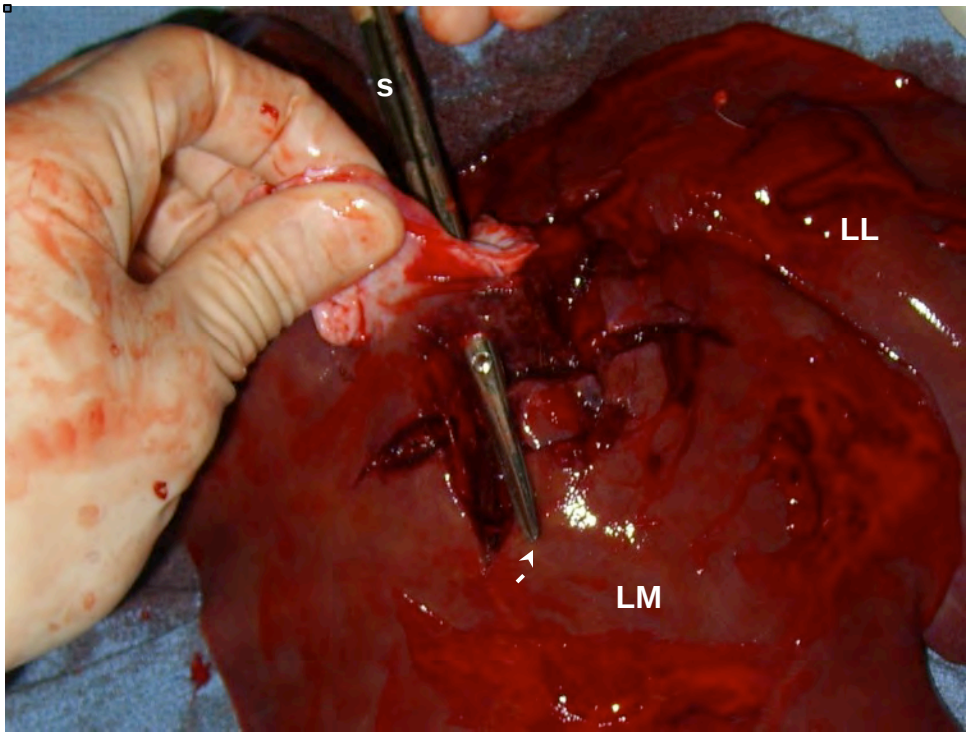

Figure 16: liver *ex vivo* from Swine 96, superior aspect, showing central liver injury. Scissors (s) has been inserted through the suprahepatic vena cava into the hepatic vein supplying the left medial (LM) lobe, and then out through the injury site. This vein was lacerated. White arrow = tip of scissors.

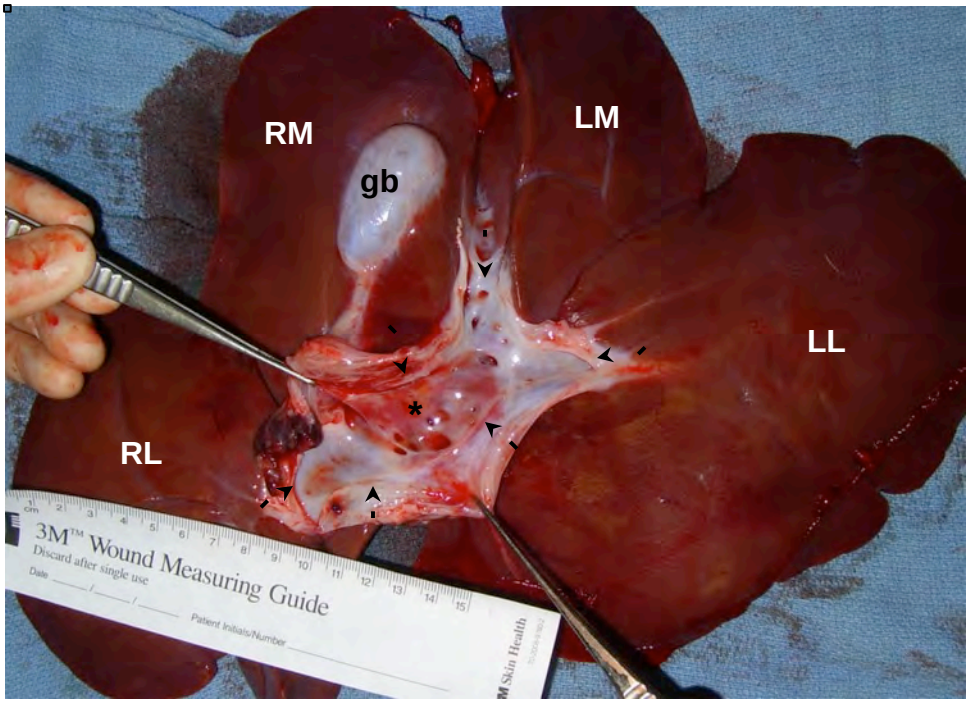

Figure 17: liver *ex vivo* from Swine 96, showing inferior aspect of liver with portal vein opened along its inferior surface (black arrows). Note hematoma in back wall of portal vein (*).

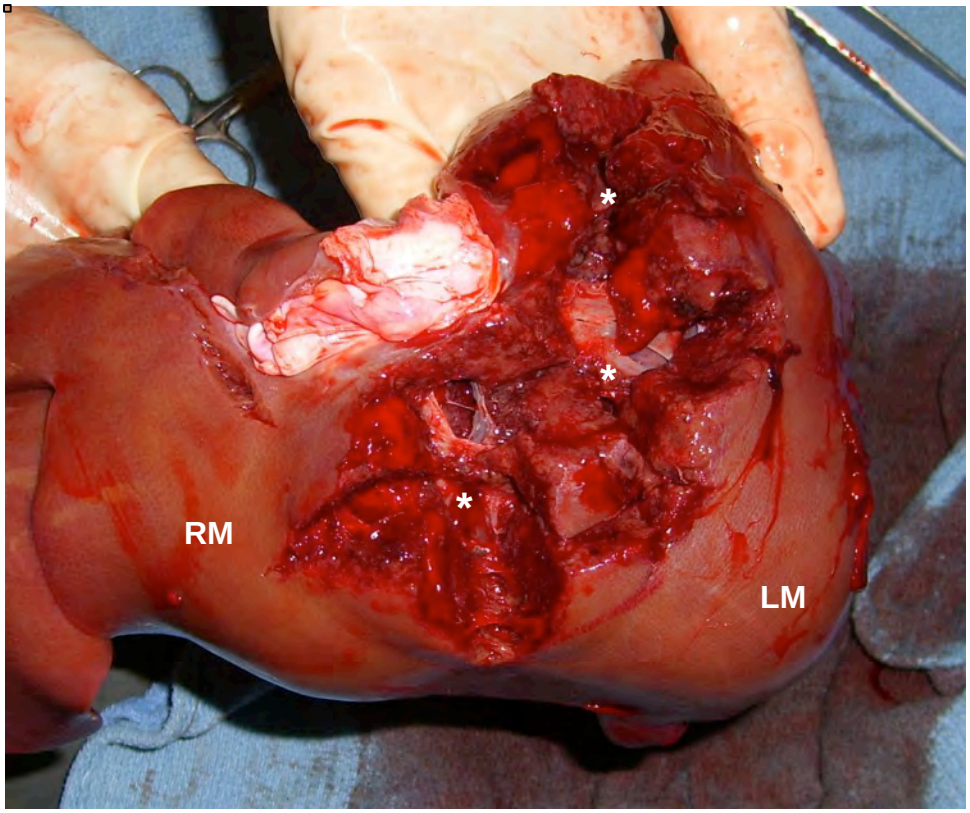

Figure 18: liver *ex vivo* from Swine 96, showing superior aspect of liver injury. Hands are splaying the injury open from below to show extent of the wounds. Center of each clamp strike indicated with an asterisk (*).

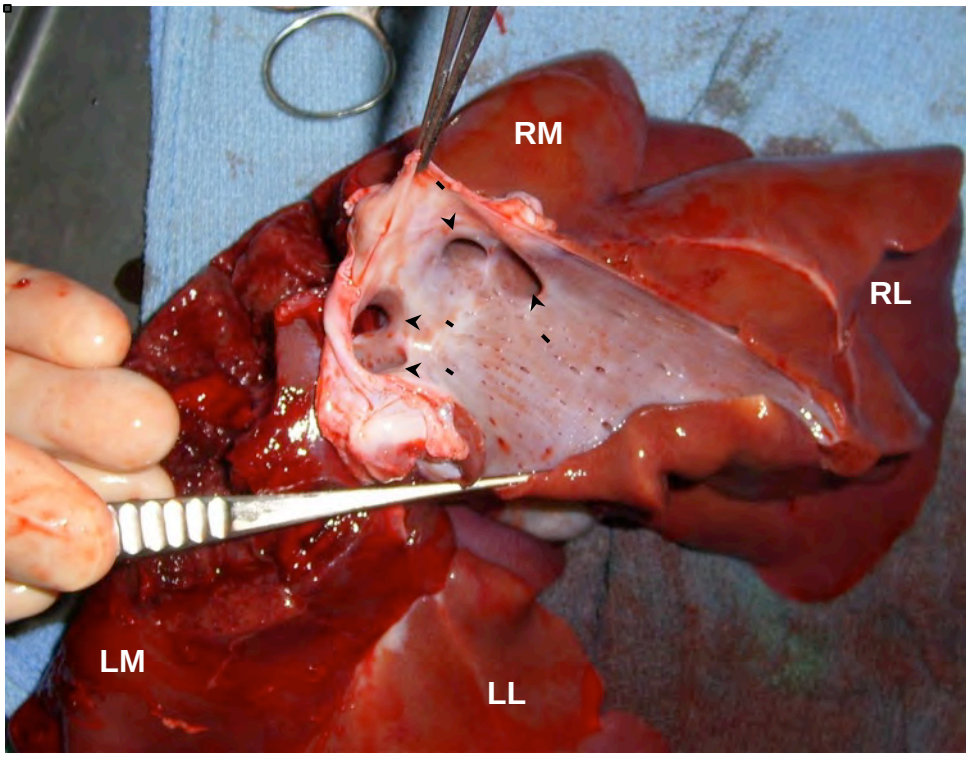

Figure 19: liver *ex vivo* from Swine 96, showing posterior aspect of liver, looking into the vena cava, which has been opened posteriorly along its axis. Black arrows indicate orifices of the hepatic veins. These openings are where the scissors is inserted to determine if a hepatic vein has been lacerated.

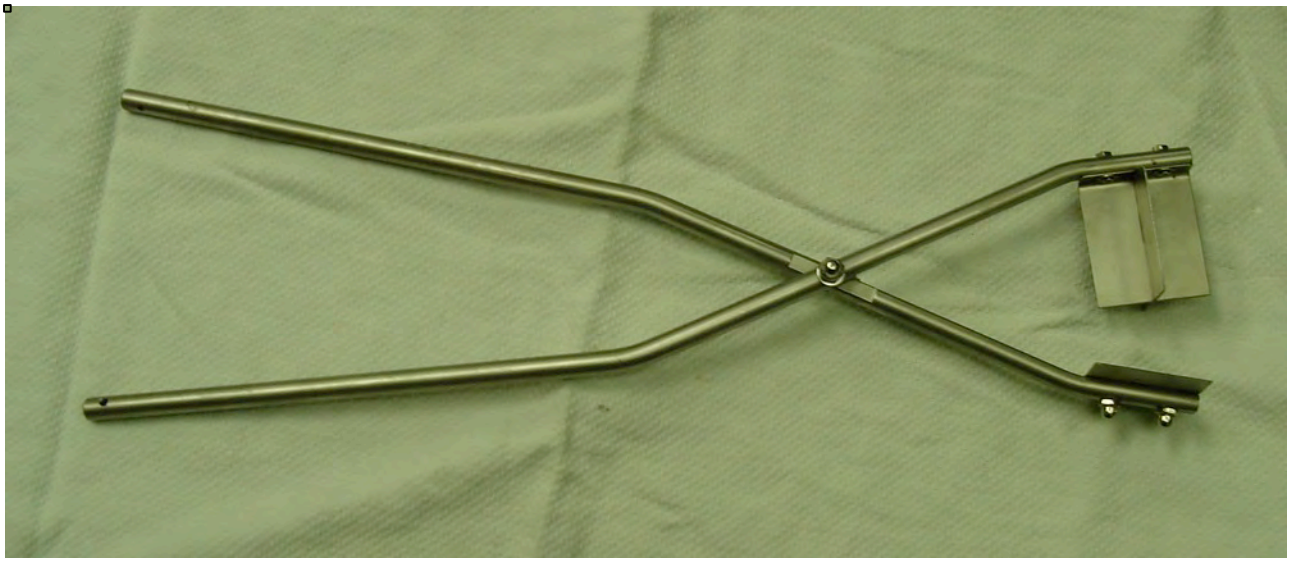

Figure 20. Liver injury clamp.

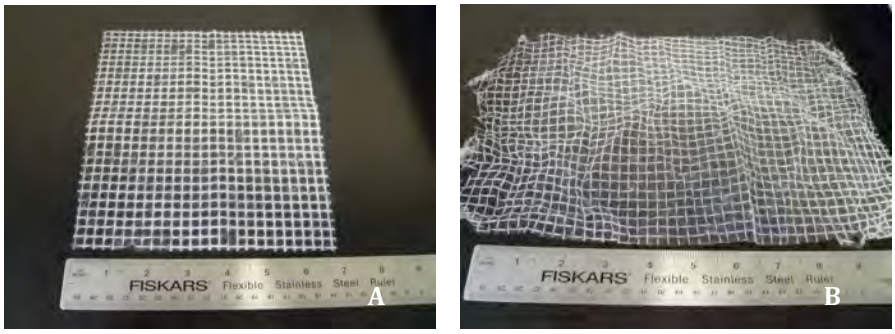

Figure 21. Macroscopic structure of microfibrous meshes: (A) PCL; (B) PLA. Note the gross resemblance to cotton gauze.

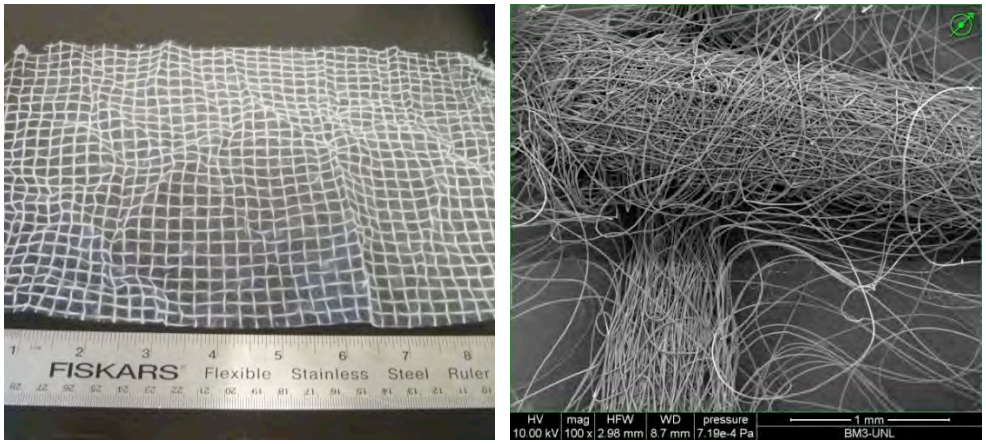

Figure 22. PCL (MW = 45 kDa) microfibrous bandage structure. An intersection of two macrofibers is shown in the right panel.

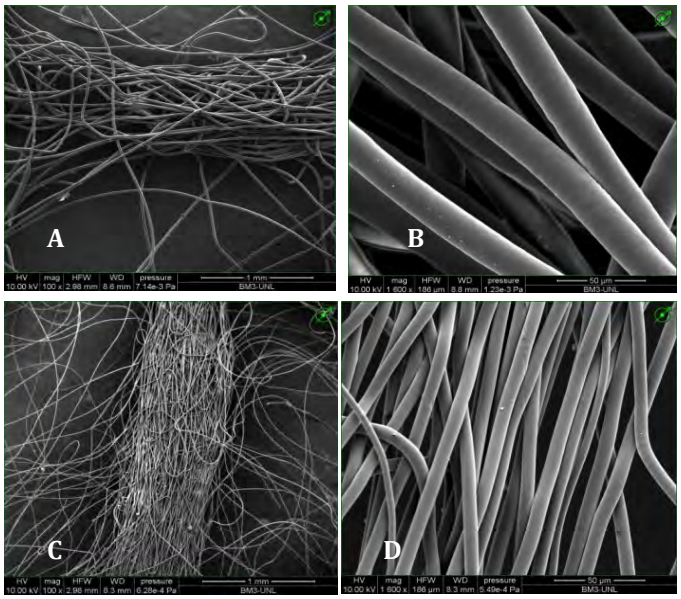

Figure 23. SEM images of PCL (A, B) and PLA (C, D) microfibers, produced with the new hybrid method (EHD + dry fiber spinning). Measure bars in lower right of each frame are 1 mm (A, C) or 50 μm (B, D).

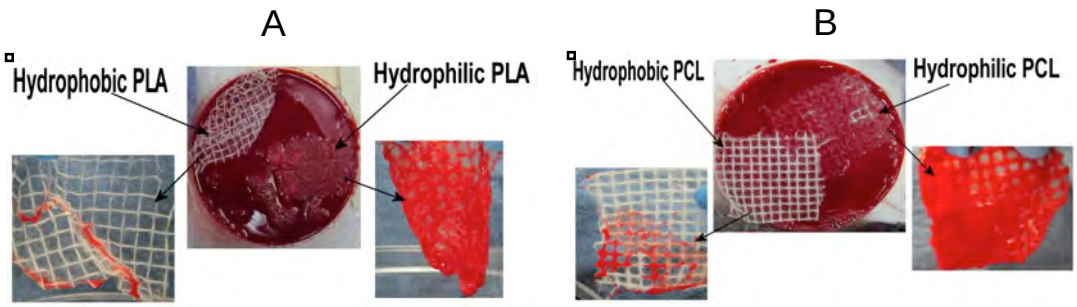

Figure 24. Ex situ swine blood absorption test. (A) PLA; (B) PCL.

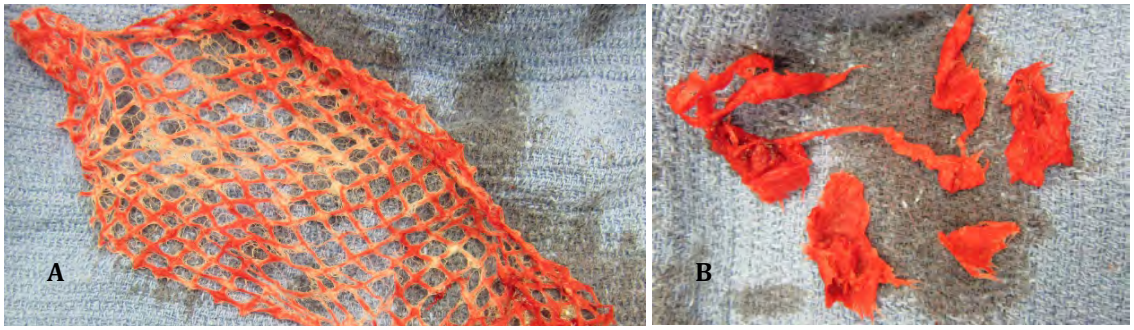

Figure 25. Explanted microfibrous meshes 1 h after treatment of liver injury. (A) PCL; (B) PLA.

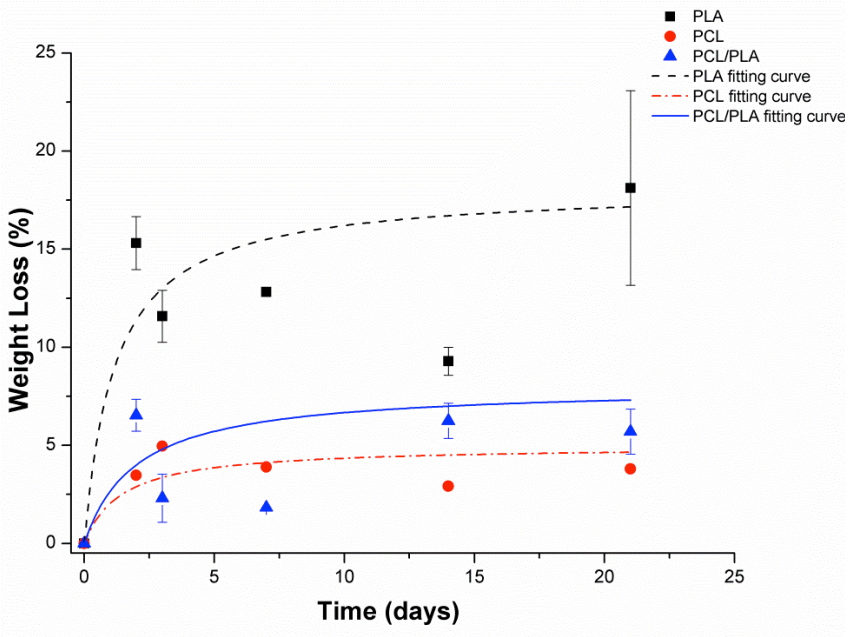

Figure 26. %Weight loss of the PLA, PCL and PCL/PLA mesh after incubation in simulated body fluid Error bars = standard deviations, where available. Fitted curves also are shown.

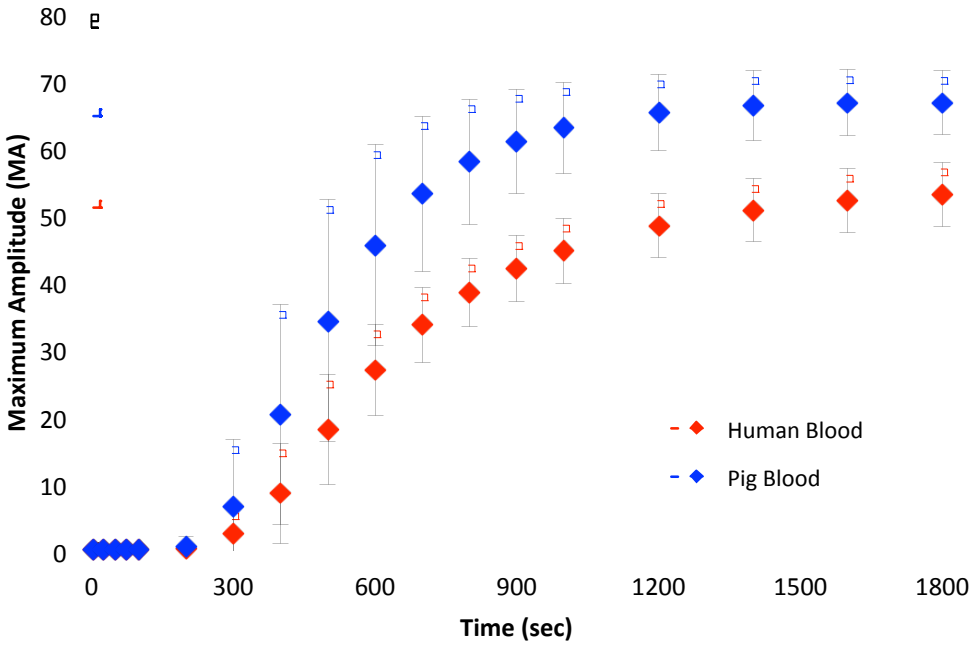

Figure 27. TEG of initial blood samples from swine (N = 68) used in liver injury studies, compared with normal human donors. Each data point is a mean ± standard deviation.

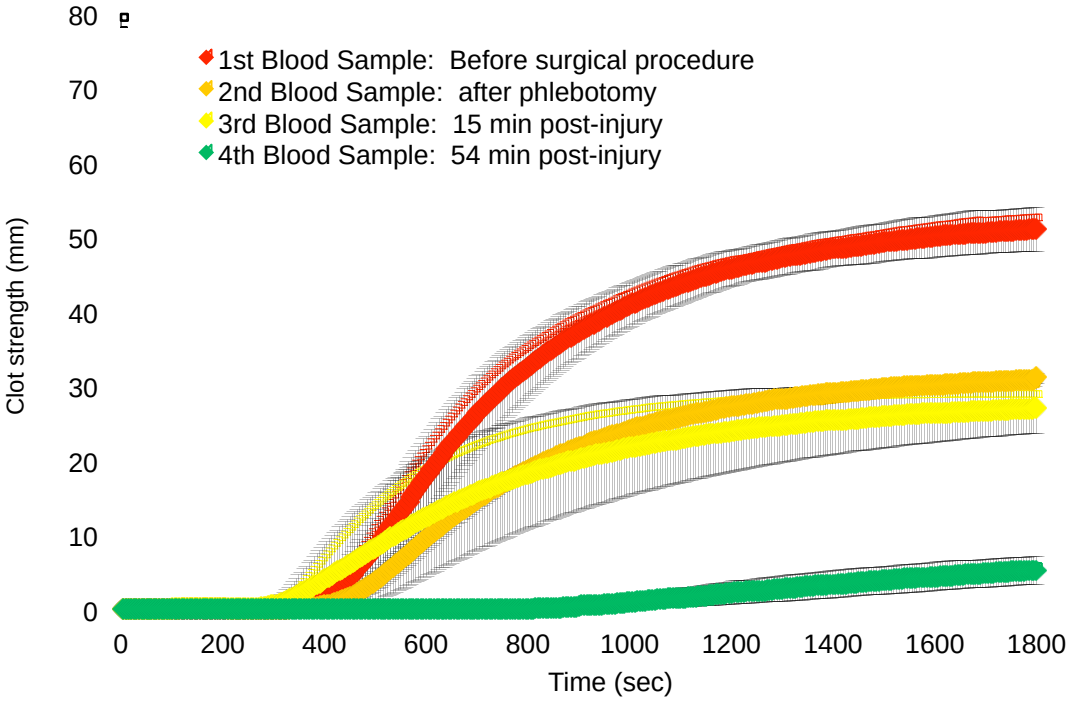

Figure 28. TEG of blood samples from swine (N = 25) used in liver injury studies, using the hypothermic hemodiluted model.

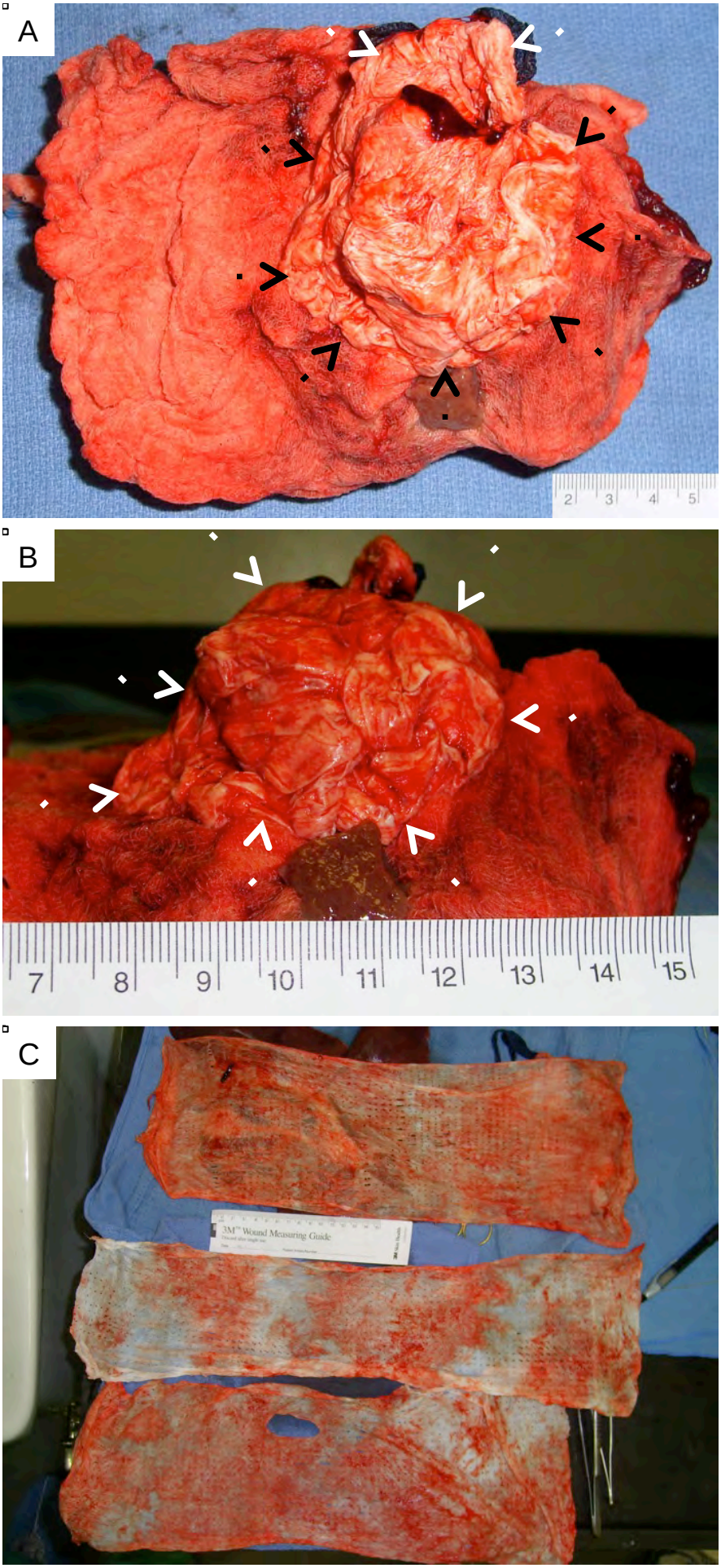

Figure 29. PLA dressing ex vivo, Swine 73. Treatment bandage was 4 ply, nanofiber sheet configuration (total dry weight = 18 g), perforated; unfolded area approx. equivalent to area of unfolded 4x4 cotton sponge, wetted with LFS (~75 mg FI present, along with FIIa and FXIIIa) just prior to bandage insertion into the wound.

(A) Superior view; arrows indicate balled-up PLA sheets, which have formed a cast of the cavitary liver injury.
(B) Side view; arrows indicate balled-up PLA sheets, again showing a cast of the injury.
(C) PLA sheets from A & B now unfolded, showing penetration of blood into the bandage.

APPENDICES / SUPPORTING DATA

2012 Annual Report, Award Number: W81XWH-11-1-0836

Item	Description	Pages
A1	Statement of Work (from original award application)	48
A2	Acronyms	49
A3	Correspondence with ISR regarding Tasks 5, 6, and 7	50-53
A4	Manuscript on recombinant fibrinogen (submitted to *Biomacromolecules* Oct 2012)	54-84
A5	Sample of VS data acquired with each swine procedure	85
A6	Sample of laboratory tests obtained at each swine procedure	86
A7	Sample swine datasheet recorded with each swine procedure	87-90
A8	State of NE Dept of Economic Development Approval Letter	91
A9	Abstract on recombinant fibrin sealant (*J Surg Res* 2011;165:317)	92
A10	Abstract on human fibrinogen (Brighton UK presentation, July 2012)	93
A11	Poster on hemostatic devices (2011 ACS meeting)	94-111
A12	rLFS vs. Tisseel™ manuscript in preparation	112-124

Appendix A1

Proposal Title: “Technologies for Hemostasis and Stabilization of the Acute Traumatic Wound”
PI: Carlson, Mark A.

STATEMENT OF WORK

No.	Task description	Site	Year	Aim
1	Purification/generation of pd-FI and rFXIIIA2-a	UNL	1-3	1
2	Generation of ultrafine particles for tamponade carrier foam	LNK	1-3	1
3	Testing of candidate tamponade carrier & FS foams	LNK & UNL	1-2	1
4	Testing of single foams in rabbits (tamponade carrier & FS foams separately)	UNMC	1	1
5	Development & engineering of dual foam candidate devices	LNK & UNL	1-2	1
6	Testing of dual foam in rabbits	UNMC	2-3	1
7	Engineering scale-up of optimized candidate particles	LNK	2-3	1
8	Testing of dual foam in swine noncompressible model (laparotomy with 2˚ closure)	UNMC	3-4	1
9	Delivery of candidate field-ready dual foam device	UNL & LNK	3	1
10	Testing of dual foam in swine noncompressible model (closed penetrating wound)	UMM	3	1
11	Delivery of report on final recommended product description for dual foam device for treatment of noncompressible hemorrhage	LNK, UNL, UNMC, UMM	4	1
12	Delivery of resorbable bandage for final preclinical study in hypothermic coagulopathic model	LNK	1	2
13	Delivery of fibrin sealant for final preclinical study in hypothermic coagulopathic model	UNL	1	2
14	Final preclinical study of resorbable bandage in for hypothermic coagulopathic model (swine)	UNMC	1	2
15	Delivery of report on final recommended product description for resorbable fibrin sealant bandage for treatment of compressible coagulopathic hemorrhage	LNK, UNL, UNMC	2	2

[SoW taken from original application that was uploaded to Grants.gov in March 2011]

Appendix A2: Acronyms

ACURO	Animal Care and Use Review Office
DEAE	diethylaminoethanol
EHD	electrohydrodynamics
ETCO2	end tidal carbon dioxide
FI	Factor I (fibrinogen)
FIIa	activated Factor II (thrombin)
FN	fibronectin
FS	fibrin sealant
FXIII	Factor XIII (cross-linking factor)
Hb	hemoglobin
HPC	hydroxypropylcellulose
IACUC	Institutional Animal Care and Use Committee
ISR	Institute of Surgical Research
IVC	inferior vena cava
LFS	Liquid Fibrin Sealant
LNK	LNKChemsolutions, LLC
LR	Lactated Ringers solution
MAP	mean arterial pressure
nhpp	normal human plasma pool
PCL	polycaprolactone
pd	plasma derived
PLA	polylactic acid
PT	protime
rFXIIIA2-a	activated recombinant Factor XIII
SBF	simulated body fluid
SDS PAGE	sodium dodecyl sulfate polyacrylamide gel electrophoresis
SEM	scanning electron microscopy
TEA	triethanolamine
TEG	thromboelastography
UNL	University of Nebraska—Lincoln
UNMC	University of Nebraska Medical Center

Monday, August 20, 2012 10:43:10 AM CT

Subject: 4public: Proposed migration to exclusive use of the swine model for USAMRMC# 10091006
Date: Monday, August 20, 2012 10:41:21 AM CT
From: Carlson, Mark A
To: Michael Dubick Dr CIV USA MEDCOM AISR, Bijan Kheirabadi, Wenjun Martini
CC: William Velander, Gustavo Larsen

Bijan Kheirabadi
Wenjun Martini
Mike Dubick
ISR, San Antonio

Project: Technologies for Hemostasis and Stabilization of the Acute Traumatic Wound (USAMRMC# 10091006)
Topic: Swine vs. Rabbit subjects

All,

I wanted to propose a change in the scientific protocol to the above study. Currently we are using a combination of rabbit and swine models in the development of our hemostatic devices. As you may recall during our visit to the ISR on April 3, 2012, my collaborators (Bill Velander and Gustavo Larsen) and I suggested the possibility of eliminating the rabbit model from this project, and performing all of the proposed procedures in swine. Recently my collaborators and I discussed this issue further, and we feel that it would be beneficial to move to exclusive use of the swine model, primarily because of cost, consistency, and relevance.

At our institution, we currently can obtain a 3 month, ~33 kg male swine for $100. The cost for a 3.2 kg rabbit is $192. The updated per diem costs for swine vs. rabbits at our institution are $8 and $4, respectively. At this per diem rate, the swine would have to be house for 23 extra days before the total costs would exceed that of a rabbit. Since this project consists of nonsurvival procedures only, it will be less expensive to use swine instead of rabbits.

In addition, my collaborators and I believe that swine model represents a more accurate model of severe clinical hemorrhage than the rabbit, particularly with respect to blood volume and the ability to tolerate blood loss. Because of this difference in modeling, it is possible that some of the acute studies in rabbits would need to be repeated in swine, for confirmation purposes. So we think it would make more sense just to perform all acute studies in swine.

When it comes time to perform long-term survival studies for toxicology, then we certainly can go back to the rabbit model, since this model will be cheaper for experiments 30+ days in duration. For acute studies of device efficacy, however, we believe that it will be cheaper and more clinically relevant to focus on the swine model.

Please let us know your thoughts. If you are in agreement with our proposed migration to exclusive use of the swine model for nonsurvival studies of device efficacy, then we will negotiate the change in the animal protocol with our local IACUC and then ACURO.

Thank you,
Mark

Mark A. Carlson, MD, FACS
Professor
Department of Surgery
Department of Genetics, Cell Biology, and Anatomy
University of Nebraska Medical Center
VA Nebraska Western-Iowa Health Care System
Surgery 112, VA Medical Center
4101 Woolworth Ave

Subject: RE: 4public: Proposed migration to exclusive use of the swine model for USAMRMC# 10091006 (UNCLASSIFIED)

Date: Monday, August 20, 2012 10:59:40 AM CT

From: Kheirabadi, Bijan Dr CIV USA MEDCOM AISR

To: Carlson, Mark A, Dubick, Michael A Dr CIV USA MEDCOM AISR, Martini, Wenjun Dr CIV USA MEDCOM AISR

CC: William Velander, Gustavo Larsen

Classification: UNCLASSIFIED
Caveats: NONE

I agree with you. Conducting the efficacy studies in swine makes more sense specially given the high cost of rabbit experiments.
Bijan

-----Original Message-----
From: Carlson, Mark A [mailto:macarlso@unmc.edu]
Sent: Monday, August 20, 2012 10:41 AM
To: Dubick, Michael A Dr CIV USA MEDCOM AISR; Kheirabadi, Bijan Dr CIV USA MEDCOM AISR; Martini, Wenjun Dr CIV USA MEDCOM AISR
Cc: William Velander; Gustavo Larsen
Subject: 4public: Proposed migration to exclusive use of the swine model for USAMRMC# 10091006

Bijan Kheirabadi
Wenjun Martini
Mike Dubick
ISR, San Antonio

Project: Technologies for Hemostasis and Stabilization of the Acute Traumatic Wound (USAMRMC# 10091006)
Topic: Swine vs. Rabbit subjects

All,

I wanted to propose a change in the scientific protocol to the above study. Currently we are using a combination of rabbit and swine models in the development of our hemostatic devices. As you may recall during our visit to the ISR on April 3, 2012, my collaborators (Bill Velander and Gustavo Larsen) and I suggested the possibility of eliminating the rabbit model from this project, and performing all of the proposed procedures in swine. Recently my collaborators and I discussed this issue further, and we feel that it would be beneficial to move to exclusive use of the swine model, primarily because of cost, consistency, and relevance.

At our institution, we currently can obtain a 3 month, ~33 kg male swine for $100. The cost for a 3.2 kg rabbit is $192. The updated per diem costs for swine vs. rabbits at our institution are $8 and $4, respectively. At this per diem rate, the swine would have to be house for 23 extra days before the total costs would exceed that of a rabbit. Since this project consists of nonsurvival procedures only, it will be less expensive to use swine instead of rabbits.

In addition, my collaborators and I believe that swine model represents a more accurate model of severe clinical hemorrhage than the rabbit, particularly with respect to blood volume and the ability to tolerate blood loss. Because of this difference in modeling, it is possible that some of the acute studies in rabbits would need to be repeated in swine, for confirmation purposes. So we think it would make more sense just to perform all acute studies in swine.

Subject: RE: 4public: Proposed migration to exclusive use of the swine model for USAMRMC# 10091006 (UNCLASSIFIED)

Date: Monday, August 20, 2012 1:40:16 PM CT

From: Martini, Wenjun Dr CIV USA MEDCOM AISR

To: Carlson, Mark A, Dubick, Michael A Dr CIV USA MEDCOM AISR, Kheirabadi, Bijan Dr CIV USA MEDCOM AISR

CC: William Velander, Gustavo Larsen

Classification: UNCLASSIFIED
Caveats: NONE

Dr Carlson,
Yes, I agree with your change and justification. Thanks.
Dr Martini

-----Original Message-----
From: Carlson, Mark A [mailto:macarlso@unmc.edu]
Sent: Monday, August 20, 2012 10:41 AM
To: Dubick, Michael A Dr CIV USA MEDCOM AISR; Kheirabadi, Bijan Dr CIV USA MEDCOM AISR; Martini, Wenjun Dr CIV USA MEDCOM AISR
Cc: William Velander; Gustavo Larsen
Subject: 4public: Proposed migration to exclusive use of the swine model for USAMRMC# 10091006

Bijan Kheirabadi
Wenjun Martini
Mike Dubick
ISR, San Antonio

Project: Technologies for Hemostasis and Stabilization of the Acute Traumatic Wound (USAMRMC# 10091006)
Topic: Swine vs. Rabbit subjects

All,

I wanted to propose a change in the scientific protocol to the above study. Currently we are using a combination of rabbit and swine models in the development of our hemostatic devices. As you may recall during our visit to the ISR on April 3, 2012, my collaborators (Bill Velander and Gustavo Larsen) and I suggested the possibility of eliminating the rabbit model from this project, and performing all of the proposed procedures in swine. Recently my collaborators and I discussed this issue further, and we feel that it would be beneficial to move to exclusive use of the swine model, primarily because of cost, consistency, and relevance.

At our institution, we currently can obtain a 3 month, ~33 kg male swine for $100. The cost for a 3.2 kg rabbit is $192. The updated per diem costs for swine vs. rabbits at our institution are $8 and $4, respectively. At this per diem rate, the swine would have to be house for 23 extra days before the total costs would exceed that of a rabbit. Since this project consists of nonsurvival procedures only, it will be less expensive to use swine instead of rabbits.

In addition, my collaborators and I believe that swine model represents a more accurate model of severe clinical hemorrhage than the rabbit, particularly with respect to blood volume and the ability to tolerate blood loss. Because of this difference in modeling, it is possible that some of the acute studies in rabbits would need to be repeated in swine, for confirmation purposes. So we think it would make more sense just to perform all acute studies in swine.

Subject: RE: 4public: Proposed migration to exclusive use of the swine model for USAMRMC# 10091006 (UNCLASSIFIED)

Date: Tuesday, August 21, 2012 7:41:25 AM CT

From: Dubick, Michael A Dr CIV USA MEDCOM AISR

To: Carlson, Mark A, Kheirabadi, Bijan Dr CIV USA MEDCOM AISR, Martini, Wenjun Dr CIV USA MEDCOM AISR

CC: William Velander, Gustavo Larsen

Classification: UNCLASSIFIED
Caveats: NONE

This is still OK with us.

-----Original Message-----
From: Carlson, Mark A [mailto:macarlso@unmc.edu]
Sent: Monday, August 20, 2012 10:41 AM
To: Dubick, Michael A Dr CIV USA MEDCOM AISR; Kheirabadi, Bijan Dr CIV USA MEDCOM AISR; Martini, Wenjun Dr CIV USA MEDCOM AISR
Cc: William Velander; Gustavo Larsen
Subject: 4public: Proposed migration to exclusive use of the swine model for USAMRMC# 10091006

Bijan Kheirabadi
Wenjun Martini
Mike Dubick
ISR, San Antonio

Project: Technologies for Hemostasis and Stabilization of the Acute Traumatic Wound (USAMRMC# 10091006)
Topic: Swine vs. Rabbit subjects

All,

I wanted to propose a change in the scientific protocol to the above study. Currently we are using a combination of rabbit and swine models in the development of our hemostatic devices. As you may recall during our visit to the ISR on April 3, 2012, my collaborators (Bill Velander and Gustavo Larsen) and I suggested the possibility of eliminating the rabbit model from this project, and performing all of the proposed procedures in swine. Recently my collaborators and I discussed this issue further, and we feel that it would be beneficial to move to exclusive use of the swine model, primarily because of cost, consistency, and relevance.

At our institution, we currently can obtain a 3 month, ~33 kg male swine for $100. The cost for a 3.2 kg rabbit is $192. The updated per diem costs for swine vs. rabbits at our institution are $8 and $4, respectively. At this per diem rate, the swine would have to be house for 23 extra days before the total costs would exceed that of a rabbit. Since this project consists of nonsurvival procedures only, it will be less expensive to use swine instead of rabbits.

In addition, my collaborators and I believe that swine model represents a more accurate model of severe clinical hemorrhage than the rabbit, particularly with respect to blood volume and the ability to tolerate blood loss. Because of this difference in modeling, it is possible that some of the acute studies in rabbits would need to be repeated in swine, for confirmation purposes. So we think it would make more sense just to perform all acute studies in swine.

Appendix A4 (31 pages total)

A recombinant human fibrinogen that produces thick fibrin fibers with increased wound adhesion and clot density

Jennifer Calcaterra,[†] Kevin E. Van Cott,[†] Stephen P. Butler,[‡] Geun Cheol Gil,[†] Marta Germano,[§] Harrie A. van Veen,[§] Kay Nelson,[§] Erik J. Forsberg,[a] Mark A. Carlson,[b] and William H.Velander[†,*]

[†] Department of Chemical & Biomolecular Engineering, University of Nebraska, Lincoln, NE 68588-0643;
[‡] Department of Biochemistry, Virginia Polytechnic Institute and State University, Blacksburg, VA 24061;
[§] Pharming Group NV, Leiden, Netherlands 2300 AL;
[a] Formerly: Infigen, Inc., DeForest, WI, Currently: WiCell Research Institute, Madison, WI 53707-7365;
[b] Department of Surgery, University of Nebraska Medical Center and the Omaha VA Medical Center, Omaha, NE 68105

Human fibrinogen is a biomaterial used in surgical tissue sealants, scaffolding for tissue engineering, and wound healing. Here we report on the post-translational structure and functionality of recombinant human FI (rFI) made at commodity levels in the milk of transgenic dairy cows. Relative to plasma-derived fibrinogen (pdFI), rFI predominately contained a simplified, neutral carbohydrate structure and >4-fold higher levels of the γ'-chain transcriptional variant known to interact with Factor XIII. In spite of these differences, rFI and pdFI were kinetically similar with respect to the thrombin catalyzed formation of protofibrils and Factor XIIIa-mediated formation of cross-linked fibrin polymer. However, electron microscopy showed rFI produced fibrin with much thicker fibers with less branching than pdFI. *In vivo* studies in a swine liver transection model showed that relative to pdFI, rFI made a denser, more strongly wound-adherent fibrin clot that more rapidly established hemostasis.

Keywords:

Fibrinogen, fibrin polymer, recombinant protein, tissue adhesion, tissue sealant

1. INTRODUCTION

Known as coagulation Factor I (FI), fibrinogen is a complex protein which polymerizes to form a wound adherent fibrin barrier that stops bleeding and acts as a scaffold for healing.[1-4] During the healing process, the fibrin clot is enzymatically digested and reabsorbed.[2, 4] These characteristics make FI naturally useful as a biomaterial in surgical tissue sealants[5-7] and as an important tool in tissue engineering.[8-11] For decades, FI has been used in the treatment of hemorrhage incurred on battlefields, in civilian trauma[12] and in surgical procedures.[13] The therapeutic transplantation of tissue made from autologous cells frequently uses a provisional matrix made of cross-linked fibrin to help culture and then deliver layers of cells into debrided wound sites.[10] Because of its role in making fibrin polymer, FI is a protein present at a high concentration of 2-4 g/l in human plasma[14] and its clinical applications typically use large 0.1-2 gram doses.[5] Unfortunately, a safe and abundant supply of plasma-derived FI (pdFI) is limited worldwide by the availability of pathogen screened plasma.[15, 16] Surgical applications for tissue sealants[13] in the United States indicate that FI would need to be manufactured at amounts greater than several metric tons per annum (Supporting Information, Table S1).

In addition to the commodity amounts needed, the complexity of FI presents a significant biosynthetic challenge even to the capabilities of most mammalian cells. For example, after transcription of three separate genes, the human liver translates and assembles two Aα, two Bβ and two γ-polypeptides into hexameric FI having a molecular weight of 340 kDa.[17, 18] Assembly arises from the restrictive pooling of free chains within the endoplasmic reticulum prior to secretion as a holoprotein. In addition, there are two variations of the γ-chain. About 11% of pdFI contain a subpopulation of the γ-chain (γ') which is a result of an alternative mRNA splicing event that replaces the four amino acid residues on the carboxy-terminal of the γ-chain with a 20 amino acid fragment.[19, 20] The γ' and γ subpopulations are both physiologically important.[21-24] The main FI functions of activation, assembly into protofibrils and fibrin crosslinking are also affected by post-translational sulfation,[25] phosphorylation,[26] and glycosylation.[27, 28] Importantly,

the γ'-chain content and the post-translational modifications of FI have been associated with opposing changes in fibrin fiber diameter, porosity and degree of branching.[27, 29-31] Past reports show that the impact of increased γ' content on fibrin formation is slowed fibrin polymerization, decreased fiber diameter with increased branching that produces smaller pores.[29-31] In contrast, *in vitro* deglycosylation of FI produced fibrin structure with a larger fiber diameter, decreased branching and larger pores. Deglycosylation also resulted in increased polymerization rates but no change in the activation kinetics of FI.[27] The physiologic significance of FI with an *in vivo* modified glycoform has not been reported. Indeed, there is currently no clear understanding between altering FI structure and the hemostatic barrier function at a wound site.

Over the past two decades, we and other laboratories have studied the biosynthesis of recombinant human fibrinogen (rFI) made in the milk of transgenic mice.[32-35] However, the small amount of rFI produced in mice limited detailed molecular and material characterization where *in vivo* studies such as on fibrin tissue adhesion were not possible. Here we provide the first report on the biosynthesis and material characterization of rFI made in the milk of cloned, transgenic dairy cows. To our knowledge, rFI is one of the most challenging biomacromolecules to ever be produced in transgenic livestock. We evaluate the post-translational modifications made by the mammary epithelia relative to the human liver. The molecular function of the rFI *in vitro* is examined by turbidimetric and viscoelastic properties as related to the formation of fibrin protofibrils and a crosslinked fibrin clot. We also study the physical structure of rFI fibrin by electron microscopy. The hemostatic function and wound adhesion of rFI is examined in an *in vivo* porcine hepatic injury model and by immunohistochemistry of the fibrin-wound interface.

2. EXPERIMENTAL SECTION

2.1. Materials. All reagents were obtained from Sigma unless otherwise specified. Plasma-derived human thrombin (pdFIIa), plasma-derived FI (pdFI) depleted of plasminogen,

von Willebrand factor and fibronectin, and bovine fibrinogen (bFI) was bought from Enzyme Research Labs (South Bend, IN). Recombinant human thrombin (rFIIa) was purchased from ZymoGenetics (Seattle, WA). Anhydrous dimethyl sulfoxide (DMSO), sodium hydroxide, and methyl iodide were obtained from Sigma (St. Louis, MO). PNGase F was purchased from New England Biolabs (Beverly, MA).

2.2. Transgene construction. The use of bovine αS1-casein promoter to direct mammary epithelial expression has been previously described.[36] The complete 5.2 kbp human Aα, 7.6 kbp Bβ, and 8.5 kbp γ fibrinogen genes were cloned from a human genomic library contained within a P1-bacteriophage derived artificial chromosome (PAC) in *Escherichia coli* cells from Genome Systems, Inc. (St. Louis, MO). All three transgenes were constructed using the 6.2 kbp bovine αS1 casein 5'-upstream promoter linked to the genomic fibrinogen coding sequences followed by each chain specific 3'UTR. The following linearized transgene constructs resulted in a: 16.7 kbp 5'-bovine αS1-casein, α fibrinogen gene (Supporting Information, Figure S1A); a 18.3 kbp 5'-bovine αS1-casein, β fibrinogen gene (Supporting Information, Figure S1B); and 21.7 kbp 5'-bovine αS1-casein, γ fibrinogen gene (Supporting Information, Figure S1C). These constructs were co-transfected into a female genital ridge cell lineage using calcium phosphate precipitation (CalPhos, Clontech, Mountain View, CA) to make founder animals by nuclear transfer.[37]

2.3. Southern Blot analysis. Genomic cow DNA was isolated from blood using Broodram procedure and subjected to restriction enzyme digestion with either BsrGI, HindIII or BglII as per the manufacturer's instructions (New England BioLabs, Ipswich, MA). Digests were loaded on a 0.8% agarose gel and subjected to electrophoresis for 4 hours at 120V. The gel was washed in 0.25N HCl for 15 min then 0.5N NaOH for 30 min before transferring to a MagnaCharge membrane (GE Healthcare, Uppsala, Sweden) using the Turbo blot system from BioRad (Hercules, CA). The αS1 casein probe was generated by PCR using Kirkegaard & Perry Laboratories's (KPL) Detector Biotinylation kit (Gaithersburg, MD). The 500 bp probe

corresponding to a region from 200 to 700 bp upstream from transcriptional start in the casein gene (5' UTR promoter region) was used to detect the endogenous αS1 gene and each fibrinogen transgene. After crosslinking, the membrane was probed and detected using the KPL AP-Chemiluminescent Blotting kit per manufacturer's instructions. Hybridization was carried out at 50°C and high stringency wash at 60°C.

2.4. Purification. rFI was purified from 32 liters of milk collected on eight lactation days from two transgenic cows (Foxy and Fantasy) of the BFI2n8c83-EGFIneo lineage. Processed in 4L batches, rFI was purified by a two-column purification procedure using cation exchange (CIEX) and hydrophobic interaction chromatography (HIC). Transgenic milk was clarified by adding ethylene diamine tetracetic acid (EDTA) to a final concentration of 50 mM and defatted by centrifugation (1600g, 20 min, 4°C). The clarified milk loaded on a Fractogel EMD SE (Merck, Darmstadt, Germany) column (10/20 cm) equilibrated in 20 mM sodium phosphate, pH 7.0. After loading, the column was washed with five volumes of the same buffer and bound proteins were eluted with a linear salt gradient from 0 to 0.5 M NaCl in 10 column volumes at a linear flow rate of 60 cm/h. Elution fractions containing rFI were pooled, diluted (1:1) with 1 M ammonium sulphate and loaded on a Butyl Sepharose (GE Healthcare, Uppsala, Sweden) column (10/15 cm) equilibrated in 50 mM sodium phosphate pH 7.0 + 0.5 M ammonium sulphate. After loading and washing, the column was eluted with a linear salt gradient from 0.5 to 0 M ammonium sulphate in 10 column volumes at a linear flow rate of 60 cm/h. Elution fractions containing rFI were pooled, concentrated and buffer exchanged to 20 mM sodium citrate pH 7.0 + 0.15 M NaCl. Purified rFI from the 4L processing batches were pooled. The purified protein was subsequently filtered over 0.22 μm and stored at -70°C until use. The step yields of the column purifications were ~60%; the overall yield of rFI was ~40%. Purity was evaluated by size exclusion chromatography. After being passed through a 0.20 μm nylon filter (Millipore, Billerica, MA), 0.5 ml of purified rFI was passed through a TSK-G3000SW$_{xL}$ (Tosoh Biosciences, South San Francisco, CA) column (14 ml, 30 cm length, 7.8 mm ID) attached to a

Knauer HPLC System at 0.5 ml/min for 45 minutes and data were collected by a photodiode array (PDA) with a 1 mm flow cell and analyzed by EZChrom Elite software.

2.5. SDS-PAGE and Western blot. Nonreduced and reduced FI samples of purified pdFI, rFI and bovine fibrinogen (bFI) and transgenic and non-transgenic milks were evaluated by sodium dodecylsulfate-polyacrylamide gel electrophoresis (SDS-PAGE) on 4-12% NuPage® Bis-Tris gels (Invitrogen, Carlsbad, CA). Gels were then stained with Colloidal Blue (Invitrogen, Carlsbad, CA) or electroblotted onto Immun-Blot™ polyvinylidene fluoride (PVDF) membranes (BioRad, Hercules, CA) for immunobloting. Blots were probed with a polyclonal antibody for human FI (USBiological, F4200-07C, Swampscott, MA).

2.6. γ- and γ'-chain content. FI samples (200 µg) were deglycosylated with Peptide N-Glycosidase F (PNGase F, New England Biolabs, Ipswich, MA), adjusted to 3M GuHCl, reduced for one hour with tris(2-carboxyethyl)phosphine (TCEP, 5 mM final concentration, Pierce, Rockford, IL), alkylated for 30 minutes with iodoacetamide (15 mM final concentration), and then adjusted to 0.2% (v/v) formic acid. Analysis was performed on an Agilent 6210 ESI-TOF MS with an Agilent 1200 capLC using liquid chromatography coupled to electrospray time-of-flight mass spectrometry (LC-ESI-TOF-MS). The column was an Agilent Poroshell 300SB-C8 with dimensions of 0.5 mm ID and 7.5 mm L (Agilent Technologies, Santa Clara, CA). The flow rate was 20 microliters/minute, and the gradient program consisted of injection in 5% acetonitrile (HPLC-grade) in 0.1% formic acid followed by washing and then a linear gradient of 1%/minute to 55% acetonitrile in 0.1% formic acid. MS data were acquired in positive mode. The raw data were deconvoluted with Agilent's Qualitative Analysis software (v B.01.03) to generate the zero-charge spectra. The corresponding peak abundances were used to estimate the amounts of each species.

2.7. Fibrinopeptide phosphorylation. Fibrinopeptides A (FpA) and B (FpB) were obtained by incubating rFI and pdFI (10 mg/ml) with rFIIa (236 U/ml) at 37°C for 60 min. Phosphorylation was identified by a LC-MS/MS system which included a Dionex U3000 nanoflow HPLC system

with a UV detector and an Applied Biosystems 4000 Q-Trap triple quad/ion trap mass spectrometer. The samples were injected onto a Dionex Acclaim Pepmap C18 trap column (Thermo Scientific, Rockford, IL) and the peptides were eluted by a linear gradient of 15-40% acetonitrile in 0.1% formic acid. Data were analyzed manually to confirm phosphorylation sites using theoretical m/z values calculated from the UCSF Protein Prospector MS-Product website and Analyst 1.4.2. The fibrinopeptide release chromatograms showed that the FpA from pdFI consisted of two peaks: a fronting shoulder that accounted for ~20-30% of the peak area, and the main peak. The fronting shoulder is the phosphorylated at Ser3. Comparison of the rFI FpA elution time indicated that the majority of rFI was phosphorylated at Ser3. This was confirmed by LC-MS/MS analysis as described in supplemental data.

2.8. Glycosylation analysis. Sialylation profiling of rFI N-glycans was performed by normal phase high performance liquid chromatography (NP-HPLC) using the method of Anumula and Dhume.[38] For ESI-MS/MS analysis of the glycans, rFI was incubated with PNGase F. Released N-glycans were separated from proteins using C18 Extract Clean columns (100 mg, 1.5 mL, Alltech, Deerfield, IL), eluted with 2 × 0.5 mL of solvent 0.1% (w/v) TFA in 50% acetonitrile/50% water, and dried by speed-vac (Labconco CentriVap, Kansas City, MO). The dried glycan sample was dissolved with a DMSO/NaOH suspension (100 µL) in 1.5mL centrifuge tube, and allowed to sit at room temperature for 30 minutes with occasional vortexing. Methyl iodide (50 µL) was added and the mixture was vortexed for 60 minutes. After the reaction, 100 µL of DMSO/NaOH suspension and 50 µL of methyl iodide were added again and vortexed for 60 minutes. 500 µL of chloroform was added and washed repeated with ice-chilled water until the aqueous phase became neutral. The organic phase was dried under speed vac for MS analysis. MS analysis was performed on a 4000 Q-Trap hybrid triple quadruple/ion trap system (Applied Biosystems, Foster City, CA) with a MicroIon Spray II ion source. Premethylated N-glycan was prepared in 70% acetonitrile/30% water. The sample solution was directly infused using a syringe pump at 0.3 µL/min. Possible structures were proposed by

analyzing MS spectra and searching theoretical precursor ion mass on web-based Glycomod. The structures were determined by analyzing the corresponding MS/MS spectra and matching with calculated fragment ion mass consistent with the precursor ion definition using Glycoworkbench.[39]

2.9. Thrombin-catalyzed activation. The thrombin-catalyzed release of fibrinopeptides A (FpA) and B (FpB) from rFI and pdFI (Enzyme Research Labs, South Bend, IN) was determined based on the method from Gorkun et al.[40] Two levels were used: 1) pdFI or rFI (0.1 mg/ml) incubated with rFIIa (0.01 U/ml) as described previously;[40] and 2) pdFI or rFI (0.5 mg/ml) incubated with rFIIa (0.05 U/ml). Reversed-phase high-performance liquid chromatography (HPLC) was used to monitor fibrinopeptides on a Waters 2695 Alliance with a Waters 2996 PDA detector using a Jupiter C18 column (300 Å, 2 mm x 150 mm, 5 µm particles) (Phenomenex, Torrance, CA). Waters Empower software was used to generate calibration curves (R^2>0.996 for FpA and FpB) using commercial standards (Sigma, St. Louis, MO) and integrate peak areas for quantification. Results from duplicates were averaged and plotted at each time point. Data were plotted as percent release with respect to time assuming 100% release at 180 minutes.

2.10. Thrombin-catalyzed protofibril formation. Polymerization of pdFI and rFI after treatment with thrombin was measured by changes in turbidity over time at 350 nm with a Beckman Coulter General Purpose spectrophotometer (Brea, CA) as previously described.[40] pdFI or rFI (0.2 or 9 mg/ml) was loaded into a 10 mm optical path microcuvette. Thrombin (0.1 U/ml or 106 U/ml, respectively) was added. The change in turbidity was monitored at 350 nm for 30 minutes at 25^{o}C.

2.11. Factor XIIIa catalyzed molecular crosslinking. Activated recombinant factor XIIIA subunit (rFXIIIa) was produced in *Pichia pastoris* as previously described.[41] The specific activity of the rFXIIIa was measured to be 7,000 U/mg using Pefakit (Pentapharm, Norwalk, CT). pdFI (Enzyme Research, South Bend, IN) was depleted of constitutive FXIII contamination by immunoaffinity purification using an anti-FXIII monoclonal antibody (Green Mountain Antibodies,

Burlington, VT). Crosslinking of FI by rFXIIIa was analyzed as previously described.[40] rFI or pdFI (0.38 mg/ml) was incubated with rFIIa (1 U/ml) and four levels of rFXIIIa (1, 25, 50 and 100 U/ml) for 0, 2.5, 5, 10 and 15 minutes at 24°C. FI was also incubated with thrombin without rFXIIIa for 15 minutes, respectively. Crosslinking was studied by reducing SDS-PAGE (4-12% Bis-Tris NuPAGE) stained with Colloidal Blue (Invitrogen, Carlsbad, CA). The pdFI and rFI samples treated with rFIIa and 25 U/ml rFXIIIa for 15 minutes were electroblotted onto polyvinylidene fluoride (PVDF) membrane (Millipore, Billerica, MA) by applying 30 volts for one hour and stained with Colloidal Blue. The bands at approximately 130 and 150 kDa were excised and the first ten amino acids in the N-terminal of each were sequenced by Edman degradation with an Applied Biosystems 494 Procise automated sequencer. N-terminal sequencing was performed by the University of Nebraska Medical Center's Protein Structure Core Facility.

2.12. Viscoelastic characterization. Clot kinetics and strength were evaluated by thromboelastography (TEG) which was performed on solutions containing purified rFI or pdFI, rFXIIIa and rFIIa with a Thromboelastograph® (TEG®) Hemostasis System 5000 series (Haemoscope Corp., Niles, IL). rFI or pdFI (9 mg/ml) was incubated at 37°C with rFIIa (53 U/ml) with rFXIIIa (2,429 U/ml). As a reference, normal citrated human blood (340 µl, N = 20 donors) was combined with 200 mM $CaCl_2$ (20 µl) as instructed by the TEG manufacturer. The TEG Analytical Software (version 4.2.2, Haemoscope, Niles, IL) calculated time to clot initiation (R), time to achieve a clot firmness of 20mm (K) and maximal clot strength (MA). Each sample was run in triplicate so mean and standard deviation could be calculated. The data were exported and analyzed in Microsoft® Excel.

2.13. Scanning electron microscopy. Scanning electron microscopy was utilized to examine the structure of fibrin clots formed by rFI and pdFI. FI (0.5 mg/ml) was incubated with rFIIa (0.5 U/ml) for one hour at room temperature. Samples underwent 2.5% glutaraldehyde fixation, stepwise ethanol and hexamethyldisilazane dehydration, and sputter coated with gold-

palladium. Clots were imaged by a scanning electron microscope (S4700 Field-Emission SEM, Hitachi, Tokyo, Japan) at 15 kV and a magnification of 10,000x. Average fiber diameters were measured from 20 fibers. The number of branch points was determined in ten 1.4 μm^2 areas. Fiber diameters and branch points were statistically compared by *t* test with an α of 0.05.

2.14. Tissue sealant function. Crossbred commercial (domestic) swine obtained from UNL Agricultural Research and Development Center (Mead, NE) were anesthetized with isoflurane (1-2%) supplemented with oxygen (1-2 L/min) throughout the procedure. A carotid arterial catheter for pressure monitoring and blood sampling, and a jugular venous catheter for fluid and medication administration were placed via surgical cutdown in the left neck. Blood samples from each pig were drawn before, during and after surgery and tested by thromboelastography (TEG) to identify and select pigs with normal clotting parameters and to monitor changes in endogenous coagulation parameters throughout surgery due to blood loss or haemodilution by Lactated Ringers solution. The liver was exposed through a midline incision. A scissoring injury clamp[42-44] with X-shaped blades (5 cm width and breadth) was applied through the central portion of the liver, adjacent to the vena cava as described previously.[12] The resultant injury was a jagged, stellate laceration 8-10 cm in diameter, completely through the organ. Such injuries were treated in 10 pigs with LFS (7 mg/ml pdFI or rFI (N = 1 and 9, respectively), 1,740 U/ml rFXIIIa, 85 U/ml rFIIa, 12 mM $CaCl_2$; total of 6 ml) applied with a Tisseel® Duploject® dual-syringe system (Baxter Healthcare Corporation) over 30 seconds to several minutes followed by 3-5 minutes of manual compression. Euthanasia was performed while the animal was under deep isoflurane anesthesia. Sodium pentobarbital (380 mg/mL, 10 mL IV) was administered, and 1 minute later the animal underwent bilateral diaphragm incisions with transection of the supradiaphragmatic vena cava and aorta. All procedures performed during this research were approved by the Institutional Animal Care and Use Committee of the Omaha VA Medical Center.

2.15. Immunohistochemistry. Adherence of the human fibrin made from rFI and pdFI to wounded tissue was examined by immunohistochemistry. Wedge-shaped hepatic excisions (base of 1 cm and height of 1 cm) were made along a lobar edge. Fibrin sealant (FS), consisting of 9 mg/ml FI (pdFI or rFI), 2,460 U/ml rFXIII, 106 U/ml rFIIa and 12 mM $CaCl_2$, was applied by spray device to the wound for about 35 seconds. Approximately 18 mg FI, 5,000 U rFXIIIa and 210 U rFIIa was applied to each wedge. Liver sections from untreated and rFI and pdFI sealant treated wedge excisions were fixed in 10% neutral-buffered formalin, dehydrated and embedded in paraffin. Specimens were sliced (5 μm), mounted on slides, dewaxed and processed with Dako TRS antigen retrieval solution (Dako, Carpentaria, CA). After blocking endogenous alkaline phosphatase and peroxidase activity, the specimens were incubated with an anti-porcine fibrinogen antibody (Kamiya Biomedical Company, Seattle, WA) and exposed with HRP/DAB+. After blocking remaining peroxidase activity associated with the anti-porcine fibrinogen antibody, specimens were incubated with an anti-human fibrinogen antibody (Abcam, Inc., Cambridge, MA) and exposed by alkaline phosphatase-based Permanent Red (Dako, Carpentaria, CA). The specimens were subsequently conterstained with Mayer's hematoxylin. DAKO EnVision™ G|2 Doublestain System (Dako, Carpentaria, CA) was used for signal detection.

3. RESULTS

3.1. Somatic cell transfection and nuclear transfer. The characterization of the transgenic cow clonal lineage BFI2n8c83-EGFIneo (termed "Fancy") is presented here as an example of a stable, cloned α-S1 casein-FI genotype. Using Southern analysis, we characterized the presence of each of the three α-S1 casein-FI transgenes (Supporting Information, Figure S1D) in Fancy's DNA isolated from leukocytes harvested from whole blood. Three restriction endonuclease digestions were chosen to yield fragments containing a common

element of the α-S1 casein promoter while having differently sized sequences unique to each fibrinogen gene. The specificity of the probes for each of the BsrGI, HindIII, and BglII digests of Fancy's and control bovine DNA was demonstrated by the presence of endogenous casein signals in both. The control DNA lacked signals associated with the human FI sequences of the reference transgene mixture. In contrast, Fancy's DNA contained hybridization signals specific to the digests of the reference α-S1 casein rFI transgene mixture and eight or more copies of each Aα-, Bβ- and γ-transgene. Two other cows of the Fancy clonal lineage (Foxy and Fantasy) showed similar copy numbers and Southern analysis results.

3.2. rFI assembly, concentration and purification. Fancy's milk was collected, skimmed and the resulting skimmed milk examined using Colloidal blue stained SDS-PAGE and Western analysis under non-reducing (Figure 1 A and B, lane 8) and reducing (Figure 1 C and D, lane 8) conditions. We estimated the concentration of assembled rFI in the milk to be 2-4 g/L in three cows of the Fancy clonal lineage using densitometric analysis of Western blots with human pdFI as a reference. Western analysis using a polyclonal antibody confirmed the identity of the main 340 kDa species as assembled human FI. The M_r of Aα-, Bβ- and γ-chains of pdFI and rFI were nearly identical at about 66.5, 52.0 and 46.5 kDa, respectively (Figure 1 C and D) with a stoichiometric presence of 1:1:1 as analyzed by SDS-PAGE. The Aα-chain of pdFI and rFI appeared as doublet bands which has been reported previously for pdFI.[45] SDS-PAGE partially resolved γ- and γ'-chains (Figure 1C, lane 4). The hexameric nature of pdFI and rFI was corroborated by the 340 kDa M_r under nonreducing conditions. Some smaller amounts of FI reactive species with higher and lower M_r than the 340 kDa band were present in the skimmed milk (Figure 1B, lane 8). Some of these species were similar to those found in pdFI (Figure 1B, lane 2) and thus could have been unassembled Aα-chains.

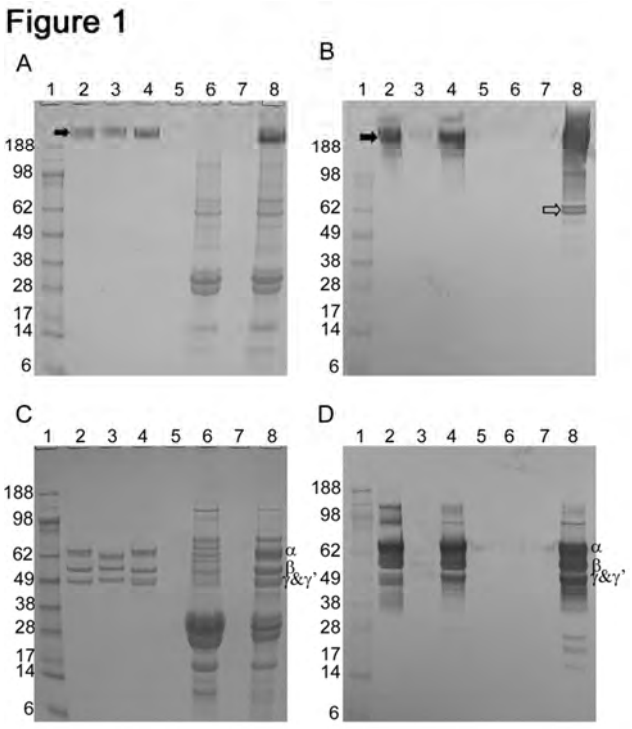

Figure 1. Expression of rFI in bovine milk. rFI expressed in the milk of transgenic cows was evaluated by SDS-PAGE gel electrophoresis under (A) nonreducing and (C) reducing conditions and Western Blot probed with goat polyclonal antibody for human FI under (B) nonreducing and (D) reducing conditions. Each panel contains a molecular weight marker (*lane 1*), purified, human pdFI (*lane 2*), bovine pdFI (*lane 3*), transgenic human rFI (*lane 4*), a blank lane (*lane 5*), nontransgenic skimmed cow milk (*lane 6*), a blank lane (*lane 7*) and transgenic skimmed cow milk (*lane 8*). The Mr of the assembled fibrinogen (340 kDa) is indicated by closed arrows in the upper panels and each individual Aα, Bβ and γ-chains of FI are indicated by α, β, and γ&γ', in the lower panels. The open arrow indicates free Aα.

For the analysis presented here, approximately 38 g of rFI was purified from 32 L of milk from eight lactation days of two transgenic cows (Foxy and Fantasy). As detected by electrophoresis, rFI was purified to a single species using a two-step sequence of cation exchange (CIEX) and hydrophobic interaction chromatography (HIC). The purity was estimated to be >98% (Figure 1 A and C, lane 4 and Figure S2 in Supporting Information) with a yield of >40%. Purified rFI was examined for the presence of bovine fibrinogen (bFI). Differences in the molecular size of assembled pdFI, bFI and rFI samples were readily discriminated from each other using SDS-PAGE under reducing conditions (Figure 1C). The side-by-side comparison of the individual FI chains using electrophoresis and LC-ESI-TOF-MS showed no discernible contamination of bFI in the rFI sample. The bFI content in this sample is likely to be <2%.

Taken together, rFI was sufficiently isolated from other milk proteins enabling the characterization of its structure and related biological activity *in vitro* and *in vivo*.

3.3. γ- and γ'-chain content. The γ' content of rFI was investigated using mass spectrometry on deglycosylated, reduced, and alkylated samples. The theoretical molecular weight (MW_{avg}) for the γ and γ' chains after this sample treatment is 47,039 and 49,054 Da, respectively, with each sulfation adding 80 Da to the γ'-chain. In both pdFI (Figure 2A) and rFI (Figure 2B), the γ-chain (47,039 Da) was the major translated species (extra carbamidomethylation of the γ-chain, an artifact of the sample processing, is seen in both pdFI and rFI). The γ'-chain of pdFI is sulfated at Tyr418 and/or Tyr422.[25] The C-terminal γ' peptide has two potential sites of Tyr-sulfation. pdFI essentially had all doubly-sulfated γ' (theoretical molecular weight 49,214 Da). We observed evidence of partial sulfation within the γ'-chain of rFI (theoretical molecular weight 49,134 Da). Accounting for all observed forms of the γ- and γ'-chains in the deconvoluted spectra, there was >4-fold higher γ' in rFI than the pdFI reference.

Figure 2

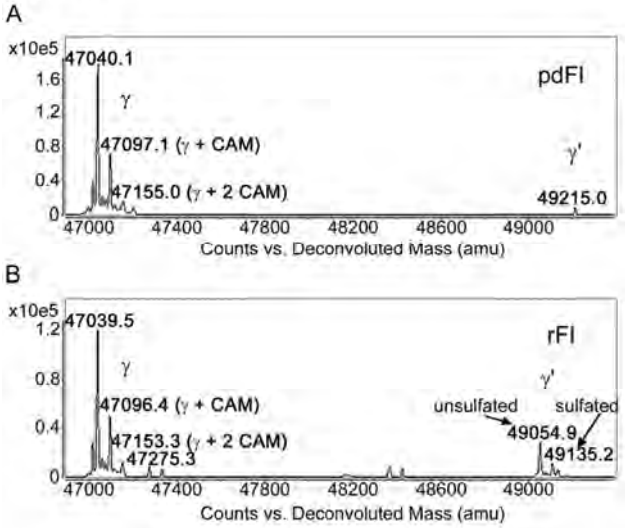

Figure 2. LC-ESI-TOF-MS analysis of γ' content. pdFI (A) and rFI (B) were treated with PNGase F, reduced, and alkylated. The total γ- vs. γ'-chain analysis indicated a >4-fold higher γ' content in rFI compared to pdFI. Extra alkylation of γ resulting from carbamidomethylation is annotated as γ + CAM.

3.4. rFI biochemical features. Phosphorylation, sulfation and glycosylation of rFI were analyzed by HPLC and LC-MS. The degree of phosphorylation of fibrinopeptide A (FpA) of rFI and reference pdFI after treatment with thrombin was evaluated by reverse phase C-18 HPLC (Figure 3A) and confirmed by LC-MS/MS (Figure 3B). Greater than 90% of the transgenic FpA was phosphorylated in contrast to 20-30% phosphorylation of FpA from the pdFI reference.

Figure 3

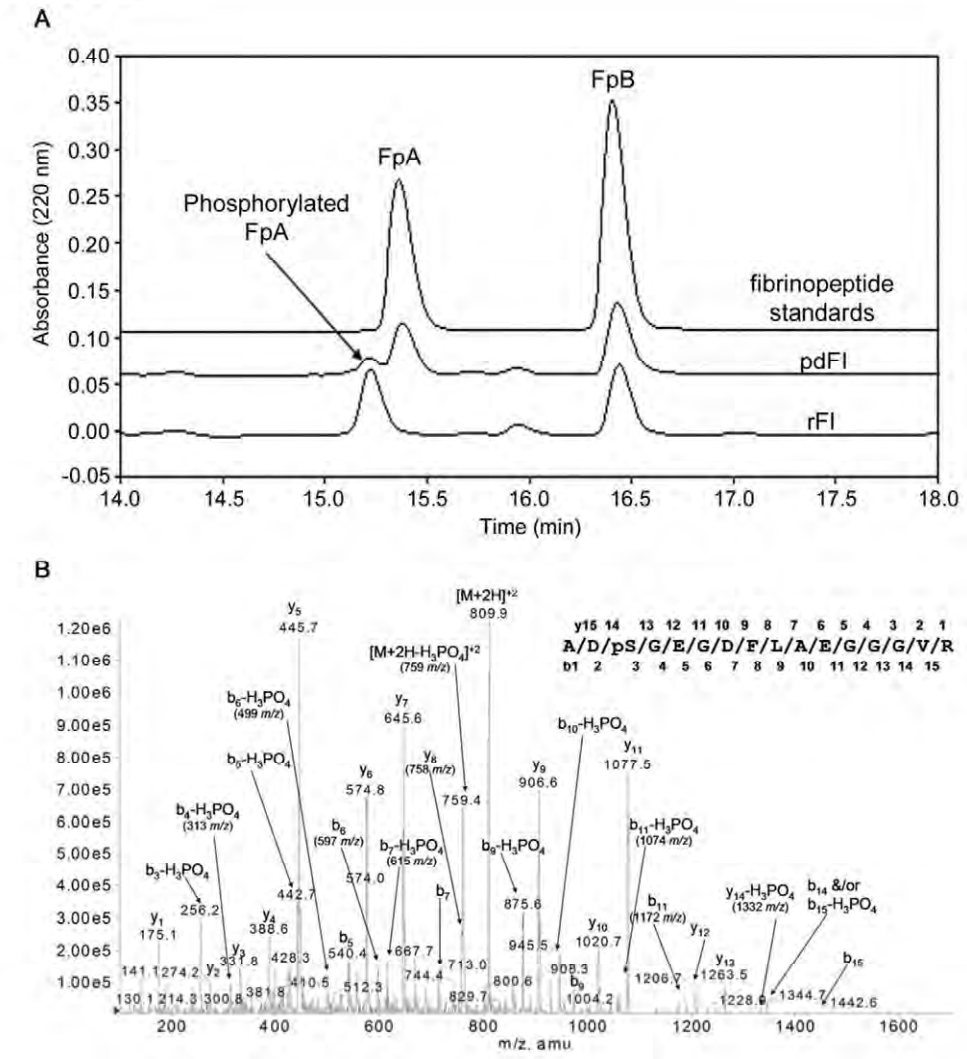

Figure 3. Fibrinopeptide phosphorylation of rFI. (A) Phosphorylation of fibrinopeptides. FpA and FpB released into the supernatant from fibrin clots formed by the treatment of pdFI and rFI (10 mg/ml) with thrombin (236 U/ml) were analyzed by C-18 HPLC and LC-MS as described in the experimental protocol. Synthetic FpA and FpB peptides were used as non-phosphorylated reference standards. Peak assignment is indicated above the corresponding peaks. (B) MS/MS spectrum of FpA released from thrombin treatment of rFI, confirming phosphorylation at Ser3. In CID, phosphorylated serine residues undergo a characteristic neutral loss of H_3PO_4 (98 amu). This characteristic loss is evident for the

precursor ion ($[M+2H - H_3PO_4]^{+2}$ = 759 m/z), the *b* fragment ions starting with b_3 ($b_3 - H_3PO_4$ = 256 *m/z*), and the y_{14}- H_3PO_4 (1332 *m/z*). These results lead to the conclusion that Ser3 is phosphorylated.

Glycosylation is a primary determinant of the clearance of glycoproteins in circulation by the liver.[46] Potential sites of N-glycosylation in pdFI and rFI are at Asn364 of the Bβ-chain and Asn42 of the γ-chain where the glycans in pdFI are biantennary complex glycans with one or two sialic acids.[47] Glycosylation of the purified rFI samples was investigated by normal phase HPLC profiling and mass spectrometry. The results of the HPLC profiling for pdFI were consistent with biantennary complex glycans with one or two sialic acids (Figure 4A); however, the majority of the N-linked glycans in rFI were neutral structures (Figure 4B). N-glycans were enzymatically released from rFI and permethylated for MS and MS/MS analysis. The N-glycans of rFI were a mixture of high mannose, neutral complex, and hybrid glycans (Figure 4C). These structures displayed a whey protein glycan signature similar to those observed with bovine lactoferrin.[48] A small amount of rFI N-glycans containing one sialic acid likely were degraded during permethylation. In summary, the post-translational modifications of rFI displayed a milk protein signature which was different than that of pdFI.

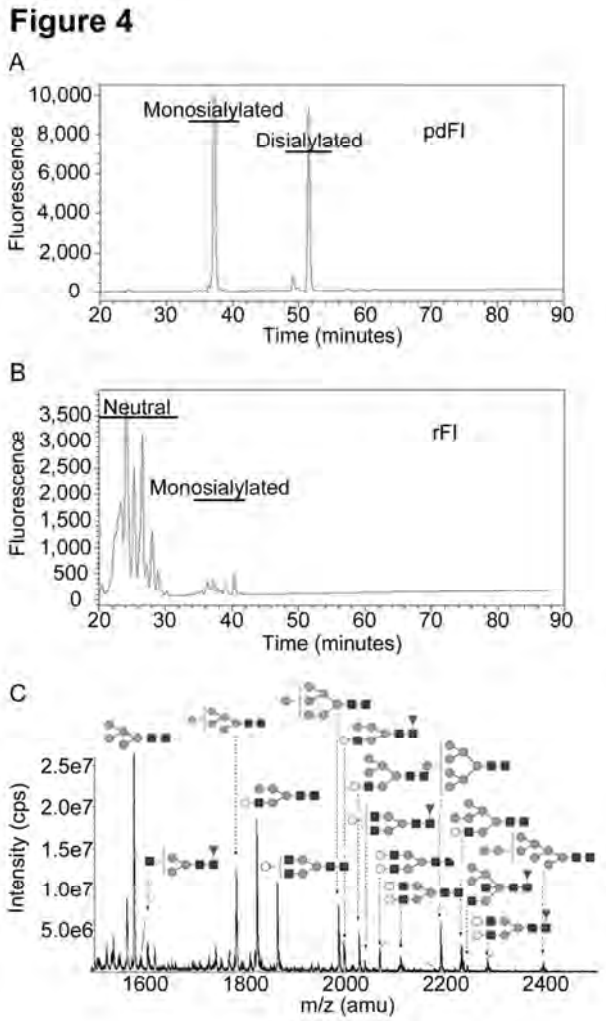

Figure 4. Biochemical features of rFI. N-glycans released by PNGase F from purified samples of pdFI and rFI were analyzed by HPLC (A and B) and mass spectrometry (C). In Panels B and C, the elution times of neutral, monosialylated, and disialylated species are indicated. In Panel D, the ESI-MS spectrum and the identified representative structures of permethylated rFI N-glycans (present as sodium adducts) are given. Identities were assigned based on the molecular mass consistency with the standard N-glycan biosynthesis scheme, and with the help of MS/MS analysis. ■ = GlcNAc; ● = Man; ▲ = Fuc; ○ = Gal; □ = GalNAc.

3.5. Activation kinetics. The thrombin-catalyzed release of fibrinopeptides A (FpA) and B (FpB) was monitored by HPLC. We studied FpA and FpB release using previously reported FI and thrombin concentrations[40] (Figure 5A) and at 5-fold higher FI and thrombin concentrations (Figure 5B) to compare pdFI and rFI activation kinetics. At both levels, FpA and FpB release kinetics were similar for pdFI and rFI in that both showed the slower release of FpB relative to FpA. Hence, the activation of rFI and pdFI were similar.

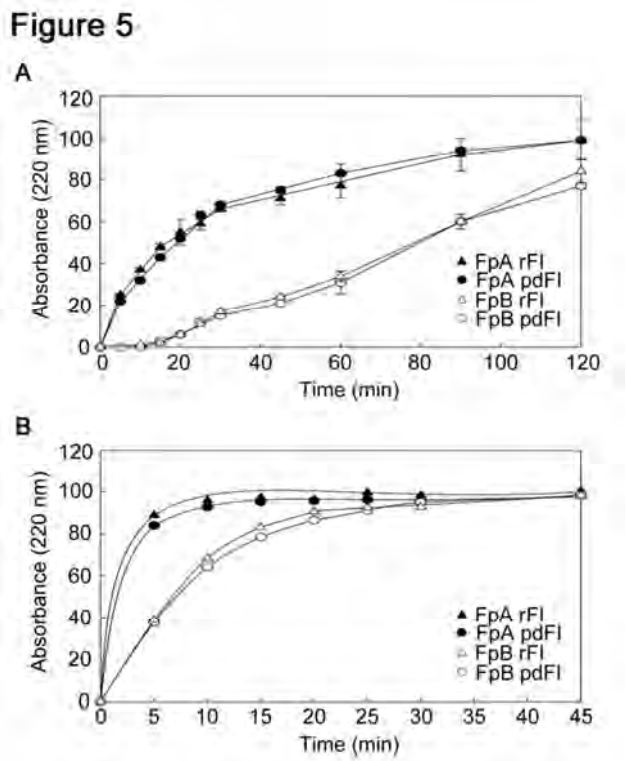

Figure 5. Activation kinetics of pdFI and rFI. The time course of the release kinetics of FpA and FpB was analyzed by HPLC at two levels: (A) rFI and pdFI (0.1 mg/ml) incubated with thrombin (0.01 U/ml), and (B) rFI and pdFI (0.5 mg/ml) incubated with thrombin (0.05 U/ml).

3.6. Fibrin protofibril formation. The rates of protofibril formation of pdFI and rFI activated by thrombin in the absence of added FXIIIa were measured by the change in turbidity (Figure 6). At 0.2 mg/mL FI and 0.1 U/mL recombinant thrombin (rFIIa), the initiation of protofibril formation as measured by the time to initial onset of turbidity was slightly faster for pdFI than rFI (Figure 6A). The rate of increase in turbidity, which is indicative of protofibril assembly,[40] and final absorbance, which is indicative of fiber diameter,[29, 30] were similar for pdFI and rFI. At 9 mg/mL FI and 106 U/mL rFIIa, the initial onset of turbidity was similar; however, the maximum absorbance was greater for pdFI than for rFI (Figure 6B). In summary, the assembly of protofibrils of activated rFI was similar to pdFI but showed some differences in asymptotic behavior as measured by turbidity.

Figure 6

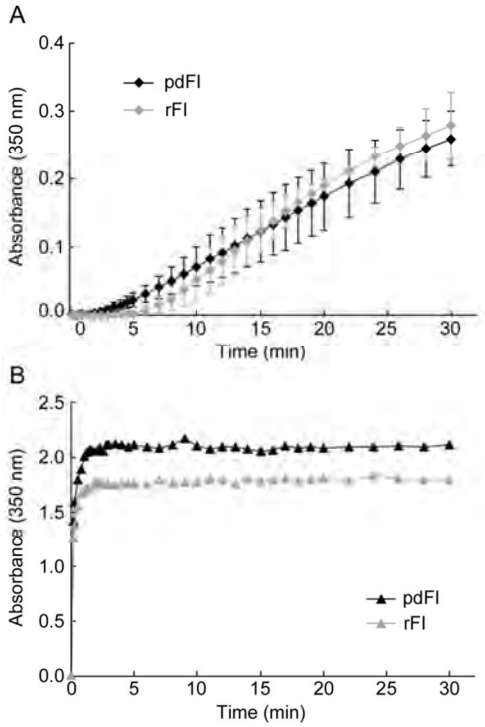

Figure 6. Fibrin protofibril formation of pdFI and rFI. Polymerization of pdFI and rFI at 0.2 mg/ml (A) and 9 mg/ml (B), initiated at time 0 with thrombin 0.1 U/ml and 106 U/ml, respectively, was monitored as the change in turbidity at 350 nm for 30 min.

3.7. Molecular crosslinking. We investigated the time course of polymerization of rFI and pdFI (0.38 mg/mL) treated with rFIIa (1 U/mL) and rFXIIIa (25 U/mL) by SDS-PAGE analysis under reducing conditions. An insoluble fibrin clot, which dissolved after treatment with reducing agent and SDS at 74^{o}C, was observed in all samples treated with rFXIIIa. The normal constitutive level of FXIII contamination present in pdFI preparations was observable by the appearance of γ-γ dimers after treatment by rFIIa alone (Figure 7A, lane 8).[49] In contrast, the absence of FXIIIa activity in the rFI was evident as no γ-γ dimers were formed after the addition of rFIIa alone (Figure 7B, lane 8). Two and a half minutes after treatment of pdFI or rFI with rFIIa, we observed a 1.5 kDa shift to lower M_r of the Aα- and Bβ-chains indicating a nearly complete conversion to their activated counterparts resulting from the release of FpA and FpB (pdFI: Figure 7A; rFI: Figure 7B). When rFXIIIa was added exogenously, γ-γ dimers between fibrin subunits of pdFI and rFI were formed at similar rates. The rate of α-chain polymerization

was similar for pdFI and rFI over the 15 minute incubation period. Similar multimerization patterns were observed for pdFI and rFI. N-terminal sequencing indicated that the band at approximately 130 kDa was an α-chain multimer (Figure 7 A and B, open arrow) and the band at approximately 150 kDa was a γ-chain multimer (Figure 7 A and B, closed arrow). Thus, rFI was kinetically similar to pdFI with respect to its molecular processing to a crosslinked fibrin clot.

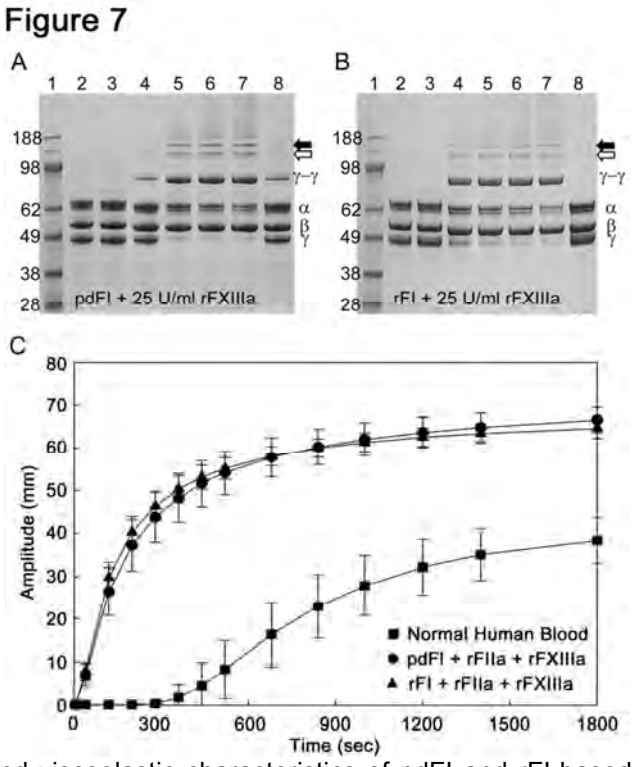

Figure 7. Crosslinking and viscoelastic characteristics of pdFI and rFI-based tissue sealants. Purified samples of pdFI and rFI (0.38 mg/ml) were treated with rFIIa (1 U/ml) and rFXIIIa at 25 U/ml (A and B, respectively). Reactions were quenched and then analyzed by SDS-PAGE under reducing conditions. Each panel has a molecular weight marker (*lane 1*). *Lane 2* contains pdFI (A) or rFI (B) prior to rFXIIIa and rFIIa treatment; *lanes 3 through 7*: FI, rFXIIIa and rFIIa incubated for 0, 2.5, 5, 10 and 15 minutes; *lane 8*: FI incubated with rFIIa only for 15 minutes. The Aα-, Bβ- and γ-chains (66, 52 and 46 kDa, respectively) of pdFI or rFI are indicated by α, β, and γ, γ- γ indicates the cross-linked γ-chains. As detected by N-terminal sequencing, the open arrow indicates an α-chain multimer and the closed arrow indicates a γ-chain multimer. Thromboelastographic comparison of rFI- and pdFI-based tissue sealants (C). TEG analysis of the kinetics of clot initiation and clot strength over time for pdFI and rFI (9 mg/ml) after treatment with rFIIa (53 U/ml) and rFXIIIa (2,429 U/ml).

3.8. Viscoelastic properties. The function of fibrin as a barrier to bleeding can be related to its viscoelastic strength. The evolution of viscoelasticity during the formation of a crosslinked

fibrin clot from rFI and pdFI were compared by TEG (Figure 7C). We used an optimized tissue sealant formulation of rFIIa, rFXIIIa and rFI or pdFI to study the differences in clot strength and viscoelastic kinetics. The average viscoelastic behavior of 20 individual human blood samples strongly contrasts the rapid clotting behavior and high strength of both rFI and pdFI. The time to clot initiation was similar for rFI (18 ± 6 sec) and pdFI (20 ± 0 sec) ($p = 0.64$, $\alpha = 0.05$). The maximum viscoelastic strength of the developing clot was about 65 mm (9,573 ± 1,115 dynes/cm^2) for pdFI and about 63 mm (8,637 ± 867 dynes/cm^2) for rFI ($p = 0.32$, $\alpha = 0.05$). In summary, both the kinetics of crosslinked fibrin clot formation and the clot strengths were equivalent for rFI and pdFI.

3.9. Scanning electron microscopy. The structure of clots formed by pdFI and rFI were compared by scanning electron microscopy (Figure 8). The fibrin from rFI had thicker fibers with larger pores and less branching than the fibrin from pdFI (Table 1). The average fiber diameter of the pdFI clot (0.10 ± 0.02 μm) was similar to diameters measured previously.[30, 31] The average fiber diameter of the rFI clot (0.19 ± 0.04 μm) was significantly greater than that of pdFI ($p < 0.001$, $\alpha = 0.05$). In contrast, the rFI fibrin clot had a significantly lower proportion of branch points per area than the pdFI fibrin clot (3.0 ± 1.4 vs. 6.0 ± 1.9; $p < 0.001$, $\alpha = 0.05$).

Figure 8

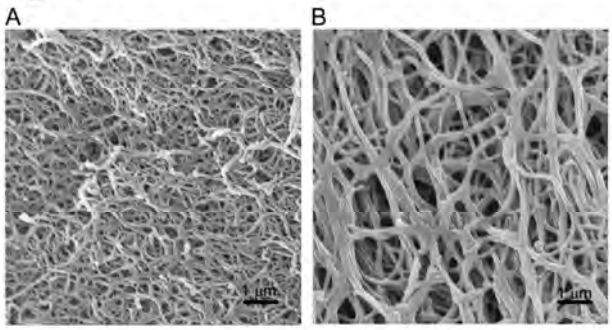

Figure 8. Scanning electron micrographs of fibrin made by pdFI and rFI. Fibrin clots were made by incubating thrombin (0.5 U/ml) with pdFI (A) or rFI (B) (0.5 mg/ml). Scale bars represent 1 μm.

Table 1. Analysis of fiber diameter and number of branch points from SEM.

	pdFI mean (SD)	rFI mean (SD)
Fiber Diameter (μm) n = 20	0.10 ± 0.02	0.19 ± 0.04 [a]
# of branch points/1.4 μm^2 n = 10	6.0 ± 1.9	3.0 ± 1.4 [a]

[a] $p < 0.001$ versus pdFI

3.10. Tissue sealant function. Since rFI had molecular and coagulation properties *in vitro* similar to those of pdFI, we evaluated the wound adherence properties of fibrin made by rFI applied to a wound *in vivo*. All of the pigs maintained similar thromboelastographic clotting parameters before, during and after surgery. rFI or pdFI was applied as a tissue sealant to a severe hemorrhage model generated from a grade V liver laceration involving the central hepatic veins.[12] The grade V liver laceration generated a jagged wound topography with severed veins up to 8 mm in diameter (Figure 9A). Untreated, this wound is a lethal, exsanguinating injury.[42] The pdFI and rFI tissue sealant was applied subsurface into the pool of blood which obscured the wound. Even in the presence of diluting amounts of blood, the tissue sealant rapidly formed an adherent clot after five minutes of manual compression. While both the pdFI-based (Figure 9B) and rFI-based (Figure 9C) tissue sealant rapidly formed an adherent barrier that stopped bleeding, qualitatively we observed that treatments with pdFI sealant became permeated with porcine blood and formed translucent clots, whereas the rFI treatments were less permeable and formed more opaque clots.

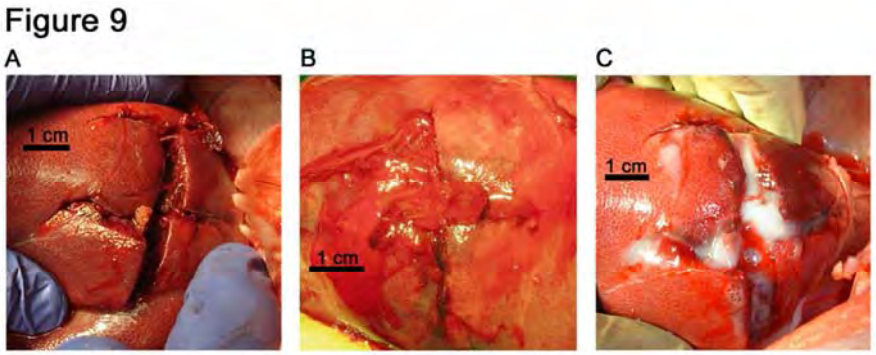

Figure 9. Evaluation of hemostatic and wound adhesive properties of rFI in a Grade V central liver laceration model in swine. (A) Laceration without fibrin sealant. (B) Laceration after application of pdFI-based tissue sealant. (C) Laceration after application of rFI-based tissue sealant. Scale bars represent 1 cm.

3.11. Immunohistochemistry. We examined the clotted wound surfaces by histological cross-sectioning and immunostaining for human and porcine FI (Figure 10 A, B and C). While the human fibrin from pdFI was well intermixed with porcine fibrin (Figure 10B), the fibrin from rFI created well delineated layers alternated with porcine fibrin (Figure 10C). We observed a relatively uniform, 100 μm thick human fibrin layer on the outer surface of the rFI sealant treated tissue. Thus, both gross visual and histological observation of the wound treated with rFI-based sealant confirmed that the resulting fibrin clot was wound adherent and intercalated with blood-borne fibrin to produce a sufficiently strong barrier to bleeding.

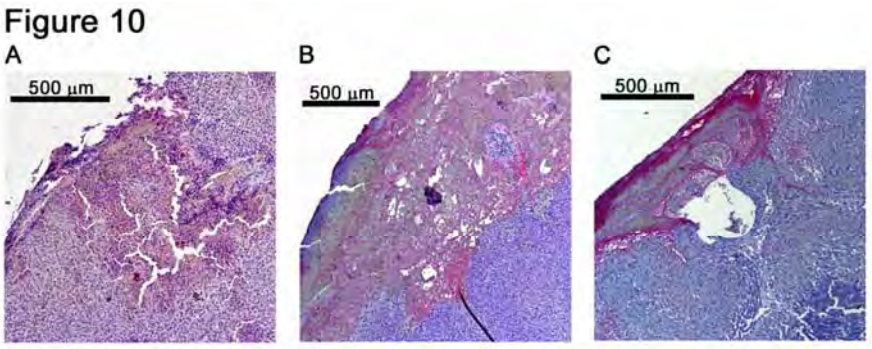

Figure 10. Histologic evaluation of the fibrin-wound interface in a liver lobe wedge excision model in swine. No fibrin sealant (A) and pdFI (B) and rFI (C) sealant treated wedge excisions were incubated with anti-porcine FI antibody stained with DAB+ (brown) and anti-human FI antibody stained with Permanent Red (pink). Scale bars represent 500 μm.

4. DISCUSSION

Our studies provide the first illumination of the *in vivo* adhesive structure and hemostatic behavior of recombinant fibrin. Importantly, the molecular complexity of FI dictates that any rFI will be a facsimile and not an exact copy of the structure and function of pdFI. For example, our rFI is perturbed by increased γ'-chain content as well as differences in the carbohydrate structure at native sites within its α-chain. Importantly, these two particular structural determinants of FI have been associated with opposing changes in fibrin fiber diameter, porosity and degree of branching.[27, 29-31] Past reports showed that increased γ/γ' heterodimer content slowed fibrin polymerization, decreased fiber diameter and increased branching resulting in smaller pores.[29-31] In contrast, deglycosylation of pdFI produced fibrin structures with larger fiber diameter, decreased branching and larger pores. Deglycosylation also resulted in increased polymerization rates but no change in the activation kinetics of pdFI.[27] Prior to this work, the physiologic significance of a post-translationally modified glycoform structure has not been reported. In addition, past work has provided no clear understanding between altering FI structure and the hemostatic barrier function that occurs at a wound site. Our work shows that changes in rFI structure might result in fibrin with improved hemostatic properties achieved without adverse effects on the speed of fibrin formation.

Our studies of rFI made in the milk of cows perturbs opposing determinants of fibrin hemostatic structure and function while making sufficient amounts for preclinical studies. We observed that the bovine mammary gland performed the same alternative mRNA splicing of the FI γ gene as the human liver resulting in the expression of the γ' variant.[19] However, the level of the γ'-chain population in rFI was strikingly higher than in pdFI. In addition, the mammary tissue also glycosylated the rFI with a neutral carbohydrate that resembled those of whey and casein milk proteins but not the ionically more bulky moiety displayed by FI made in the human liver. Surprisingly, in spite of its >4-fold higher γ' content, the resulting rFI produced fibrin with thicker

fibers, less branching and larger pores compared to pdFI. Importantly, this was accompanied by no observable slowing in the molecular kinetics of fibrin assembly. This is a similar result for fibrin made from deglycosylated pdFI having much lower levels of γ/γ'. This prior work showed that removing the charged and branched carbohydrate structure sterically affected individual profibril alignment during the assembly into fibers.[27, 28] Thus, we conclude that the perturbation to a less bulky glycoform made by the mammary gland biochemistry more strongly influenced fibrin structure over that of the γ/γ' heterodimer content.

Previous studies have given conflicting data on the effect of changes in the overall phosphorylation of pdFI where both increased and decreased phosphorylation of pdFI were correlated with increased fiber thickness.[26] However, these early studies did not elucidate the location of the phosphorylation within the pdFI and whether it occurred on the FpA activation peptide and or at other alternate phosphorylation sites which may affect fibrin structure. Here, the phosphorylation of the rFI was 3-fold higher than pdFI and it occurred exclusively from increased phosphorylation of the FpA activation peptide which is removed upon activation. The higher FpA phosphorylation in rFI likely reflects the very efficient phosphorylation of these same motifs in milk caseins.[50] Perhaps more importantly, both FpA/FpB release kinetics and early phase turbidity kinetics were similar for pdFI and rFI. These kinetics are associated with the start of protofibril formation and are in agreement with past studies. Thus, we conclude that there was little observable impact by the higher phosphorylation that occurred in rFI.

Our porcine hepatic injury model consisted of a stellate laceration[42] imposed under normal coagulation potential. It produced severe solid organ hemorrhage primarily from venous blood flow and a rough wound topography of exposed collagen surfaces to examine fibrin adherence. While having equivalent thromboelastic kinetics and strength as measured *in vitro*, the pdFI-based tissue sealant made a translucent and less hemostatic clot than the rFI when applied to a wound surface. In contrast, the fibrin generated from rFI made an opaque white and adherent clot which more rapidly resulted in hemostasis. Furthermore, the histology of the

wounds treated by pdFI and rFI showed a strong contrast in clot structure leading to hemostasis: the fibrin from the rFI was adherent as a dense stratum less than 100 um thick while the pdFI was well mixed into the wound and diluted with endogenous pig fibrin to a depth of about 300 um or more. This is consistent with our macroscopic observation that the rFI clot was not permeated by red blood cells while the pdFI clot was blood red in color. This reflects the different fiber structure seen in our SEM results and is likely caused by the presence of the sterically less bulky carbohydrate that is the signature glycosylation pattern of mammary tissue.[48] Based upon the wound adherence and hemostatic characteristics of rFI, we are currently conducting preclinical studies that will statistically compare the efficacy of a rFI-based tissue sealant to commercial-grade tissue sealant in a cold hemodilution, hypocoagulopathic grade V+ porcine liver injury model.[12] With respect to the potential impact of the rFI fibrin matrix on healing and reabsorption, these future *in vivo* studies will include the examination of clot stability during the healing process in a swine liver injury survival model. The potential for the future production of a first generation tissue sealant engineered to have improved hemostatic behavior is shown by our estimates of the commodity scale production of rFI by the cows of this study (Supporting Information, Table S2). We estimate that fewer than 300 cows can translate to the production of one metric ton of purified rFI that would help meet clinical needs worldwide.

5. CONCLUSION

This study describes the production, purification and molecular characterization of large amounts of rFI produced in the milk of transgenic dairy cows. The rFI produced by transgenic cows was fully assembled and produced at 2-4 g/L. Despite differences in γ' content, glycoform and phosphorylation content of FpA, the kinetic and viscoelastic attributes of fibrin formation by rFI were similar to those by pdFI. The fibrin from rFI had significantly thicker fibers and a lower proportion of branching than clots from pdFI. We then used this material as a tissue sealant to study the function of fibrin made from rFI in a porcine hepatic injury model. In two different

swine liver surgical trauma models, rFI formed a more opaque, histologically dense, wound-adherent fibrin clot that more rapidly stopped bleeding than pdFI.

ASSOCIATED CONTENT

(1) Schematic illustrations of the three separate FI transgenes used in making the transgenic cows and a corresponding Southern blot, (2) flow diagram of the purification process of rFI from milk and purity of rFI by size exclusion chromatography. This material is available free of charge via the Internet at http://pubs.acs.org.

AUTHOR INFORMATION

Corresponding Author

William H. Velander, Department of Chemical & Biomolecular Engineering, University of Nebraska – Lincoln Othmer Hall, Room 207, 820 N. 16th Street, Lincoln, NE 68588, wvelander2@unl.edu, phone: (402) 472-3697, fax: (402) 472-6989.

Notes

The academic institution of W.H.V. has licensed recombinant fibrinogen technology to Pharming Group NV. W.H.V. has no financial interest in Pharming Group NV. M.G., H.V.V. and K.N. are employees of Pharming Group NV.

ACKNOWLEDGEMENTS

We are grateful to Dr. Jason Johanning and Dr. Iraklis Pipinos for their assistance in the surgical procedures. Thanks to Dr. Mehmet Inan for the production of rFXIIIa and L. Smoyer of the University of Nebraska for technical assistance. We would like to acknowledge Dr. Roman Drews and the late Dr. William Drohan and Dr. Henryk Lubon for their contributions while at the American Red Cross Jerome Holland Laboratory. This research was primarily supported by a USA Medical Material Development Activity of the Army grant (W81XWH-05-1-0527) to W.H.V,

the American Red Cross and Pharming Group NV. This study is the result of work supported in part with resources and the use of facilities at the Omaha VA Medical Center.

REFERENCES

(1) Ferry, J. D. *Proc.Natl.Acad.Sci.U.S.A.* **1952,** *38*, 566-9.
(2) Mosesson, M. W. *J Thromb Haemost* **2005,** *3*, 1894-904.
(3) Ariens, R. A.; Lai, T. S.; Weisel, J. W.; Greenberg, C. S.; Grant, P. J. *Blood* **2002,** *100*, 743.
(4) Laurens, N.; Koolwijk, P.; De Maat, M. P. M. *Journal of Thrombosis and Haemostasis* **2006,** *4*, 932.
(5) Spotnitz, W. D.; Burks, S. *Transfusion* **2008,** *48*, 1502-16.
(6) Achneck, H. E.; Sileshi, B.; Jamiolkowski, R. M.; Albala, D. M.; Shapiro, M. L.; Lawson, J. H. *Ann Surg* **2010,** *251*, 217-28.
(7) Elvin, C. M.; Brownlee, A. G.; Huson, M. G.; Tebb, T. A.; Kim, M.; Lyons, R. E.; Vuocolo, T.; Liyou, N. E.; Hughes, T. C.; Ramshaw, J. A. M.; Werkmeister, J. A. *Biomaterials* **2009,** *30*, 2059-2065.
(8) Gray, J. L.; Kang, S. S.; Zenni, G. C.; Kim, D. U.; Kim, P. I.; Burgess, W. H.; Drohan, W.; Winkles, J. A.; Haudenschild, C. C.; Greisler, H. P. *J Surg Res* **1994,** *57*, 596-612.
(9) Pellegrini, G.; Ranno, R.; Stracuzzi, G.; Bondanza, S.; Guerra, L.; Zambruno, G.; Micali, G.; De Luca, M. *Transplantation* **1999,** *68*, 868-79.
(10) Linnes, M. P.; Ratner, B. D.; Giachelli, C. M. *Biomaterials* **2007,** *28*, 5298-5306.
(11) Dainiak, M. B.; Allan, I. U.; Savina, I. N.; Cornelio, L.; James, E. S.; James, S. L.; Mikhalovsky, S. V.; Jungvid, H.; Galaev, I. Y. *Biomaterials* **2009,** *31*, 67-76.
(12) Delgado, A. V.; Kheirabadi, B. S.; Fruchterman, T. M.; Scherer, M.; Cortez, D.; Wade, C. E.; Dubick, M. A.; Holcomb, J. B. *J. Trauma: Inj., Infect., Crit. Care* **2008,** *64*, 75-80.
(13) Spotnitz, W. D.; Prabhu, R. *J.Long.Term.Eff.Med.* **2005,** *15*, 245.
(14) Fenger-Eriksen, C.; Lindberg-Larsen, M.; Christensen, A. Q.; Ingerslev, J.; Sorensen, B. *Br. J. Anaesth.* **2008,** *101*, 769-773.
(15) Burnouf, T.; Goubran, H. A.; Radosevich, M.; Sayed, M. A.; Gorgy, G.; El-Ekiaby, M. *Vox Sang.* **2006,** *91*, 56-62.
(16) Horowitz, B.; Busch, M. *Transfusion* **2008,** *48*, 1739-53.
(17) Doolittle, R. F. *Annu.Rev.Biochem.* **1984,** *53*, 195.
(18) Weisel, J. W. *Adv.Protein Chem.* **2005,** *70*, 247.
(19) Chung, D. W.; Davie, E. W. *Biochemistry (N.Y.)* **1984,** *23*, 4232-6.
(20) Fornace, A. J., Jr.; Cummings, D. E.; Comeau, C. M.; Kant, J. A.; Crabtree, G. R. *J.Biol.Chem.* **1984,** *259*, 12826-30.
(21) Uitte de Willige, S.; de Visser, M. C. H.; Houwing-Duistermaat, J. J.; Rosendaal, F. R.; Vos, H. L.; Bertina, R. M. *Blood* **2005,** *106*, 4176-4183.
(22) Mosesson, M. W.; Cooley, B. C.; Hernandez, I.; Diorio, J. P.; Weiler, H. *Journal of thrombosis and haemostasis JTH* **2009,** *7*, 102-10.
(23) Cheung, E. Y. L.; Uitte de Willige, S.; Vos, H. L.; Leebeek, F. W. G.; Dippel, D. W. J.; Bertina, R. M.; de Maat, M. P. M. *Stroke* **2008,** *39*, 1033-1035.
(24) Lovely, R. S.; Falls, L. A.; Al-Mondhiry, H. A.; Chambers, C. E.; Sexton, G. J.; Ni, H.; Farrell, D. H. *Thromb.Haemost.* **2002,** *88*, 26-31.
(25) Farrell, D. H.; Mulvihill, E. R.; Huang, S. M.; Chung, D. W.; Davie, E. W. *Biochemistry (N.Y.)* **1991,** *30*, 9414-20.
(26) Martin, S. C.; Ekman, P.; Forsberg, P. O.; Ersmark, H. *Thromb. Res.* **1992,** *68*, 467-73.
(27) Langer, B. G.; Weisel, J. W.; Dinauer, P. A.; Nagaswami, C.; Bell, W. R. *J.Biol.Chem.* **1988,** *263*, 15056-63.
(28) Marchi, R.; Arocha-Pinango, C. L.; Nagy, H.; Matsuda, M.; Weisel, J. W. *Journal of thrombosis and haemostasis JTH* **2004,** *2*, 940-8.
(29) Gersh, K. C.; Nagaswami, C.; Weisel, J. W.; Lord, S. T. *Thromb. Res.* **2009,** *124*, 356-363.
(30) Cooper, A. V.; Standeven, K. F.; Ariens, R. A. *Blood* **2003,** *102*, 535-40.
(31) Siebenlist, K. R.; Mosesson, M. W.; Hernandez, I.; Bush, L. A.; Di Cera, E.; Shainoff, J. R.; Di Orio, J. P.; Stojanovic, L. *Blood* **2005,** *106*, 2730-2736.
(32) Prunkard, D.; Cottingham, I.; Garner, I.; Bruce, S.; Dalrymple, M.; Lasser, G.; Bishop, P.; Foster, D. *Nat.Biotechnol.* **1996,** *14*, 867.
(33) Butler, S.; O'Sickey, T.; Lord, S.; Lubon, H.; Gwazdauskas, F.; Velander, W. *Transgenic Res.* **2004,** *13*, 437.
(34) Lubon, H.; Paleyanda, R. K.; Velander, W. H.; Drohan, W. N. *Transfus Med Rev* **1996,** *10*, 131-43.

(35) Butler, S. P.; Van Cott, K.; Subrumanian, A.; Gwazduaskas, F. C.; Velander, W. H. *Thromb.Haemost.* **1997,** *78*, 537.
(36) Platenburg, G. J.; Kootwijk, E. P. A.; Kooiman, P. M.; Woloshuk, S. L.; Nuijens, J. H.; Krimpenfort, P. J. A.; Pieper, F. R.; de Boer, H. A.; Strijker, R. *Transgenic Res.* **1994,** *3*, 99-108.
(37) Forsberg, E. J.; Strelchenko, N. S.; Augenstein, M. L.; Betthauser, J. M.; Childs, L. A.; Eilertsen, K. J.; Enos, J. M.; Forsythe, T. M.; Golueke, P. J.; Koppang, R. W.; Lange, G.; Lesmeister, T. L.; Mallon, K. S.; Mell, G. D.; Misica, P. M.; Pace, M. M.; Pfister-Genskow, M.; Voelker, G. R.; Watt, S. R.; Bishop, M. D. *Biol. Reprod.* **2002,** *67*, 327-333.
(38) Anumula, K. R.; Dhume, S. T. *Glycobiology* **1998,** *8*, 685-694.
(39) Ceroni, A.; Dell, A.; Haslam, S. M. *Source Code Biol. Med.* **2007,** *2*.
(40) Gorkun, O. V.; Veklich, Y. I.; Weisel, J. W.; Lord, S. T. *Blood* **1997,** *89*, 4407.
(41) Park, D.-S.; Kim, J.-H.; Lee, S. W.; Jeong, J.-M. *Biotechnol. Lett.* **2002,** *24*, 97-101.
(42) Holcomb, J. B.; Pusateri, A. E.; Harris, R. A.; Charles, N. C.; Gomez, R. R.; Cole, J. P.; Beall, L. D.; Bayer, V.; MacPhee, M. J.; Hess, J. R. *J Trauma* **1999,** *46*, 49-57.
(43) Holcomb, J. B.; Pusateri, A. E.; Harris, R. A.; Reid, T. J.; Beall, L. D.; Hess, J. R.; MacPhee, M. J. *J Trauma* **1999,** *47*, 233-40; discussion 240-2.
(44) Pusateri, A. E.; Modrow, H. E.; Harris, R. A.; Holcomb, J. B.; Hess, J. R.; Mosebar, R. H.; Reid, T. J.; Nelson, J. H.; Goodwin, C. W., Jr.; Fitzpatrick, G. M.; McManus, A. T.; Zolock, D. T.; Sondeen, J. L.; Cornum, R. L.; Martinez, R. S. *J. Trauma: Inj., Infect., Crit. Care* **2003,** *55*, 518-526.
(45) McDonagh, R. P., Jr.; McDonagh, J. M.; Blomback, M.; Blomback, B. *FEBS (Fed. Eur. Biochem. Soc.) Lett.* **1971,** *14*, 33-6.
(46) Morell, A. G.; Gregoriadis, G.; Scheinberg, I. H.; Hickman, J.; Ashwell, G. *J.Biol.Chem.* **1971,** *246*, 1461-7.
(47) Townsend, R. R.; Hilliker, E.; Li, Y. T.; Laine, R. A.; Bell, W. R.; Lee, Y. C. *J.Biol.Chem.* **1982,** *257*, 9704-10.
(48) Spik, G.; Coddeville, B.; Mazurier, J.; Bourne, Y.; Cambillaut, C.; Montreuil, J. *Adv. Exp. Med. Biol.* **1994,** *357*, 21-32.
(49) Siebenlist, K. R.; Meh, D. A.; Mosesson, M. W. *Biochemistry (N.Y.)* **1996,** *35*, 10448-53.
(50) Bingham, E. W.; Farrell, H. M., Jr. *J.Biol.Chem.* **1974,** *249*, 3647-51.

Table of Contents Graphic

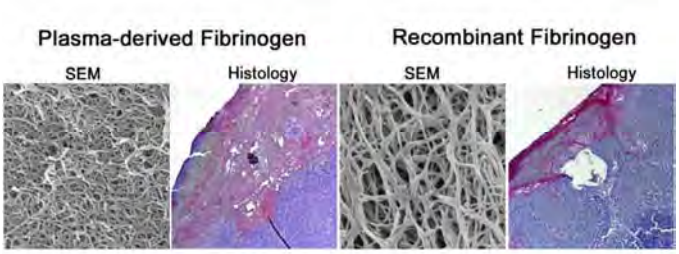

Appendix A5

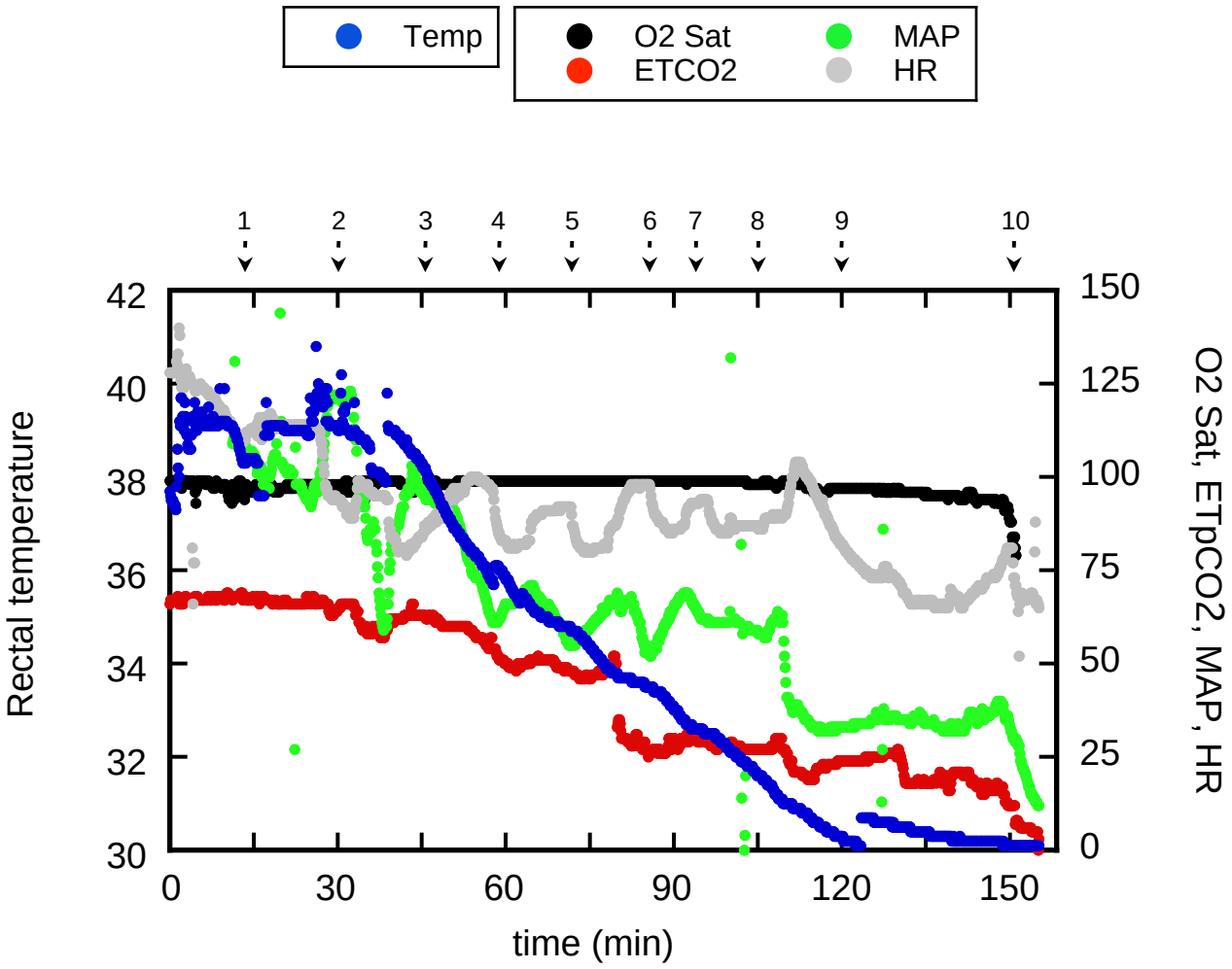

VS data from swine no. 55 (2011-12-16) recorded continuously with Bionet BM5 Vet monitor

1 = Art line established; lab draw* no. 1
2 = Splenectomy followed by 1300 mL LR
3 = Begin first fluid exchange (500 mL)
4 = Begin second fluid exchange (500 mL)
5 = Begin third fluid exchange (500 mL)
6 = Begin fourth fluid exchange (200 mL)
7 = Lab draw no. 2, then 1000 mL LR
8 = Central liver injury
9 = Lab draw no. 3
10 = no BP at 47 min post-injury; lab draw no. 4

*Lab draw = TEG, PT/PTT, ABG, Hct/Hb, plt, fibrinogen

Appendix A6. Sample of laboratory tests obtained at each swine procedure (subject 71).

value	(initial)	(pre-injury)	(15 min post-injury)	(46 min** post-injury)
pH	7.42	7.43	7.46	7.65
pO2 (mm Hg)	512	527	540	486
pCO2 (mm Hg)	38.8	33.1	29.4	16.4
HCO3 (mmol/L)	24.6	21.6	20.8	18.0
base excess (mmol/L)	0.7	-1.8	-2.5	-4.1
O2 sat	na	na	na	na
Hb (ABG)	11.5	9.0	3.5	1.0
Hb (g/dL)	11.2	4.9	2.8	0.8
Hct (%)	33.9	15.6	9.1	3.1
Plt (x 1,000/µL)	516	40	26	17
QFA (mg/dL)*	93	31	fail	fail
PT (s)	11.4	17.7	fail	fail
INR	1.0	1.6	fail	fail
APTT (s)	18.3	22.9	fail	fail

*QFA = quantitative fibrinogen assay, based on von Clauss method (clotting time).
**Subject died at 53 min

I. OVERVIEW
Date: June 22, 2012
Swine no: 73
Model: swine, hypothermic hemodiluted central liver injury model, as described in *J Trauma* 2008; 64: 75-80
Treatment: PLA nanofiber sheet, perforated, 4 ply, treated with polysorbate, wet with rFS
Personnel: Carlson, Wheeler, Cavanaugh, Hansen, Calcaterra, Noriega

---

II. PRE-INJURY PHASE

Start time: 7:45 AM
Swine sex: male
Date swine received from UNL Mead: 06/20/2012
Pre-procedure wt: 33.4 kg (73.5 lb)

Anesthetic Induction: Telazol (4.4 mg/kg), Ketamine (2.2 mg/kg), Xylazine (2.2 mg/kg), given as single IM shot
Anesthetic maintenance: 1% inhalational isoflurane

Lines/tubes/monitors

1. Endotracheal tube with ETCO2 monitor
2. EKG clips
3. Left ear vein angiocath (20g) for supplemental LR
4. Right carotid artery angiocath (20g), cutdown; for BP monitor
5. Right jugular vein angiocath (16g), cutdown; connected to rapid infusion pump
6. Left femoral artery angiocath (16g), cutdown; for phlebotomy
7. Transabdominal cystotomy (16 Fr Foley)
8. Rectal temp probe
9. Pulse oximetry

Initial VS

- HR: 104
- MAP: 106
- Temp: 38.1

Blood draw no. 1 (initial): 8:01 AM
(ABG, TEG, hematocrit/hemoglobin, PT/PTT, qualitative fibrinogen)

Splenectomy time: 8:13 AM
Spleen wt: 226 gm
LR (22˚C) infused after splenectomy: 700 mL at 150 mL/min

Time fluid exchange begun: 08:30 AM
Time fluid exchange ended: 09:08 AM
Calculated 60% blood volume withdrawn: 1501 mL
Actual blood volume phlebotomized: 1500 mL (divided into 3 x 500 mL phlebotomies)
Replacement fluid (1:1 with blood withdrawn): Hextend (4˚C), 1500 mL at 150 mL/min
Cooling methods: cold IV fluids, open abdomen, intraabdominal ice packs

Pre-injury fluid data:

- Blood loss (spleen weight + phlebotomies + incidental): 226 + 1500 + 64 = 1790 mL
- Hespan (4˚C): 1500 mL (phlebotomy replacement)
- LR (22˚C): 1550 mL (spleen replacement + incidental)

Pre-injury VS

- HR: 88
- MAP: 58
- Temp: 32.9

Blood draw no. 2 (pre-injury): 9:08 AM
(ABG, TEG, hematocrit/hemoglobin, PT/PTT, qualitative fibrinogen)

III. INJURY PHASE

Time of liver injury: 9:19 AM
Injury type: double application of clamp through central liver, directly anterior to IVC
Duration of free-bleed period: 30 sec
Treatment immediately after free-bleed:
PLA nanofiber sheets x 3 (perforated, 4 ply, pretreated with polysorbate, wet with rFS) stuffed directly into injury; laparotomy pads placed over dome of liver (n = 3) and under liver (n = 1). (Technique: the three PLA sheets first were completely unfolded, then balled up, then soaked with a spray of rFI, all prior to the injury. The injury then was performed, followed by 30 sec free-bleeding. Just prior to bandage application, all three PLA sheets were dunked into a tray containing a solution of rFIIa and rFXIIIa, and were thoroughly soaked. The activated bandages then were stuffed into the wound as a unit. Time from soaking with FII & FXIII to wound insertion was 10 sec. This bandage insertion time was longer because the PLA sheets did not retain well into the wound recess after insertion. The sheets had to be held in place with one hand while the other hand was placing the cotton lap pads over the top.)
Blood loss during free-bleed period: 368 mL

Time resuscitation initiated: immediately at time of injury
Resuscitation fluid: Hextend (37˚C)
Target MAP for resuscitation (90% of pre-injury MAP): 52 mm Hg

---

IV. POST-TREATMENT PHASE

Blood draw no. 3 (15 min post-injury): 09:34 AM
(ABG, TEG, hematocrit/hemoglobin, PT/PTT, qualitative fibrinogen)

15 min post-injury VS

- HR: 43
- MAP: 96
- Temp: 31.1

Blood draw no.4: 9:43 AM
(ABG, TEG, hematocrit/hemoglobin, PT/PTT, qualitative fibrinogen)

Survival at 120 min post-injury : no

Time of death: 09:45 AM
Interval from injury to death/euthanasia: 26 min
Amount resuscitation fluid given: 3000 mL at 150 mL/min
Target MAP attained: no

Post-treatment fluid data:

- Blood loss (intraabdominal suctioning + pads/gauze): 3743 + 471 = 4214 mL
- IV fluid given: Hextend (37˚C): 3000 mL

V. POST-DEATH PHASE

Findings upon abdominal exploration: liters of unclotted blood, no red clots. The bandages were in appropriate position. There was no adherence between the PLA sheets and the wound bed. The balled-up PLA sheets themselves were quite firm and formed a perfect mold (or cast) of the liver wound (see Figure 1, attached). The PLA sheets were stuck to the cotton lap pads (Figure 1). The sheets were subsequently unfolded, and ~80% of the total surface area had been saturated with blood (Figure 1).

Ex vivo liver examination:

- Number of retrohepatic veins lacerated: 2 (both large)
- IVC intact: yes
- Portal vein injury: no
- Other: none
- Liver wt: 879 gm

Tissue harvested: skin for keratinocyte culture

VI. COMMENTS

Treatment failure with the nanofiber PLA sheets (pretreated with polysorbate, wet with rFS). Large blood loss; no bandage adherence; early death. Today's bandage material essentially was the same iteration that was successful in the liver resection model (normothermic, normal clotting subjects, with a smooth bandage:wound interface). The cold coagulopathic model will need something different; I think we need to get some degree of adhesion to the wound surface. Here are my thoughts/opinions:

- This subject's starting MAP (58) was marginal…I'm not sure how valid today's data was because of this low starting MAP. We did give some extra fluid prior to injury in an attempt to bring the MAP up, but this did not have much effect. Not sure why this subject's MAP was low compared to the other subjects.
- I did not like the way the PLA sheet configuration worked with the deep liver wound. The balled-up sheets slid and rolled around too much as I was trying to insert them. They would not stay in place with a single shove; I had to hold them in with one hand while I placed the cotton lap pads over the top of them. For this reason alone I would prefer going back to a open-mesh configuration (i.e., cotton sponge mimic) for this liver laceration model. The cotton sponge configuration wound stay in the wound after insertion.
- We may need to consider upping the amount of exogenous fibrinogen that goes into the wound. All three synthetic bandages wet with rFS that we have used to date have not demonstrated any clot beyond the confines of the bandage. There simply may not be enough endogenous fibrinogen in the cold coagulopathic model to form clots outside of the confines of the bandage.

- Perhaps we could try a PCL/PLA composite wet with rFS; alternatively, we could try wetting the cotton gauze sponges with rFS & see if the control material can do any better with the biologics.

VII. PLAN

Plan: next subjects will be on Thu June 28th and Fri June 29nd. As I mentioned above, I would prefer to use a cotton sponge mimic (instead of the sheets) for handling issue discussed above. Regarding the adherence & clot formation issues, I think we should have some more discussions of these problems.

Dave Heineman
Governor

State of Nebraska
DEPARTMENT OF ECONOMIC DEVELOPMENT
P.O. Box 94666
Lincoln, Nebraska 68509-4666 USA
Phone (402) 471-3111
Toll Free (800) 426-6505
Fax (402) 471-3778
Statewide Relay (800) 833-0920 (voice)
www.neded.org

August 15, 2012

Gustavo Larsen, Principal
LNK Chemsolutions, LLC
4701 Innovation Drive
Lincoln, NE 68521

RE: Phase one research and development grant from the Nebraska Research and Development Program authorized under Section 81-12,161, Nebraska Revised Statutes (2011) of the Business Innovation Act ("R&D Program").

Notice of Approval

Dear Gustavo:

It is a pleasure to inform you that LNK Chemsolutions, LLC has been approved for a Nebraska Applied Research and Development Grant (R & D) up to the amount of $100,000 for the purposes of determining the greatest efficacy and optimization of a hemostatic patch (PLA bandage containing human clotting factors) in a hepatic resection model of swine. Your project was approved for funding based upon information contained within your R&D Program application, including but not limited to, information demonstrating the required 1:1 match from outside funds, which was identified in the latest budget from LNK Chemsolutions, LLC , as proceeds from a grant from the U.S. Department of Defense.

It is important that you understand that while costs may be incurred at this time, only eligible expenses will be reimbursable under the guidelines of the Eligible expenses will be outlined in a grant contract, which will be sent to you at a later date. The contract will reflect a project period starting **June 1, 2012** after which LNK Chemsolutions may incur eligible project costs of which 50% may be reimbursed from the grant proceeds provided they are incurred prior to **September 1, 2013**.

The grant contract will also include provisions related to the term of the grant, reporting requirements, and the reimbursement process.

Please understand that up until execution of the grant contract, costs will be incurred at your own risk, and only eligible expenses will be reimbursable after full execution of the grant contract. **If you have any questions regarding this information, contact the program administrator, Stew Jobes at (402) 471-3114 or by email at stew.jobes@nebraska.gov; or Eric Zeece at (402) 471-3777 or by email at eric.zeece@nebraska.gov.**

We congratulate LNK Chemsolutions, LLC, and look forward to actively working with you in carrying out your project.

Sincerely,

Stew Jobes
Economic Development Program Manager

cc: Eric Zeece, Libby Elder

of the RBC-age groups in ADP induced aggregation. None of the TEG parameters of enzymatic clotting function (R, delta), fibrin cross-linking (angle), thrombin induced platelet aggregation (MA, G), or fibrinolysis (LY30) were significantly different between RBC-age groups. There were no significant differences in Hct and PLT counts between the different samples studied. **Conclusions:** Storage of RBCs ≥21 days may be responsible for decreased platelet function when transfused. An association has been noted between RBC age and the AA pathway during platelet aggregation. Further *in vivo* studies are needed to determine if platelet dysfunction related to transfusion of RBCs ≥21 days is contributory to poor clinical outcomes.

RBC age (days)	Enzymatic Activity (R)	Thrombin Generation (Delta)	Rate of Clot Formation (Angle)	Maximum Amplitude (MA)	Clot Strength (G)	Lysis at 30 min. (LY30)	ADP inhibition	AA inhibition
1	4.73±0.9	1.0±0.3	51.0±3.4	58.7±4.4	8.3±2.1	0.5±0.3	5.1±0.9	1.4±1.1
14	5.0±1.1	0.8±0.5	60.7±5.1	61.7±3.7	9.7±1.5	0.4±0.3	3.9±1.5	7.9±3.8
21	4.9±1.3	0.8±0.3	62.3±2.9	62.4±3.0	10.0±1.7	0.1±0.1	5.2±4.4	34.6±7.4*,**
42	5.5±1.1	0.6±0.2	59.8±3.9	61.6±4.0	9.6±2.2	0.1±0.1	4.4±2.7	43.6±18.0*,**

* $P<0.05$ vs. RBC-day 1, ** $P<0.05$ vs. RBC-day 14, .

44.4. A Totally Recombinant Factor XIII-Supplemented Fibrin Sealant. M. A. Carlson,[1] W. H. Velander,[2] I. I. Pipinos,[1] J. M. Johanning,[1] J. Calcaterra[2]; [1]University of Nebraska Medical Center, Omaha, NE; [2]University of Nebraska Lincoln, Lincoln, NE

Introduction: Plasma-derived (pd) fibrin sealants (FS) have had limited applications because of cost, supply, and utility issues. We now describe a totally recombinant Factor XIII-supplemented FS which may be able to address these issues. **Methods:** Human recombinant (r) fibrinogen (FI) and activated Factor XIII (FXIIIa) were generated in the milk of transgenic cows and in yeast, respectively; human r-thrombin (FIIa) was purchased (Recothrom®). r-FS made from these three factors was optimized with thromboelastography (TEG). pd-FS (Tisseel™) was used as directed. FS testing consisted of series of hepatic wedge excisions ("pie-slice") in domestic swine (male, 3 months, 30 kg; N = 6/group) with a constant base (1 cm) and step-wise increasing depth (0.5 to 3 cm, in 0.5 cm increments; 6 excisions/series, 2 series per swine) made on a lobar edge. Each excision was treated with up to 1 mL of FS without compression or other aid, and then hemostasis was scored: 0 = failure/minimal effect; 1 = steady bleeding; 2 = oozing; 3 = hemostatic. **Results:** Minimal factor concentrations in the r-FS which yielded optimal TEG performance (data not shown, DNS) were 9 mg/mL FI, 0.36 mg/mL FXIIIa, 106 U/mL FIIa, and 12 mM CaCl2. Removal of r-FXIIIa decreased r-FS clotting kinetics ("alpha angle") and ultimate clot strength ("maximal amplitude") by 60 and 70%, respectively (DNS). pd-FS (N = 3 lots) contained 34-53 mg/mL FI, 200-312 U/mL FIIa, and trace/undetectable FXIIIa. Ultimate clot strength at 20 min was not different between the r-FS and pd-FS (DNS), but the r-FS gained strength more quickly (time to half-maximal strength = 30 vs. 100 sec, respectively; derived value from TEG plots). Ultimate clot strength of both sealants was twice that of human whole blood (N = 22 normal donors), except that the latter had a 5-6 minute latency before detectable strength ("R value;" DNS). In the wedge resection model, the hemostatic scores of the r-FS were equivalent or better than those of the pd-FS (Figure; *$p<0.05$, Wilcoxon; each bar represents mean score±sd of 10-12 excisions). **Conclusions:** r-FS had equivalent or better hemostatic efficacy than pd-FS in this wedge resection model, despite the FI concentration in the r-FS being about one-fourth that in the pd-FS. TEG data indicated that this result was dependent on the r-FXIIIa in the r-FS. Given that r-FS production is scalable, and the fact that FXIIIa supplementation greatly reduced FI requirement without sacrificing efficacy, r-FS production cost potentially should be much less than that for pd-FS. An abundant, economic source of r-FS might lead to increased innovation in hemostasis, acute wound stabilization, and related fields.

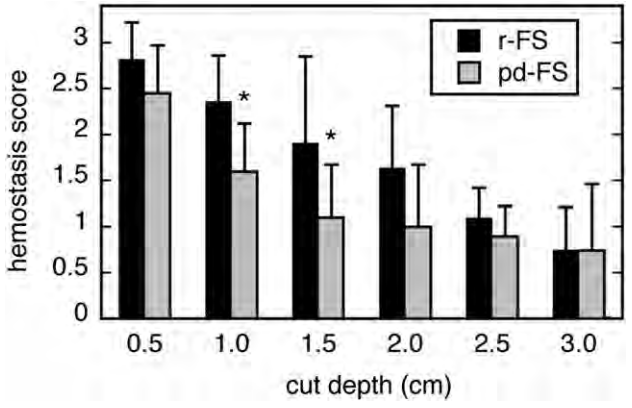

44.5. Propranolol Attenuates The Burn Induced Endoplasmic Reticulum Stress Response. M. G. Jeschke,[1,2] D. Boehning,[2] R. Kraft,[2] C. C. Finnerty,[2] D. N. Herndon,[2] J. Song[2]; [1]Sunnybrook Health Science Centre and University of Toronto, Toronto, ON; [2]Shriners Hospital for Children and UTMB, Galveston, TX

Introduction: Severe burn is associated a wide array of stress, metabolic, and physiologic processes in an attempt to restore homeostasis. The catecholamine induced stress response following severe burns is particularly exaggerated and manifests detrimentally as inflammation, insulin resistance, hypermetabolism, and associated profound protein catabolism. Recently, endoplasmic reticulum (ER) stress and the unfolded protein response (UPR) were identified as central intracellular stress signaling pathways that modulate and enhance inflammatory responses and cell death. We hypothesize that catecholamine blockade using Propranolol, a non-selective β1/2 receptor antagonist, will attenuate ER stress and lead to restored IR signaling, and improved cell survival. **Methods:** Rats received a 60% total body surface area burn and were assigned to receive 5mg/kg/day of Propranolol p.o or saline (control). On post-burn day 3 liver was harvested before and 1 min after insulin injection (1 IU/kg) into the portal vein and expression patterns of various proteins known to be involved in insulin and ER-stress signaling cascades were determined by Western blotting. Apoptosis and caspase-3 by TUNEL assay and luminescent technique, IL-6 by ELISA. **Results:** Burn induced ER stress as shown by increased expression of phospho-PKR-like ER-Kinase (PERK) and phospho-inositol requiring enzyme (IRE)-1. Induction of ER stress was associated with a significant increase of p-Jun N-terminal Kinase (JNK) ($p<0.05$). Propranolol significantly decreased the ER stress markers phospho-PERK and phospho-IRE-1 when compared with burn which was associated with significantly decreased pJNK, attenuated cell apoptosis and decreased IL-6 levels, $p<0.05$. In terms of insulin signaling, we found that burn phosphorylated insulin receptor substrate (IRS)-1 at serine 307 and de-phosphorylated at tyrosine 612 which was associated with an impaired PI3K/Akt signaling, $p<0.05$, indicating the impairment of insulin sensitivity post-burn injury. Propranolol treatment partially restored the impaired insulin signal pathway by significantly increasing IRS-1 and pAkt, $p<0.05$. **Conclusions:** Propranolol significantly alleviated the burn induced ER stress response which was associated with alleviated inflammation, improved cell viability, and improved insulin signaling.

44.6. The Role Of The Vagus Nerve In Preventing Acute Lung Injury: Uncovering the Gut-Lung Axis. M. J. Krzyzaniak, G. Cheadle, L. Reys, Y. Ortiz-Pomales, N. Lopez, A. Hageny, J. Putnam, B. Eliceiri, A. Baird, V. Bansal, R. Coimbra; University of California San Diego, San Diego, CA

Introduction: We have previously shown that vagal nerve stimulation (VNS) has a protective effect against gut epithelial barrier

HEMOSTASIS, ADHESION AND CLOT STABILITY CHARACTERISTICS OF HUMAN FIBRINOGEN PRODUCED IN THE MILK OF TRANSGENIC COWS

J. Calcaterra[1], Mark A. Carlson[2], Iraklis I. Pipinos[2], Jason M. Johanning[2], Crystal Cordes[2], H. van Veen[3], K. Nelson[4] and W.H.Velander[1]

[1] Department of Chemical and Biomolecular Engineering, University of Nebraska–Lincoln

[2] Department of Surgery, University of Nebraska Medical Center

[3] Pharming Technologies B.V., Leiden, The Netherlands

[4] Pharming Healthcare, Inc., DeForest, WI `

Objective: In the future, resuscitative and topical therapies for restoring hemostasis disrupted by trauma will likely include recombinant human fibrinogen (rFI). Previously, we found that rFI made in the milk of transgenic cows possessed many molecular properties similar to plasma-derived fibrinogen (pdFI). Here, we evaluate the wound adhesion and hemostatic behavior of rFI in a lethal pig liver injury model. We also evaluate the clot formation and stability of rFI in normal human blood *ex vivo*. **Methods:** The effects of rFI on time to clot initiation and clot strength were investigated by thromboelastography (TEG) when added to normal human blood at near hyperfibrinogenemic levels. Plasmin degradation of rFI and pdFI clots created with human thrombin and factor XIIIa (FXIIIa) were studied by TEG. The ability of rFI to covalently bind to α2-antiplasmin (A2AP) by FXIIIa was studied by SDS-PAGE and western blotting. The hemostatic efficacy of rFI as a component in a fibrin sealant was investigated *in vivo* on lethal, Grade V stellate liver lacerations in a swine model (N = 9). Adherence of the human fibrin made from rFI to wounded tissue was examined by immunohistochemistry. **Results:** The addition of rFI significantly increased thromboelastographic clot strength when added to normal human blood. Purified rFI, made in the milk of cows, did not have detectable A2AP protein or activity. As a result, plasmin (8 to 84 mU/ml) resulted in clot lysis of rFI but not pdFI (9 mg/ml). In the presence of FXIIIa, A2AP was found to covalently attach to rFI. rFI sealant resulted in a stable, wound adherent clot that stopped moderate and severe bleeding in swine hemorrhage models. **Conclusions:** These *in vivo*, *ex vivo* and *in vitro* studies indicate that purified rFI produced in the milk of transgenic cows has potentially desirable attributes for use in fibrinogen replacement therapy and as a component of fibrin sealants.

Poster presentation at the 97th Annual Clinical Congress of the American College of Surgeons (San Francisco, CA, Oct. 23-27, 2011)

DEVELOPMENT OF NOVEL HEMOSTATIC DEVICES IN SWINE HEMORRHAGE MODELS

Mark A. Carlson[1], William H. Velander[2], Gustavo Larsen[3], Jennifer Calcaterra[2], Iraklis I. Pipinos[1], Jason M. Johanning[1], Crystal Cordes[1], Sandra Noriega[3], Ruben Spretz[3], and Wilson H. Burgess[2]

[1]Department of Surgery, University of Nebraska Medical Center
[2]Department of Chemical and Biomolecular Engineering, University of Nebraska–Lincoln
[3]LNK Chemsolutions LLC, Lincoln NE

Contact: Mark A. Carlson (macarlso@unmc.edu; 402-995-5371);
www.nebraskasurgicalresearch.com

ABSTRACT

Development of advanced hemostatic technologies to treat exsanguinating hemorrhage currently is a research priority of the U.S. Department of Defense. We have been researching novel hemostatic treatments in swine hemorrhage models. The treatments consist of combinations of human clotting factors embedded in resorbable nanoengineered synthetic bandage material. These biologic-based bandages are intended to stop high-pressure and high-flow hemorrhage, and also are intended to be implantable without need for explanation. The swine hemorrhage models consist of grade V hepatic laceration, major (≥ 20%) hepatectomy, femoral arteriotomy, and infrarenal aortotomy. Primary outcome of these models (performed under general anesthesia) are survival, blood loss, and cessation of hemorrhage during a 180 min observation period. Survival models also will be included in this research, in order to determine any toxic effect from bandage implantation. Preliminary data suggests increased efficacy of the biologic bandages over control bandages (cotton gauze) in these swine hemorrhage models.

INTRODUCTION

Exsanguination is the first or second most common cause of battlefield mortality; coagulopathic hemorrhage and noncompressible hemorrhage have been especially problematic. With regard to civilian trauma, there were about 122,000 accidental deaths in the USA in 2006, which accounted for 5.0% of all mortality during that year. Violence contributes to a significant number of deaths with civilian trauma. A research priority of the US Army is to develop effective treatment for traumatic hemorrhage in subjects with noncompressible injuries and also in coagulopathic subjects. We believe that bleeding from complex wound topographies in (1) noncompressible, truncal injuries or (2) coagulopathic subjects can be treated with a resorbable synthetic matrix combined with human clotting factors. In contrast to previous hemostatic devices, we believe our engineering approach will maximize efficacy while decreasing both polymer and biologic usage, thus providing a cost-effective device. Accordingly, we have developed the ability to engineer a variety of synthetic, resorbable prototypes at nano- and micro-scale (fiber and particulate) containing minimal amounts of polymer and clotting factors. Prototype configurations range from a cotton gauze analogue to an expandable polymer. In addition, we have developed economical, abundant sources of human fibrin sealant components that are kinetically faster than commercially-available sealants. Economical, effective, and safe hemostatic devices will have great utility in the control of battlefield hemorrhage. The formulations proposed in this project could be carried and used by a soldier and/or a Forward Surgical Team. The development of effective, relatively simple, and economical methods of acute wound stabilization for noncompressible hemorrhage or coagulopathic hemorrhage would have profound impact on the survivability of battlefield trauma and would be highly valued by the DOD and other federal institutions.

METHODS/1 of 2

Each animal was fasted for 12-18 hours before surgery, with free access to water. Premedication was done with a combination of telazol (4.4mg/kg), ketamine (2.2 mg/kg), and xylazine (2.2 mg/kg), given as a single IM shot. An IV line was established in a marginal ear vein to provide supplemental medication (telazol 4.4mg/kg, ketamine 2.2 mg/kg, and xylazine 2.2 mg/kg IV as needed), and euthanasia solution at the end of the procedure. The animal was masked with isoflurane (3-4%) and supplemented with oxygen (3-5 L/min) to achieve relaxation for endotracheal intubation. Once intubation was accomplished, the animal was maintained with isoflurane (1-2%) supplemented with oxygen (1-2 L/min) throughout the procedure. A rectal temperature probe and EKG (cardiac) monitors were placed. The animal rested on a warming blanket. Mechanical ventilation was provided at a rate of 12-15 breaths per minute and a tidal volume of 5-10 mL/kg. End-tidal pCO2 was maintained at 35-45 mm Hg. The equipment required for these and subsequent procedures included an anesthesia machine, a ventilator, an end-tidal CO2 monitor, a rectal-temperature monitor, a warming blanket, an arterial pressure monitor, a Foley catheter, laparotomy and vascular surgical instruments, and a suction apparatus. Continuous vital sign data were digitally captured by a Bionet monitor.

A carotid arterial catheter for pressure monitoring and blood sampling, and a jugular venous catheter for fluid and medication administration was placed via surgical cutdown in the left neck. A midline laparotomy and splenectomy was performed to minimize autotransfusion by the contractile porcine spleen. The spleen was weighed, and warm lactated Ringer's (LR) solution was given at three times the splenic weight to replace the approximate volume of blood contained in the spleen.

A grade V hepatic injury was created with a custom-designed liver injury clamp (see Results). The X-shaped tines on this clamp were ~5 cm across. The clamp was applied twice (adjacent sites) through the central portion of the liver, adjacent to the vena cava. This technique produced a jagged, stellate-shaped lesion. The experimental treatments then were applied into this injury.

METHODS/2 of 2

Subjects were monitored for 3hr (or until death) after treatment. The subject then was euthanized, and the injured liver was removed for weighing and histology.

Euthanasia for nonsurvival procedures was performed while the animal was under deep isoflurane anesthesia. Sodium pentobarbital (380 mg/mL, 10 mL IV) was administered, and then the animal underwent bilateral diaphragm incisions with intentional exsanguination, all in accordance with the AVMA Guidelines. For the survival procedures, euthanasia was performed by first anesthetizing the animal as described for the primary procedure, and then performing the exsanguination/ diaphragm incisions.

RESULTS/FIGURE 1

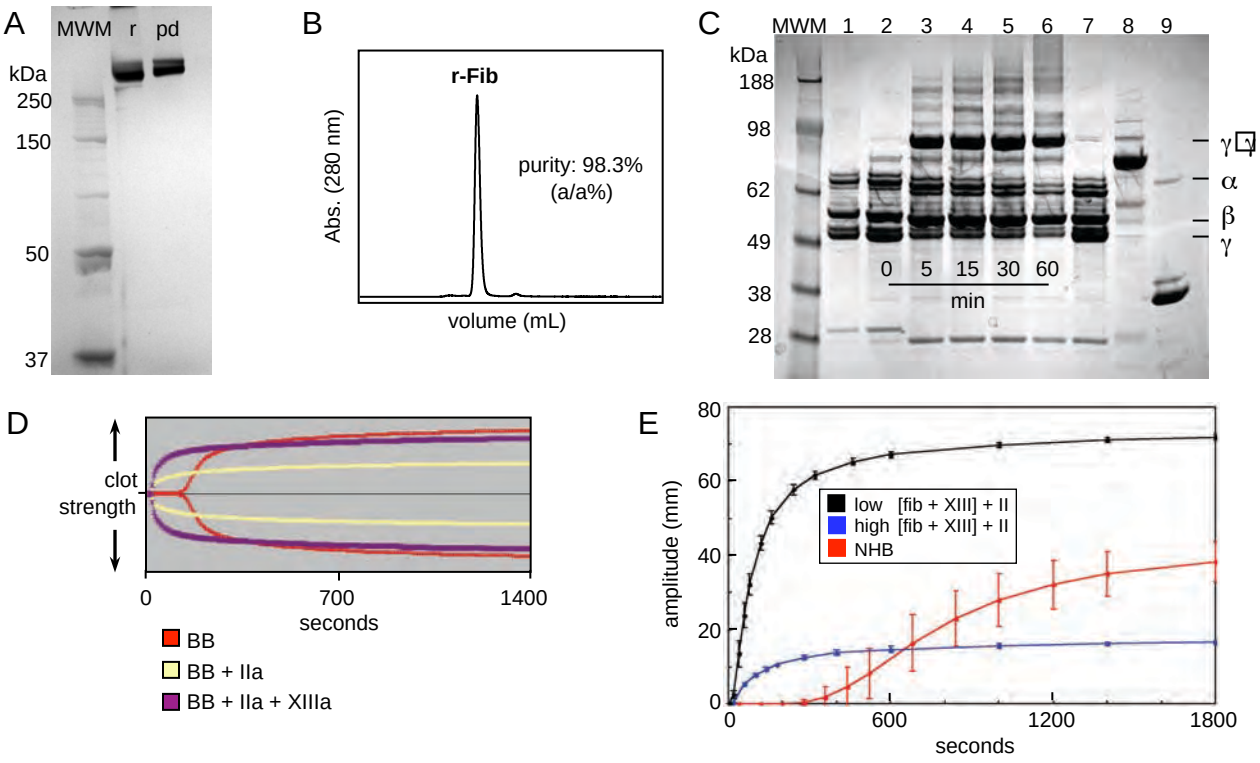

Figure 1: *In vitro* characterization of recombinant clotting factors used in this research. (A) Comparison of recombinant (r) and plasma-derived (pd) fibrinogen by non-reducing SDS-PAGE. MWM = molecular weight marker. **(B)** Size exclusion chromatography of recombinant fibrinogen; purity = 98.3%. **(C)** Formation of γ-chain cross-links in recombinant fibrinogen as analyzed by reducing SDS-PAGE. Lane 1: r-fibrinogen prior to incubation with r-FXIII and pd-thrombin; lanes 2-6: r-fibrinogen, r-FXIII and pd-thrombin incubated for various intervals; lane 7: r-fibrinogen incubated with pd-thrombin for 60 minutes; lane 8: r-FXIII prior to incubation with r-fibrinogen and pd-thrombin; lane 9: pd-thrombin prior to incubation with r-FXIII and r-fibrinogen. After 5 minutes, a majority of the γ-chains were cross-linked and the remaining chains were slowly converted to γ-γ dimers for the next 55 minutes. The recombinant fibrinogen showed very little transglutaminase activity in the presence of thrombin and no added recombinant FXIII. **(D)** TEG of lyophilized bovine blood (BB) with additions of pd-thrombin and r-FXIII. **(E)** TEG of normal human blood (NHB) and recombinant factors. Clots consisting of 8.53 μM recombinant fibrinogen, 0.09 μM r-FXIII and 3.22 μM plasma-derived thrombin (blue) have faster clot onset times but lower maximal clot strengths than NHB (red; average from 22 patients). If r-fib and r-FXIII are increased to 25.17 μM and 4.33 μM, respectively, while maintaining 3.22 μM pd-thrombin (black), then the maximal clot strengths are four-fold larger than NHB. Data are expressed as mean ± sd.

RESULTS/FIGURE 2

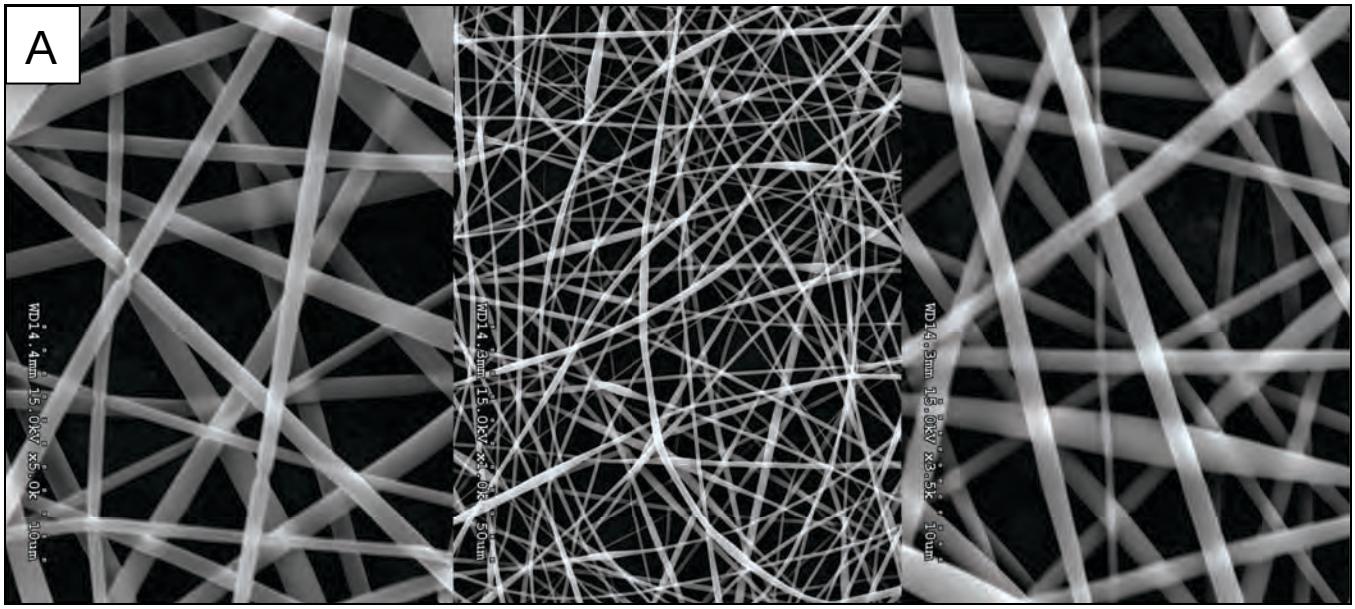

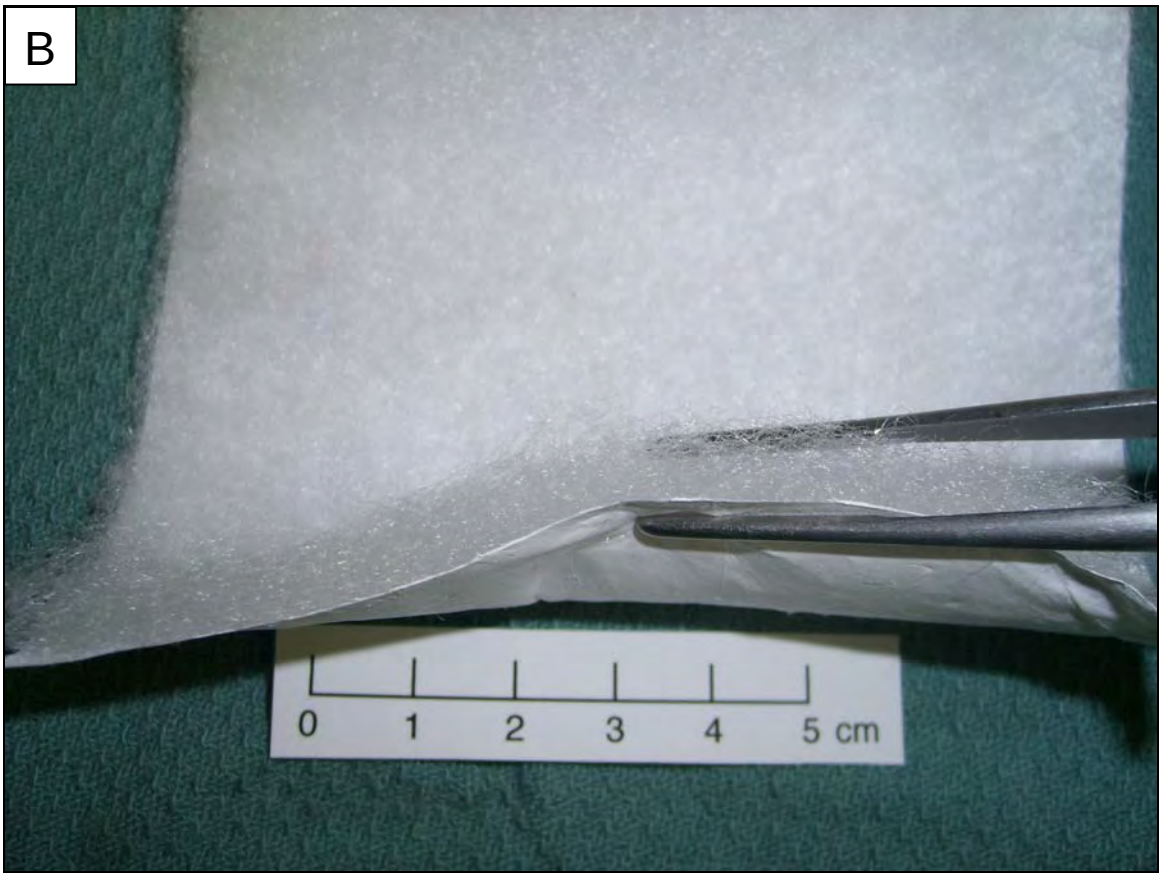

Figure 2: resorbable polylactide (PLA) bandage material. (A) Microporous PLA; fiber diameter 1 µm, pore space 5-10 µm. (B) Macro view (macroporous PLA superior, microporous PLA inferior.

Carlson/2011 ACS

RESULTS/FIGURE 3

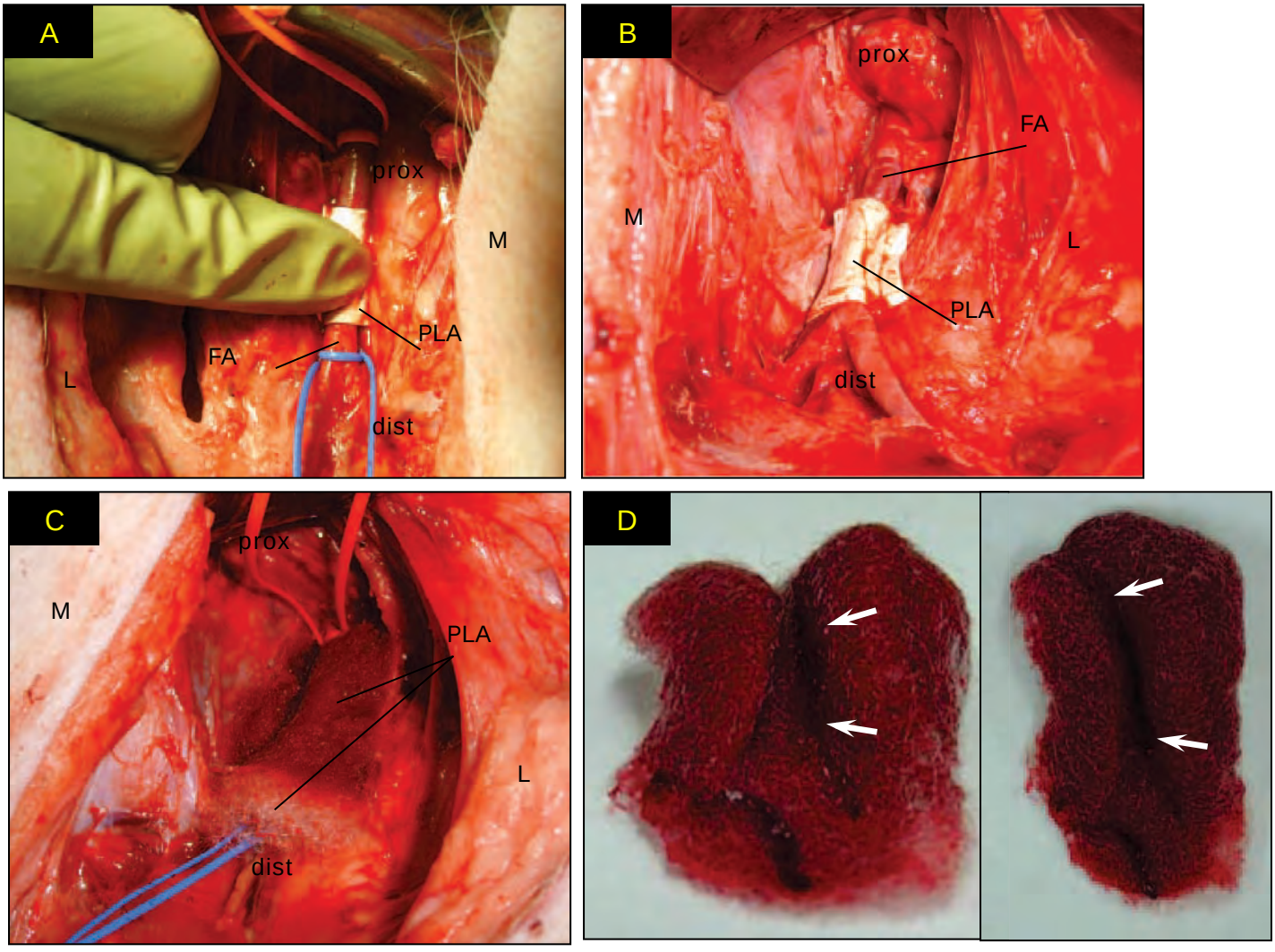

Figure 3: the swine femoral arteriotomy model. (A) The femoral artery (FA) is exposed through a groin incision (right side shown), and controlled with vessel loops. A 4 mm arteriotomy is made with a punch instrument between the loops. A dressing (microporous PLA in this image) then is applied, finger pressure is held for 5 min, and then the site is inspected for bleeding. **(B)** Hemostatic result after application of microporous PLA in 2 plies, containing thrombin and recombinant Factor XIII in the inner ply, and recombinant fibrinogen in the outer ply. Doppler flow was present in the distal artery. L = lateral; M = medial; prox = proximal; dist = distal. **(C)** Hemostatic result after application of the macroporous ("woolly") PLA in 2 layers with the same distribution of clotting factors as in B. Doppler flow was present in the distal artery. **(D)** Appearance of a macroporous PLA bandage containing all 3 clotting factors post-removal from an arteriotomy site. Note formation of a prominent vessel groove (arrowheads) in the dressing material. This used bandage was quite firm to the touch.

RESULTS/FIGURE 4

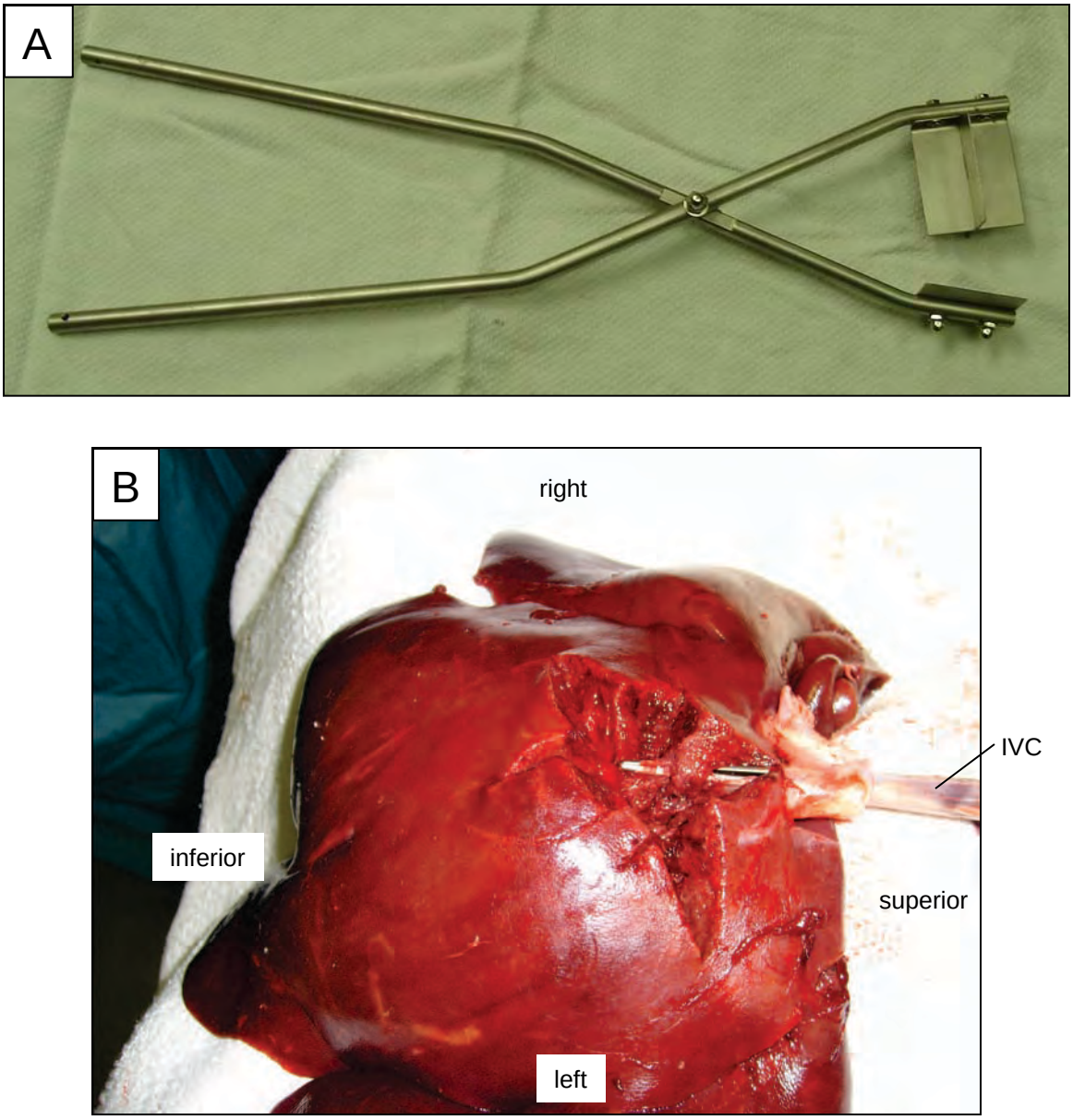

Figure 4: injury to central area of liver in swine (*ex vivo*). Liver injury clamp (A) was applied twice over the dome of the liver (B) so that the times entered just anterior to the IVC (inferior vena cava). The tines actually shredded the IVC within the liver parenchyma, as demonstrated with the tip of the Debakey forceps inserted into the IVC.

RESULTS/FIGURE 5

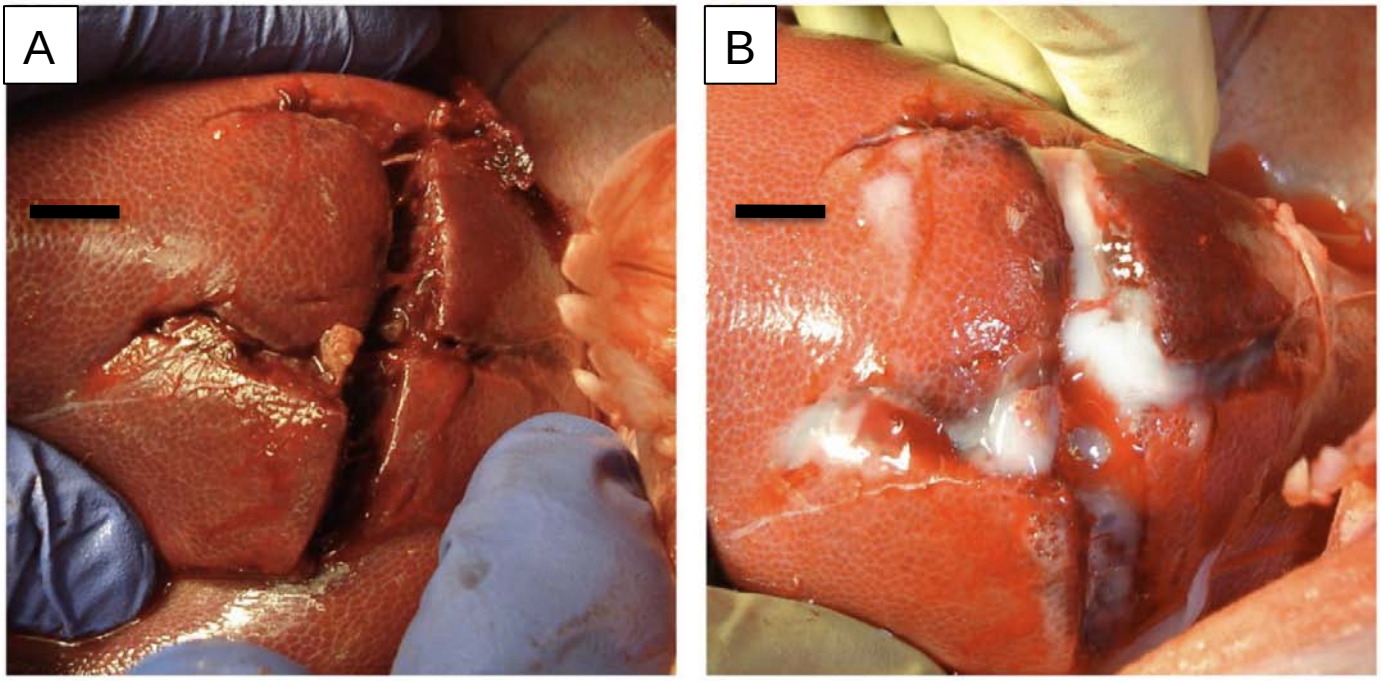

Figure 5: *in vivo* view of injury to central area of liver in swine. (A) Prior to treatment. (B) After treatment with liquid clotting factors (fibrin sealant, tri-factor: fibrinogen, thrombin, Factor XIIIa. Bars = 1 cm.

RESULTS/FIGURE 6

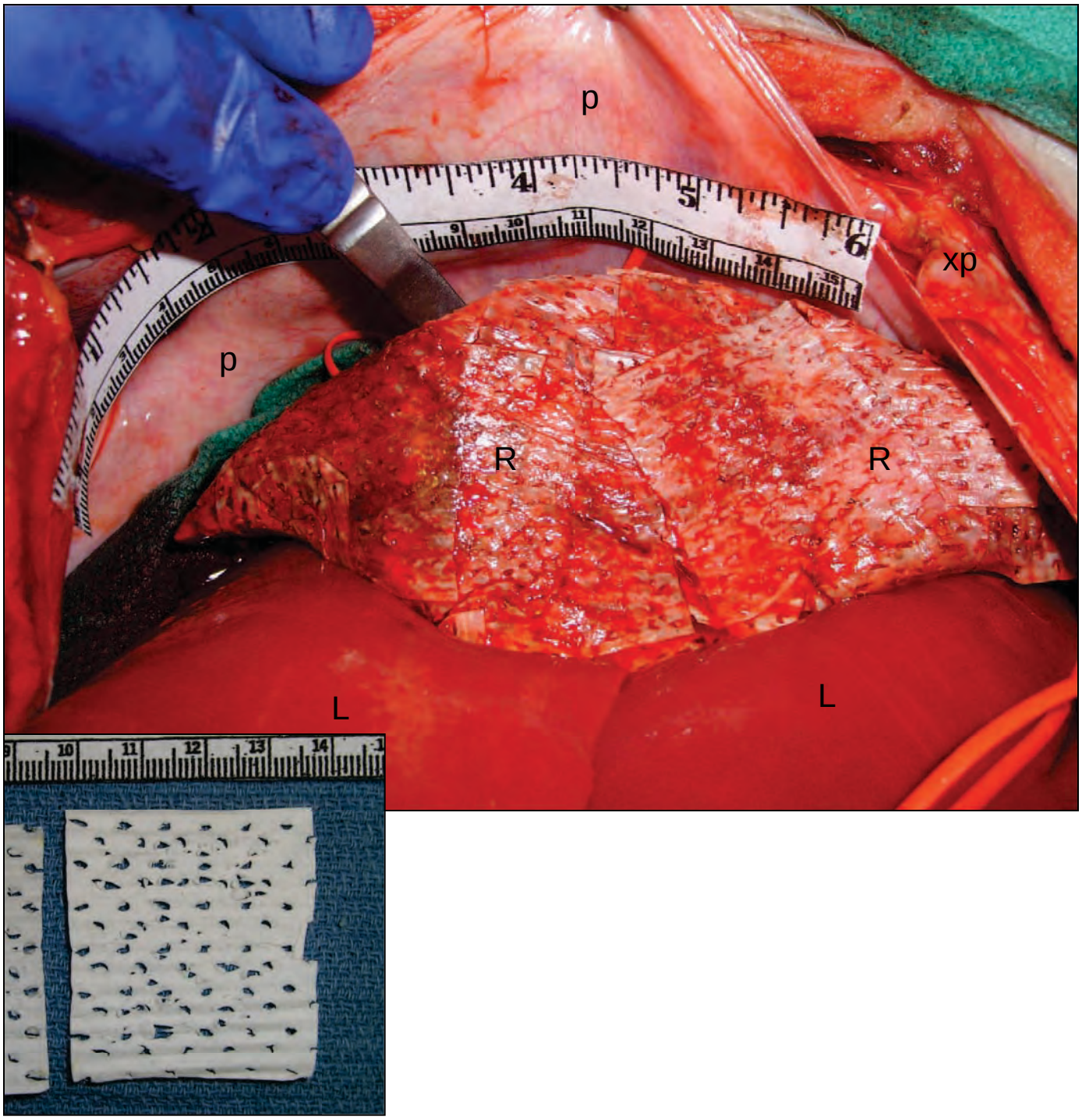

Figure 6: major liver resection, *in vivo*. Resection (R) was treated with microporous hydrophilic PLA (inset; corrugated/perforated), wet with recombinant I, IIa, & XIIIa, and with inflow/outflow occlusion. Liver clamps all released at time of photograph. Lower scale is cm/mm. L = noninvolved liver lobes; p = peritoneum; xp = xiphoid process.

RESULTS/FIGURE 7

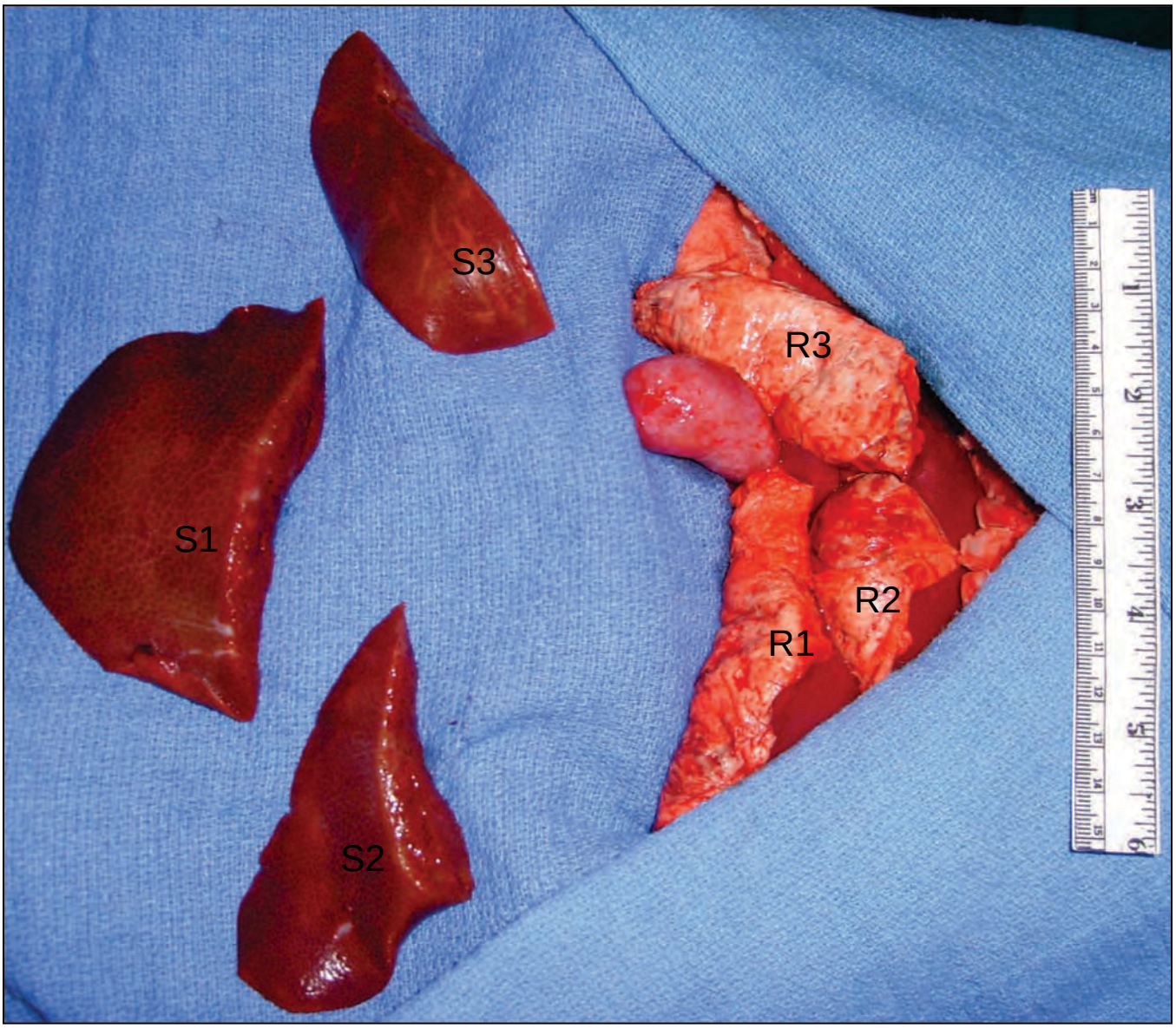

Figure 7: hepatic resections *in vivo*. Intraoperative photo. Resection sites (R1, R2, R3) and corresponding specimens (S1, S2, S3) are juxtaposed. All resections treated with clotting factors + bandage.

RESULTS/FIGURE 8

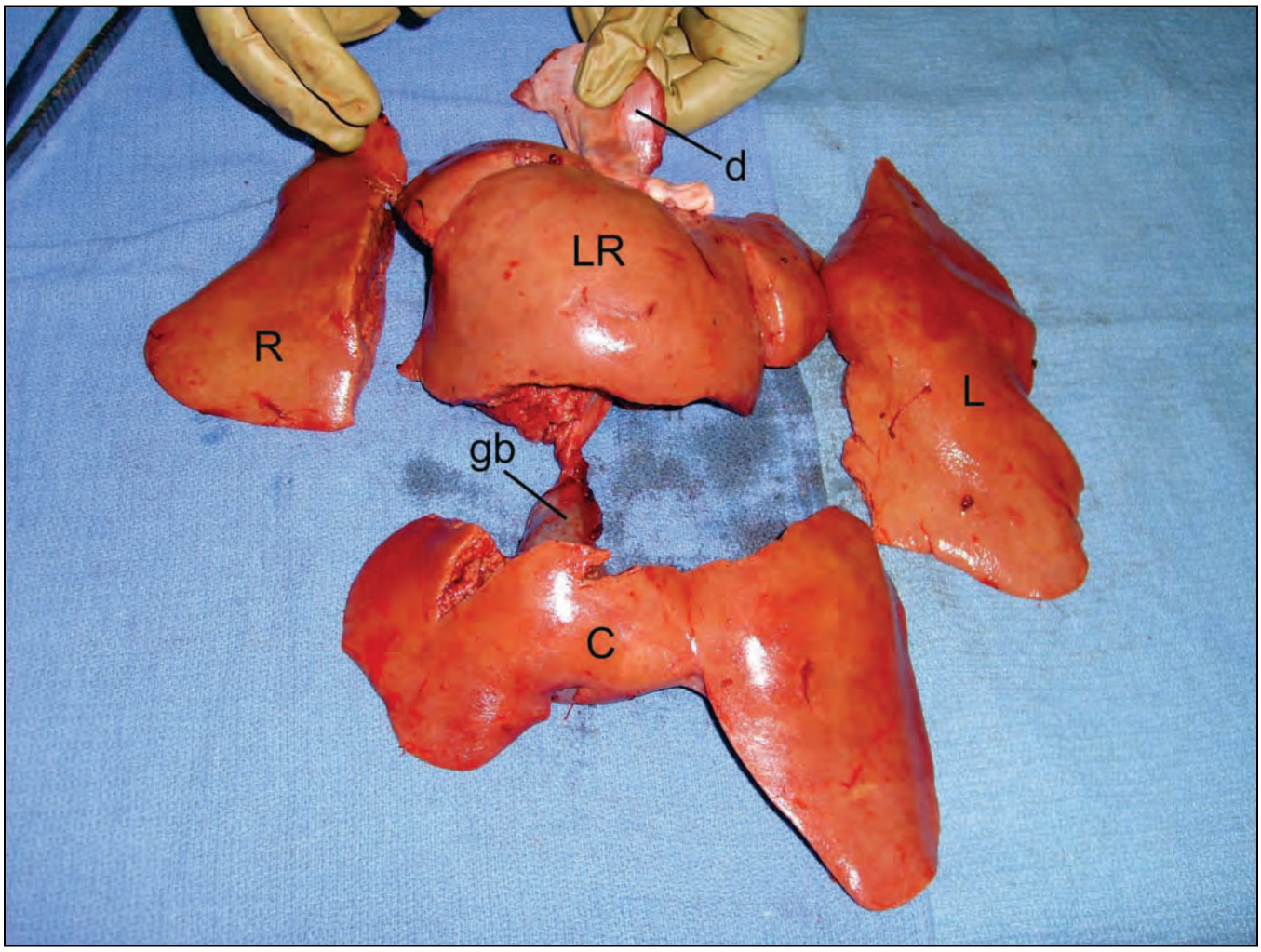

Figure 8: multiple heptatic resections (~70%), *ex vivo*. R = right segment; L = left segment; C = central segment; LR = liver remnant; d = diaphragm; gb = gallbladder. All resections controlled with combination of bandage + clotting factors, without any suturing or other hemostatic treatment.

RESULTS/FIGURE 9

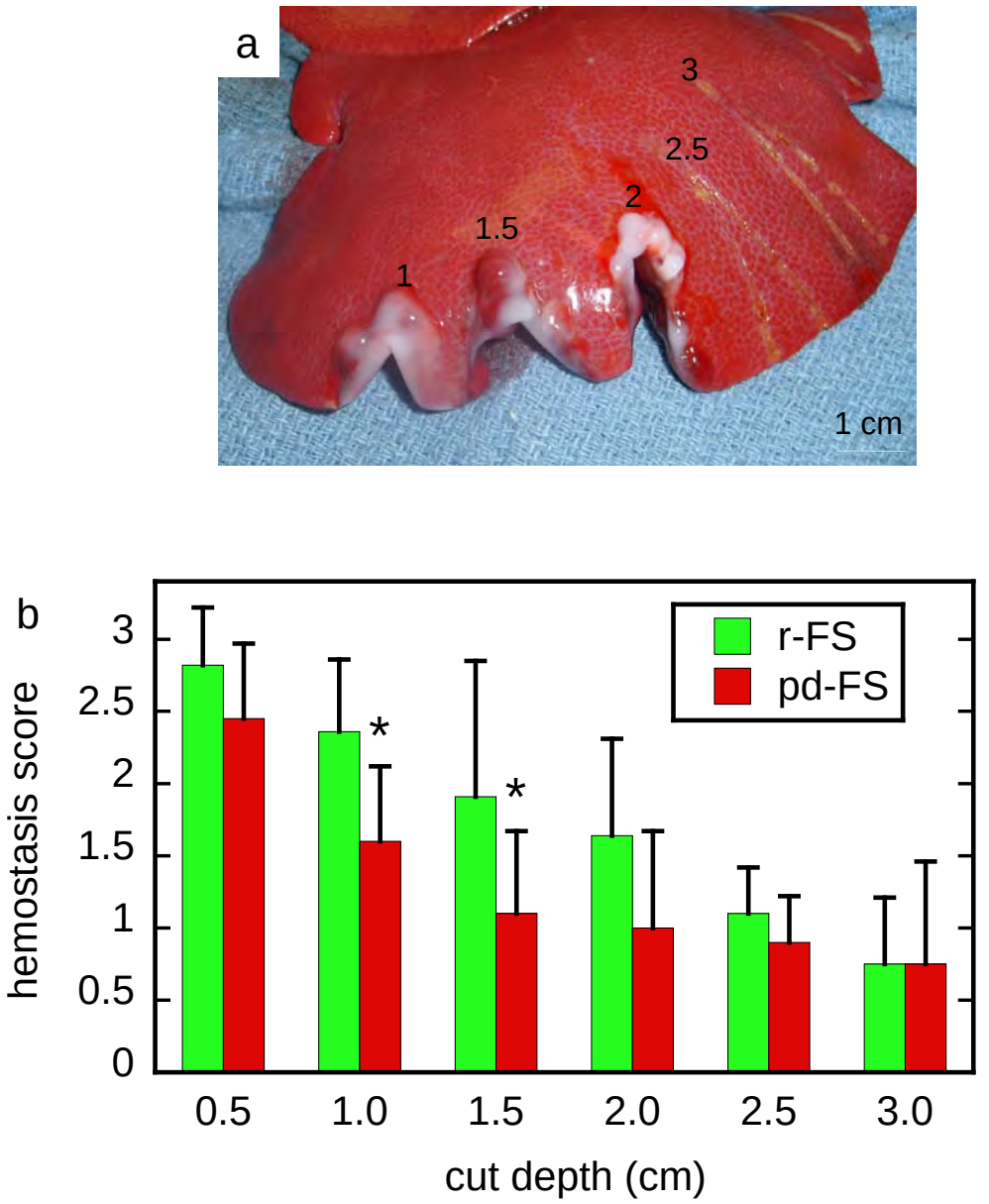

Figure 9: *ex vivo* hepatic lobar edge. (a) Crescendo series of wedge resections (depth given in cm), post-treatment with aerosolized triple-factors (r-fibrinogen, r-thrombin, r-F XIII). (b) Efficacy of recombinant vs. plasma-derived clotting factors in this model. Higher number = better hemostasis. *p < 0.05. Each bar = mean ± sd of 10 assays.

RESULTS/FIGURE 10

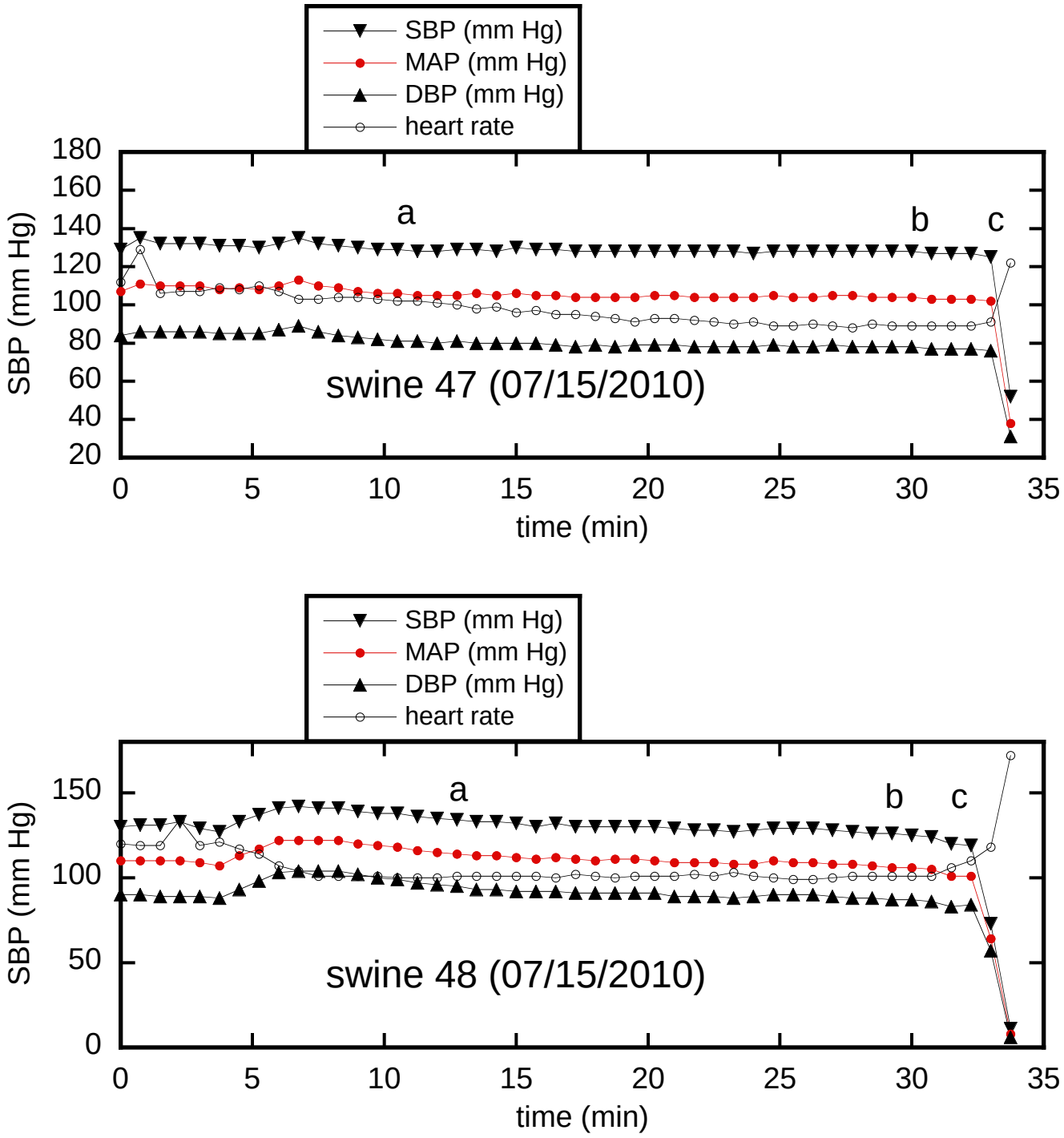

Figure 10. Vital signs of two swine undergoing wedge excisions. Recorded onto laptop directly from Bionet BM5 monitor; a = testing begun; b = testing finished; c = euthanasia with intentional exsanguination.

Carlson/2011 ACS

RESULTS/FIGURE 11

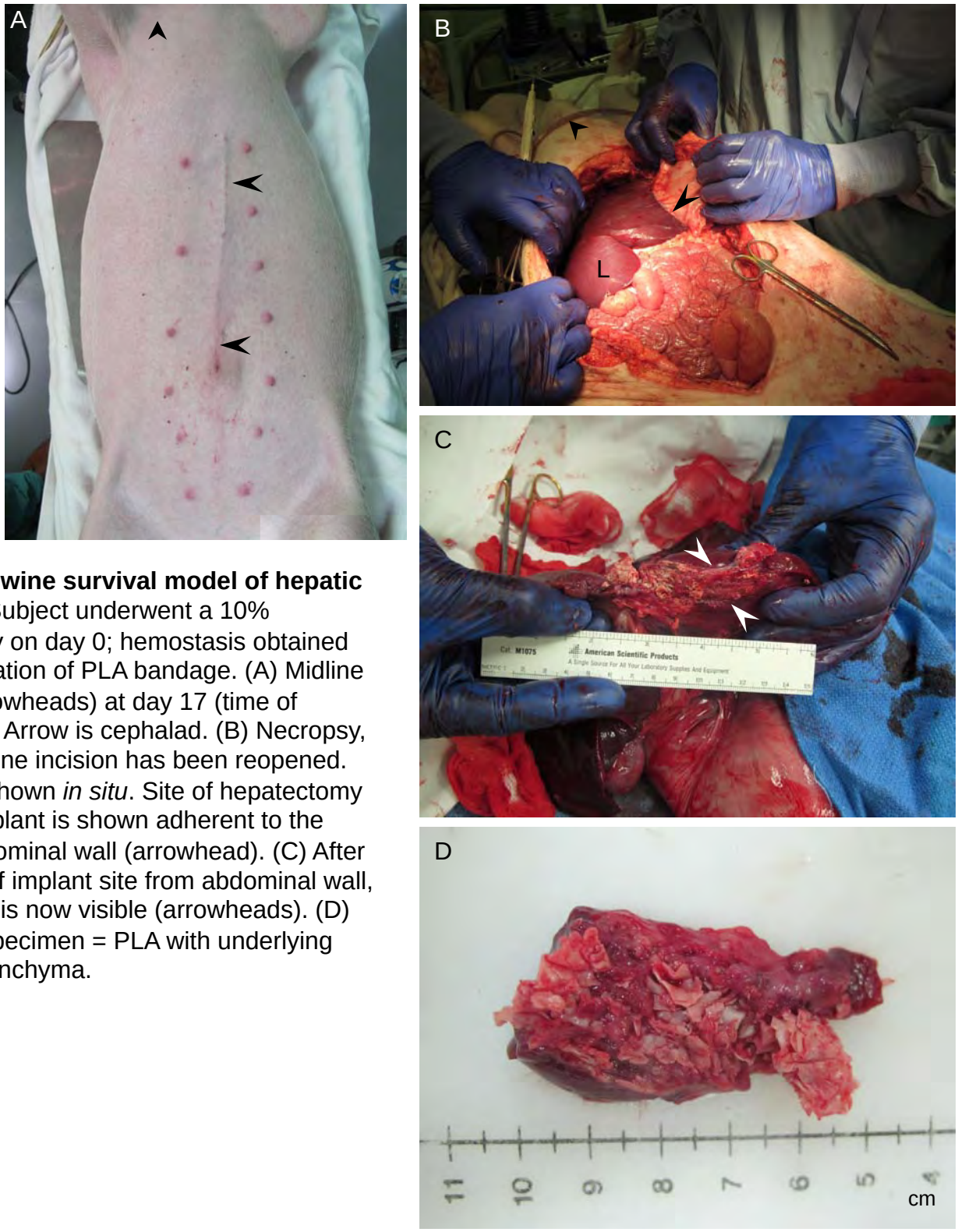

Figure 11. Swine survival model of hepatic resection. Subject underwent a 10% hepatectomy on day 0; hemostasis obtained with implantation of PLA bandage. (A) Midline incision (arrowheads) at day 17 (time of euthanasia). Arrow is cephalad. (B) Necropsy, day 17. Midline incision has been reopened. Liver (L) is shown *in situ*. Site of hepatectomy with PLA implant is shown adherent to the anterior abdominal wall (arrowhead). (C) After separation of implant site from abdominal wall, PLA implant is now visible (arrowheads). (D) Explanted specimen = PLA with underlying hepatic parenchyma.

RESULTS/FIGURE 12

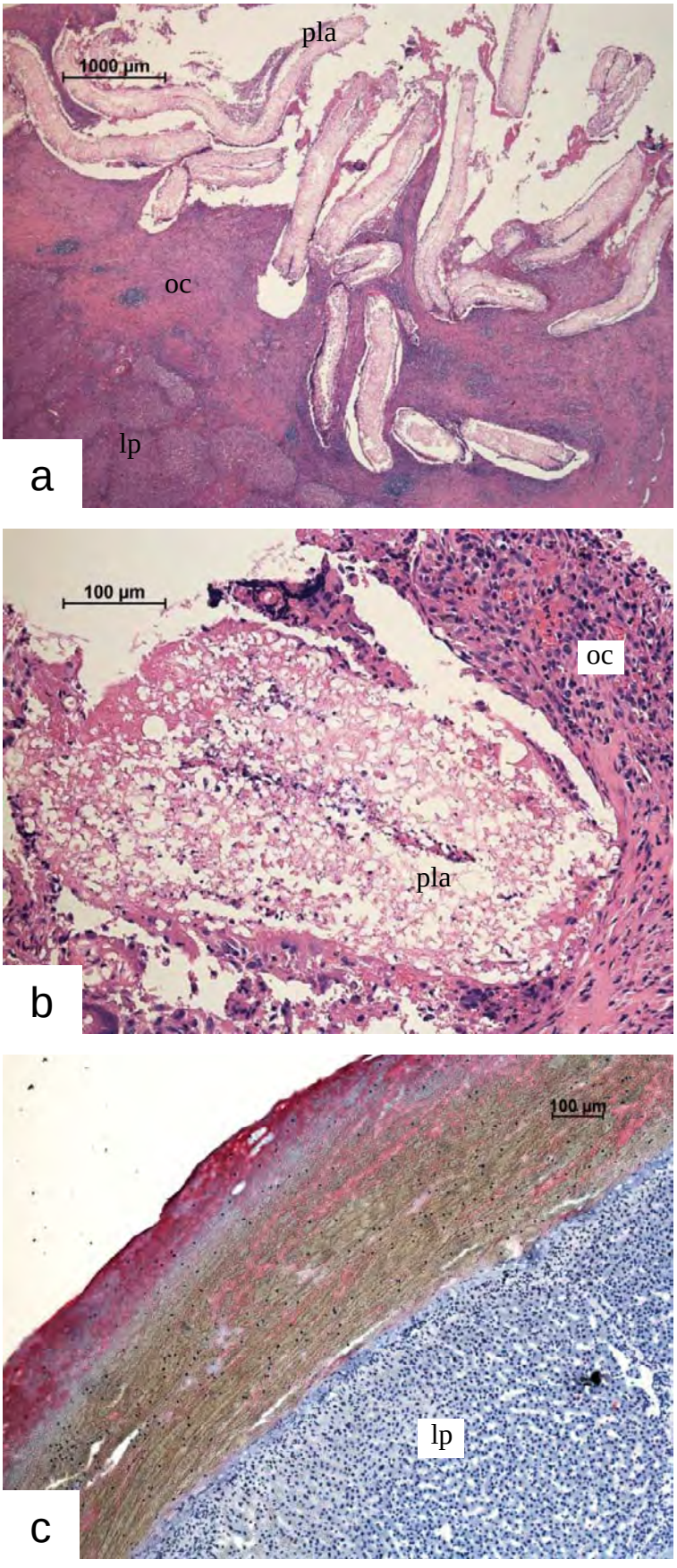

Figure 12. Histology of treated hepatic resection. (a) Interface of cut liver edge and PLA bandage at day 17 after treatment, H&E. (b) Higher magnfication from panel a. (c) Double immunohistochemistry for human fibrinogen (red) and porcine fibrinogen (brown) on the cut liver edge treated with rh-FS, day zero (hematoxylin counterstain). lp = liver parenchyma; oc = organizing clot; pla = PLA bandage.

CONCLUSIONS

- Standard swine models of severe hemorrhage were replicated at UNMC.
- Human clotting factors and resorbable PLA mesh can be formulated into a variety of hemostatic treatments.
- The above novel treatments have demonstrated preliminary efficacy in swine hemorrhage models.
- There is no preliminary evidence of toxicity with short-term implantation.

Acknowledgements: supported by grants from the Department of Defense, the National Institutes of Health, and UNMC. Also supported with resources and the use of facilities at the Omaha VA Medical Center.

Manuscript in preparation

A totally recombinant human fibrin sealant containing fibrinogen, thrombin, and Factor XIII

Mark A. Carlson[1,3,§]

William H. Velander[4]

Iraklis I. Pipinos[2,3]

Jason M. Johanning[2,3]

Crystal Krause[1,3]

Jennifer Calcaterra[4]

Departments of [1]Surgery and [2]Vascular Surgery, University of Nebraska Medical Center, Omaha, NE 68198-3280, and the [3]Veterans Administration Medical Center, Omaha NE 68105, USA

[4]Department of Chemical and Biomolecular Engineering, University of Nebraska–Lincoln, Lincoln NE 68588-0643, USA

[§]Corresponding author

Email addresses:

MAC: macarlso@unmc.edu

WHV: wvelander2@unl.edu

IIP: ipipinos@unmc.edu

JMJ: jjohanning@unmc.edu

CK: ccordes@unmc.edu

JC: jenncalc2@aol.com

Abstract

Background

Plasma-derived (pd) fibrin sealants (FS) have had limited applications because of cost, supply, and utility issues. We now describe a totally recombinant Factor XIII-supplemented FS which may be able to address these issues.

Methods

Human recombinant (r) fibrinogen (FI) and activated Factor XIII (FXIIIa) were generated in the milk of transgenic cows and in yeast, respectively; human r-thrombin (FIIa) was purchased (Recothrom®). r-FS made from these three factors was optimized with thromboelastography (TEG). pd-FS (Tisseel™) was used as directed. FS testing consisted of series of hepatic wedge excisions ("pie-slice") in domestic swine (male, 3 months, 30 kg; N = 6/group) with a constant base (1 cm) and step-wise increasing depth (0.5 to 3 cm, in 0.5 cm increments; 6 excisions/series, 2 series per swine) made on a lobar edge. Each excision was treated with up to 1 mL of FS without compression or other aid, and then hemostasis was scored: 0 = failure/minimal effect; 1 = steady bleeding; 2 = oozing; 3 = hemostatic.

Results

Minimal factor concentrations in the r-FS which yielded optimal TEG performance (data not shown, DNS) were 9 mg/mL FI, 0.36 mg/mL FXIIIa, 106 U/mL FIIa, and 12 mM CaCl2. Removal of r-FXIIIa decreased r-FS clotting kinetics ("alpha angle") and ultimate clot strength ("maximal amplitude") by 60 and 70%, respectively (DNS). pd-FS (N = 3 lots) contained 34-53 mg/mL FI, 200-312 U/mL FIIa, and trace/undetectable FXIIIa.

Ultimate clot strength at 20 min was not different between the r-FS and pd-FS (DNS), but the r-FS gained strength more quickly (time to half-maximal strength = 30 vs. 100 sec, respectively; derived value from TEG plots). Ultimate clot strength of both sealants was ~twice that of human whole blood (N = 22 normal donors), except that the latter had a 5-6 minute latency before detectable strength ("R value;" DNS). In the wedge resection model, the hemostatic scores of the r-FS were equivalent or better than those of the pd-FS (Figure; *$p < 0.05$, Wilcoxon; each bar represents mean score ± sd of 10-12 excisions).

Conclusions

r-FS had equivalent or better hemostatic efficacy than pd-FS in this wedge resection model, despite the FI concentration in the r-FS being about one-fourth that in the pd-FS. TEG data indicated that this result was dependent on the r-FXIIIa in the r-FS. Given that r-FS production is scalable, and the fact that FXIIIa supplementation greatly reduced FI requirement without sacrificing efficacy, r-FS production cost potentially should be much less than that for pd-FS. An abundant, economic source of r-FS might lead to increased innovation in hemostasis, acute wound stabilization, and related fields.

Background

Utilization of dried plasma as a topical hemostatic aid was documented in 1909.{Radosevich, 1997 #8398} The combination of relatively purified fibrinogen with thrombin to make fibrin glue was described in 1944,{Tidrick, 1944 #8399} but it was not until improved purification technology became available that fibrin sealant (or glue) became commercially available in the 1970's.{Radosevich, 1997 #8398} Since this time, the efficacy of fibrin sealant (FS) products as a topical hemostat or tissue adhesive has

been demonstrated in numerous elective clinical scenarios, including carotid endarterectomy,{Milne, 1995 #8236} total knee arthroplasty,{Levy, 1999 #8273} reoperative cardiac procedures,{Rousou, 1989 #8299} pulmonary resection,{Moser, 2008 #360} and partial nephrectomy,{Siemer, 2007 #8400}. FS alone was not useful during hepatectomy in patients,{Figueras, 2007 #7303} but FS combined with an equine collagen matrix reduced blood loss after liver resection compared with argon beam coagulation.{Frilling, 2005 #8401}

There has been interest in the development of FS-containing hemostatic devices for control of traumatic hemorrhage, particularly by the military.[ref] Topical hemostatic treatments which incorporate FS have been successfully employed in porcine models of femoral vessel injury,{Larson, 1995 #7212}{Jackson, 1997 #7213}{Holcomb, 1998 #7215} aortic injury,{Kheirabadi, 2007 #7302} severe liver injury,{Pusateri, 2003 #7298} and others. One of the notable FS-containing hemostatic devices for traumatic hemorrhage that was put to clinical use was the Dry Fibrin Sealant Dressing (DFSD), produced by the American Red Cross. This dressing contained human fibrinogen (15 mg/cm^2), human thrombin (37.5 U/cm^2), and calcium chloride (117 $\mu g/cm^2$) freeze-dried onto a 4 by 4 inch polygalactin mesh;{Pusateri, 2006 #8304} as such, the DFSD contained ~1.5 g of fibrinogen, and cost ~1,000 USD to manufacture. The DFSD was efficacious in various porcine models of lethal hemorrhage;{Holcomb, 1998 #7215}{Holcomb, 1999 #7300;Holcomb, 1999 #7284} and was anecdotally successful in military trauma, but was discontinued due to concerns about fragility and cost.{Pusateri, 2006 #8304}

[justification & advantages of a recombinant FS; background on r-FS development; lead-in to efficacy comparison against Tisseel in swine]

Methods

Clotting Factors

Description of the synthesis of human recombinant fibrinogen (huR-FI) and activated Factor XIIIa (huR-FXIIIa) in transgenic cows and yeast, along with their purification and *in vitro* characterization, will be published separately.[reference] Human recombinant activated thrombin (huR-FIIa) was purchased (Recothrom®; Zymogenetics, www.zymogenetics.com). Human plasma-derived fibrin sealant (pd-FS) was purchased (Tisseel™; Baxter BioSurgery, www.advancingbiosurgery.com/us/products/tisseel), and used per the manufacturer's instructions. Samples of normal human blood were obtained from volunteers after informed consent in a process that was approved by Institutional Review Board.

Thromboelastography

Clotting strength and kinetics of various tri-component mixtures of purified rFI or plasma-derived human fibrinogen (pdFI), rFXIII and pdFIIa or rFIIa were evaluated by thromboelastography (TEG) with a Thromboelastograph® Hemostasis System (5000 series; Haemoscope Corp., www.haemoscope.com). TEG Analytical Software (version 4.2.2, Haemoscope Corp.) collected time to clot initiation, time to achieve a clot firmness of 20mm (K), and maximal clot strength (MA). The instrument was calibrated each day

of use. Each experiment included a minimum of three replicates per treatment group. All blood samples were tested within 36 hours of phlebotomy.

Fibrinogen Immunohistochemistry

Swine liver specimens were fixed in 10% neutral-buffered formalin, dehydrated, and then embedded in paraffin blocks. All paraffin-embedded sections were cut at 5 μm, transferred to slides, and the dewaxed sections underwent antigen retrieval per the manufacturer's instructions (Dako TRS antigen retrieval solution; Dako North America, www.dako.com/us). The presence of both human and swine fibrinogen were detected by sequential dual-immunohistochemical staining followed by a Mayer's hematoxylin counterstain. Signal detection was performed using the DAKO EnVision™ G|2 Doublestain System (Dako North America) per the manufacturer's instructions. Briefly, endogenous peroxidase and alkaline phosphatase activity present in the tissue were blocked, and then the swine fibrinogen antibody (Kamiya Biomedical Company, www.kamiyabiomedical.com) was applied and visualized using HRP/DAB+. A second blocking step was performed prior to incubation with the human fibrinogen antibody (Abcam, Inc., www.abcam.com). The human fibrinogen antibody was visualized using the alkaline phosphatase-based Permanent Red (Dako North America), per the manufacturer's instructions.

Swine Hepatic Wedge Resection Model

The use of domestic swine (male, 30 kg/3 months old) for this project was approved by our Institutional Animal Care and Use Committee. Each subject was fasted

for 12 hours before surgery, with free access to water. Each subject was premedicated with telazol (4.4mg/kg), ketamine (2.2 mg/kg), and xylazine (2.2 mg/kg), as a single intramuscular injection. An intravenous line was established in a an ear vein, oral endotracheal intubation was performed, and anesthesia was maintained with 1-2% isoflurane using a Matrx VMS™ Veterinary Anesthesia Machine (Midmark Corp., www.midmark.com). Mechanical ventilation was maintained at 12-15 breaths per minute with a tidal volume of 5-10 mL/kg, in order to keep the end-tidal pCO_2 at 35-45 mm Hg. Rectal temperature, cardiac activity, and pulse oximetry was monitored with a Bionet BM5 Veterinary Monitor (Bionet America, Inc., www.bionetus.com). A carotid arterial catheter was placed for arterial pressure monitoring and blood sampling, and a jugular venous catheter was placed for isotonic fluid and medication administration, all via a surgical cutdown in the left neck.

The liver then was exposed through a midline incision. Sites for wedge-shaped ("pie-slice") hepatic excisions were lightly scored with electrocautery on the liver capsule (Figure 1a). The base of the excision was maintained constant at 1 cm. The depth of the excision ranged from 0.5-3.0 cm, in 0.5 cm increments, for a total of 6 excisions per series, all cut with scissors. The relatively small size of these excisions and the multiple liver lobe edges available permitted multiple excisions (two series of six, or 12 excisions) to be made in each subject without major blood loss. Each excision was treated with up to 1 mL of FS without compression or other aid [further description of FS applications technique]. Hemostasis was scored as follows: 0 = failure/minimal effect; 1 = steady bleeding; 2 = oozing; 3 = hemostatic.

Statistical Analysis

Results were compared by ANOVA and the unpaired t-test with an α of 0.05.

Results

Thromboelastography

Minimal factor concentrations in the r-FS which yielded optimal TEG performance (data not shown, DNS) were 9 mg/mL FI, 0.36 mg/mL FXIIIa, 106 U/mL FIIa, and 12 mM CaCl2. Removal of r-FXIIIa decreased r-FS clotting kinetics ("alpha angle") and ultimate clot strength ("maximal amplitude") by 60 and 70%, respectively (DNS). pd-FS (N = 3 lots) contained 34-53 mg/mL FI, 200-312 U/mL FIIa, and trace/undetectable FXIIIa. Ultimate clot strength at 20 min was not different between the r-FS and pd-FS (DNS), but the r-FS gained strength more quickly (time to half-maximal strength = 30 vs. 100 sec, respectively; derived value from TEG plots). Ultimate clot strength of both sealants was ~twice that of human whole blood (N = 22 normal donors), except that the latter had a 5-6 minute latency before detectable strength ("R value;" DNS).

r-FS *vs.* pd-FS in the Treatment of Hepatic Wedge Excisions

In the wedge resection model, the hemostatic scores of the r-FS were equivalent or better than those of the pd-FS (Figure; *$p < 0.05$, Wilcoxon; each bar represents mean score ± sd of 10-12 excisions).

Immunohistochemistry of r-FS applied to the Porcine Liver

Text for this sub-section.

Discussion

- Potential uses for an r-FS product (mention severe hemorrhage, e.g., noncompressible; clinical uses)
- Cost comparison with pd-FS, other economics
- Potential disadvantages of r-FS

Conclusions

r-FS had equivalent or better hemostatic efficacy than pd-FS in this wedge resection model, despite the FI concentration in the r-FS being about one-fourth that in the pd-FS. TEG data indicated that this result was dependent on the r-FXIIIa in the r-FS. Given that r-FS production is scalable, and the fact that FXIIIa supplementation greatly reduced FI requirement without sacrificing efficacy, r-FS production cost potentially should be much less than that for pd-FS. An abundant, economic source of r-FS might lead to increased innovation in hemostasis, acute wound stabilization, and related fields.

Competing interests

The authors declare no competing interests.

Authors' contributions

Preparation of clotting factors, thromboelastography: JC

Animal procedures: MAC, IIP, JMJ

Immunohistochemistry: CK

Drafting of manuscript: MAC

Overall supervision: MAC, WHV

All authors contributed to the experimental design and to the critical assessment and revision of the manuscript. All authors read and approved the manuscript in its final form.

Acknowledgements

This study is the result of work supported in part with resources and the use of facilities at the Omaha VA Medical Center. MAC and WHV were supported by grants from the NIH and the United States Department of Defense. The authors would like to acknowledge the technical assistance of Chris Hansen and Dean Heimann. The authors declare no conflicts of interest.

References

Figures

Figure 1 – Hepatic wedge excision model
Figure legend text

Figure 2 – Thromoboelastography of r-FS *vs.* pd-FS
Figure legend text.

Figure 3 – Immunohistochemistry of rHu-FS applied to porcine liver
Figure legend text.

Figure 4 – Hemostasis scores of hepatic wedge excisions treated with r-FS *vs.* pd-FS.
Figure legend text.

Tables
[pending]

Table 1 - Sample table title
Table legend text.

Additional files

Additional file 1 – video of FS application to hepatic wedge excision (dual syringe technique)

Additional file descriptions text (including details of how to view the file, if it is in a non-standard format).

Additional file 2 – video of FS application to hepatic wedge excision (aerosol technique)
Additional file descriptions text (including details of how to view the file, if it is in a non-standard format).

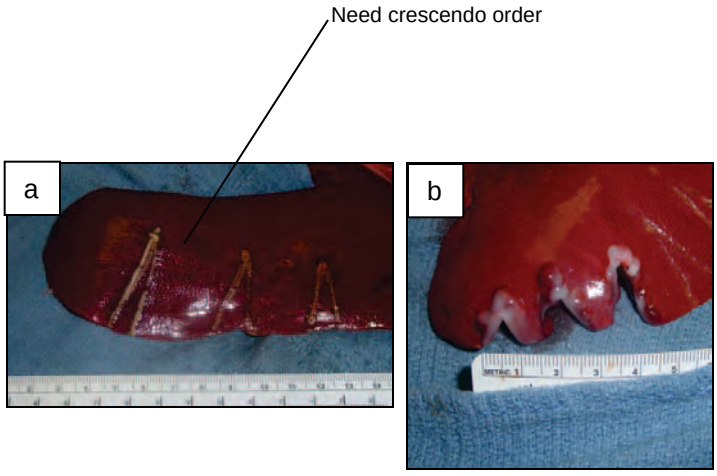

a. Tracing of hepatic wedge excisions. Scale = cm.

b. Post-treatment of hepatic wedge excisions. Scale = cm.

c. Double IHC for human fibrinogen (red) and swine fibrinogen (brown) in swine hepatic wedge excision treated with r-FS; bar = 1,000 µm.

d. Higher magnification of e; bar = 100 µm.

e. Single IHC for swine fibrinogen (brown) in swine hepatic wedge excision treated with r-FS; bar = 1,000 µm.

f. Higher magnification of g; bar = 100 µm.

Supplemental files:

- Image of hydrophilic vs. hydrophobic PLA, ex vivo
- TEG: multiple swine comparison
- TEG: one swine before, during, end of procedure
- Video of FS application to wedge cuts
- Video: swine 44, blood-letting from hepatic resection site
- raw data (spreadsheet) from hepatic resections
- raw data (spreadsheet) from wedge excisions

Figure 1 (swine model)

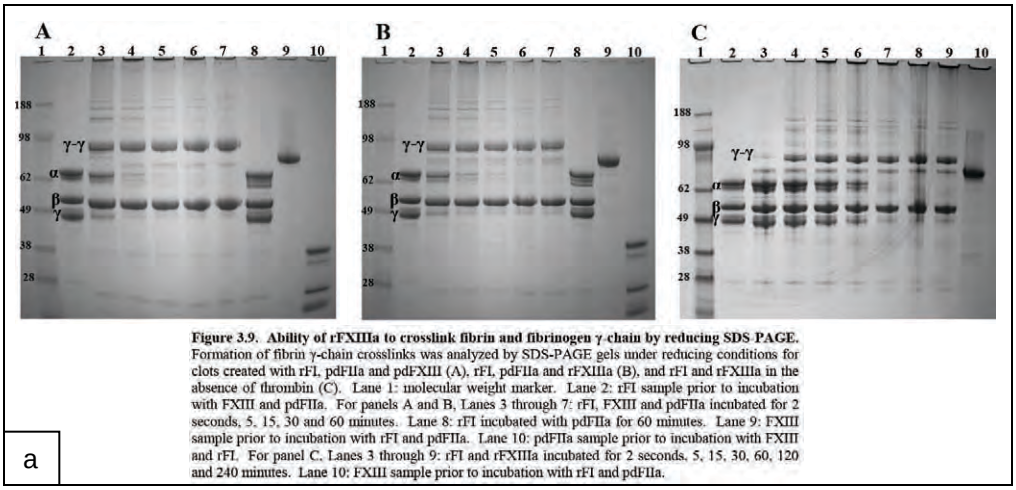

Figure 3.9. Ability of rFXIIIa to crosslink fibrin and fibrinogen γ-chain by reducing SDS-PAGE. Formation of fibrin γ-chain crosslinks was analyzed by SDS-PAGE gels under reducing conditions for clots created with rFI, pdFIIa and pdFXIII (A), rFI, pdFIIa and rFXIIIa (B), and rFI and rFXIIIa in the absence of thrombin (C). Lane 1: molecular weight marker. Lane 2: rFI sample prior to incubation with FXIII and pdFIIa. For panels A and B, Lanes 3 through 7: rFI, FXIII and pdFIIa incubated for 2 seconds, 5, 15, 30 and 60 minutes. Lane 8: rFI incubated with pdFIIa for 60 minutes. Lane 9: FXIII sample prior to incubation with rFI and pdFIIa. Lane 10: pdFIIa sample prior to incubation with FXIII and rFI. For panel C, Lanes 3 through 9: rFI and rFXIIIa incubated for 2 seconds, 5, 15, 30, 60, 120 and 240 minutes. Lane 10: FXIII sample prior to incubation with rFI and pdFIIa.

a

b

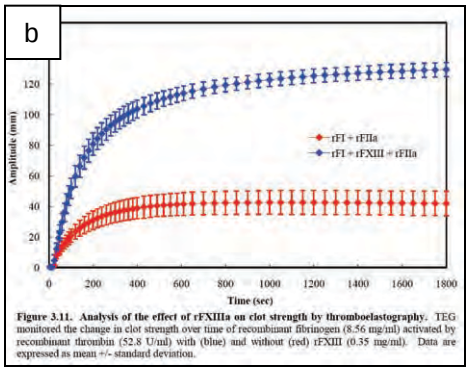

Figure 3.11. Analysis of the effect of rFXIIIa on clot strength by thromboelastography. TEG monitored the change in clot strength over time of recombinant fibrinogen (8.56 mg/ml) activated by recombinant thrombin (52.8 U/ml) with (blue) and without (red) rFXIII (0.35 mg/ml). Data are expressed as mean +/- standard deviation.

c

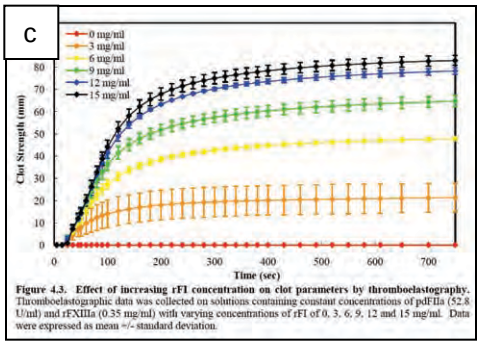

Figure 4.3. Effect of increasing rFI concentration on clot parameters by thromboelastography. Thromboelastographic data was collected on solutions containing constant concentrations of pdFIIa (52.8 U/ml) and rFXIIIa (0.35 mg/ml) with varying concentrations of rFI of 0, 3, 6, 9, 12 and 15 mg/ml. Data were expressed as mean +/- standard deviation.

d

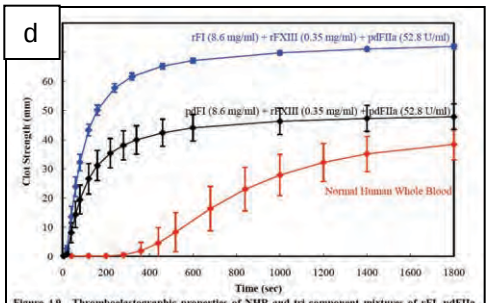

Figure 4.9. Thromboelastographic properties of NHB and tri-component mixtures of rFI, pdFIIa and rFXIIIa. Clots consisting of 8.6 mg/ml plasma-derived fibrinogen from a commercial LFS, 0.35 mg/ml rFXIII and 52.8 U/ml pdFIIa (black) have maximal clot strengths 18% greater than the average maximal strength of clots from whole blood of 22 normal donors (red). Replacing the plasma-derived fibrinogen with recombinant fibrinogen (blue) yielded clot strengths 67% greater than blood and 41% greater than that of the fibrinogen from the commercially available LFS. Data were expressed as mean +/- standard deviation.

e

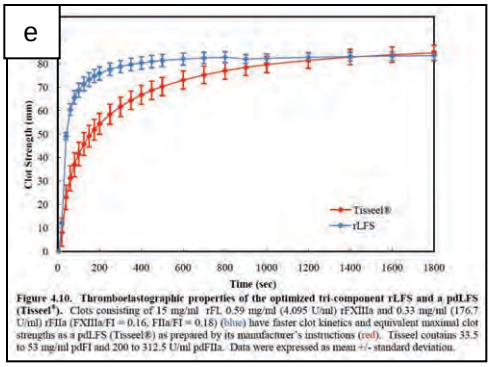

Figure 4.10. Thromboelastographic properties of the optimized tri-component rLFS and a pdLFS (Tisseel®). Clots consisting of 15 mg/ml rFI, 0.59 mg/ml (4.095 U/ml) rFXIIIa and 0.33 mg/ml (176.7 U/ml) rFIIa (FXIIIa/FI = 0.16, FIIa/FI = 0.18) (blue) have faster clot kinetics and equivalent maximal clot strengths as a pdLFS (Tisseel®) as prepared by its manufacturer's instructions (red). Tisseel contains 33.5 to 53 mg/ml pdFI and 200 to 312.5 U/ml pdFIIa. Data were expressed as mean +/- standard deviation.

Legend

Figure 2. *in vitro* characterization of r-FS
a. r-FXIIIa crosslinks FI
b. TEG: effect of r-FXIIIa in the FS
c. TEG: dose-response of r-FI in the r-FS
d. TEG: FS *vs.* whole blood
e. TEG: optimized r-FS *vs.* Tisseel

Supplemental files:

- Additional images of FI and FXIIIa characterization (electrophoresis, fibrinopeptide release, etc.)
- TEG: optimization of FXIIIa and FIIa concentration in the FS

Figure 2 (TEG)

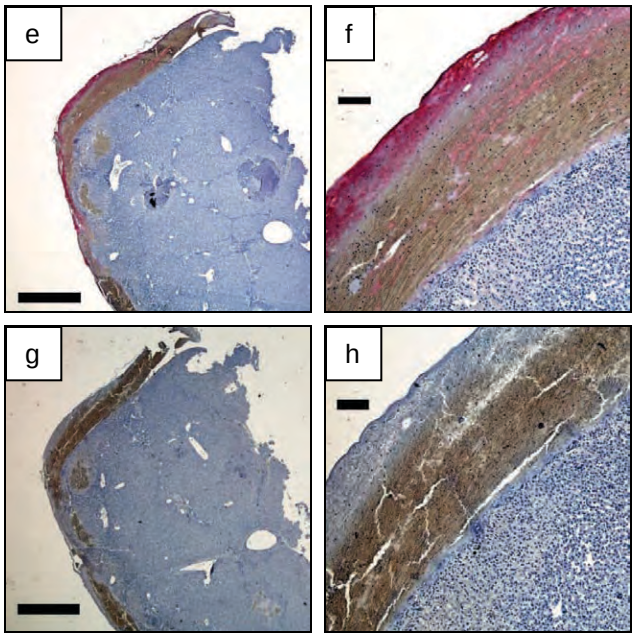

a. Tracing of hepatic wedge excisions. Scale = cm.

b. Post-treatment of hepatic wedge excisions. Scale = cm.

c. Double IHC for human fibrinogen (red) and swine fibrinogen (brown) in swine hepatic wedge excision treated with r-FS; bar = 1,000 µm.

d. Higher magnification of e; bar = 100 µm.

e. Single IHC for swine fibrinogen (brown) in swine hepatic wedge excision treated with r-FS; bar = 1,000 µm.

f. Higher magnification of g; bar = 100 µm.

Supplemental files:

- Image of hydrophilic vs. hydrophobic PLA, ex vivo
- TEG: multiple swine comparison
- TEG: one swine before, during, end of procedure
- Video of FS application to wedge cuts
- Video: swine 44, blood-letting from hepatic resection site
- raw data (spreadsheet) from hepatic resections
- raw data (spreadsheet) from wedge excisions

Figure 3 (IHC)

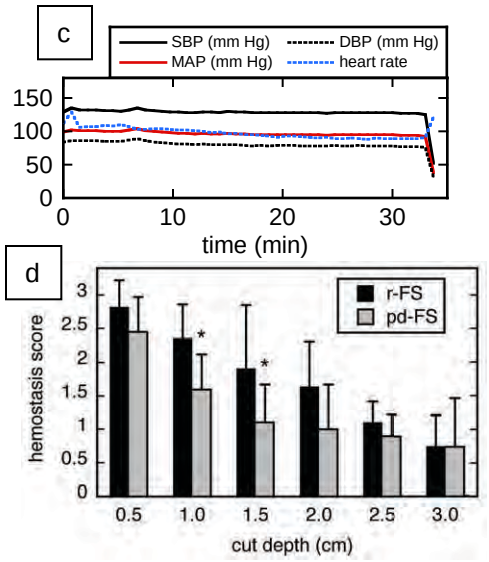

a. Sample tracing of hemodynamics during series of 12 wedge excisions.

b. Comparison of hemostasis score in wedge excisions treated with pd-FS *vs.* r-FS; $p < 0.05$, Wilcoxon.

Figure 4 (hemostasis scores)